# Impact of LEA29Y expression in a porcine heterotopic abdominal heart transplantation model

von Samjhana Shrestha

Inaugural-Dissertation zur Erlangung der Doktorwürde
der Tierärztlichen Fakultät der Ludwig-Maximilians-Universität
München

# Impact of LEA29Y expression in a porcine heterotopic abdominal heart transplantation model

von Samjhana Shrestha

aus Nepal

München 2025

Aus dem Veterinärwissenschaftlichen Department
der Ludwig-Maximilians-Universität München

Lehrstuhl für Molekulare Tierzucht und Biotechnologie

Arbeit angefertigt unter der Leitung von

Univ.-Prof. Dr. Eckhard Wolf

Angefertigt im Klinikum rechts der Isar der Technischen Universität München

Mentor: Prof. Dr. med. Christian Kupatt

Gedruckt mit Genehmigung der Tierärztlichen Fakultät

der Ludwig-Maximilians-Universität München

Dekan: Univ.-Prof. Dr. Reinhard K. Straubinger, Ph.D.

Berichterstatter: Univ.-Prof. Dr. Eckhard Wolf

Korreferent: Priv.-Doz. Dr. Susanne Zöls

Tag der Promotion: 26. Juli 2025

*For Baa, Aama and Buwa*

*and Maya*

# TABLE OF CONTENTS

# INDEX OF ABBREVIATIONS

| | |
|---|---|
| A | Adenine |
| α-1,3-gal | Galactose-alpha-1,3-galactose |
| AbdA | Abdominal aorta |
| ACTB | Beta-actin |
| AKT | Protein kinase |
| APC | Antigen presenting cell |
| AscA | Ascending aorta |
| ATP | Adenosine triphosphate |
| B2M | Beta-2-microglobulin |
| C | Cytosine |
| cAMP | Cyclic adenosine monophosphate |
| CD | Cluster of differentiation |
| cDNA | Complementary deoxyribonucleic acid |
| CFTR | Cystic fibrosis transmembrane conductance regulator |
| CRP | C- reactive protein |
| CRISPR | Clustered Regularly Interspaced Short Palindromic Repeats |
| CTL | Cytotoxic T lymphocyte |
| CTLA-4 | Cytotoxic T-lymphocyte-associated protein 4 |
| Ctrl | Control |
| CVD | Cardiovascular disease |
| CYBB | Cytochrome b-245 beta chain |
| DAMP | Damage-associated molecular patterns |
| DMD | Duchenne muscular dystrophy |
| DNA | Deoxyribonucleic acid |
| dNTP | Deoxynucleoside triphosphate |
| DSA | Donor specific antibody |
| DTH | Delayed type hypersensitivity |
| EDTA | Ethylenediaminetetraacetic acid |
| Et-OH | Ethanol |
| f | forward |
| g | units of gravity |

| | |
|---|---|
| G | Guanine |
| GAPDH | Glyceraldehyde-3-phosphate dehydrogenase |
| GGTA1 | Glycoprotein galactosyltransferase alpha |
| GHR | Growth hormone receptor |
| GTKO | Galactose-alpha-1,3-galactose knockout |
| hr | Hour |
| HE | Hematoxylin and Eosin |
| HHTx | Heterotopic abdominal heart transplantation |
| HLA | Human leucocyte antigen |
| IHC | Immunohistochemistry |
| IL | Interleukin |
| IVC | Inferior vena cava |
| IRI | Ischemia reperfusion injury |
| IFNG | Interferon gamma |
| kg | kilogram |
| KCl | Kalium chloride |
| LA | Left atrium |
| LFA | Lymphocyte function-associated antigen |
| LV | Left ventricle |
| MAC | Membrane attack complex |
| mg | milligram |
| MHC | Major Histocompatibility Complex |
| min | minute |
| ml | milligram |
| mM | milli-molar |
| MM | master-mixture |
| MMF | Mycophenolate mofetil |
| NADPH | Nicotinamide adenine dinucleotide phosphate |
| NF-KB | Nuclear factor kappa light chain enhancer of activated B cells |
| NGS | Next generation sequencing |
| NHP | Non-human primate |
| NK | Natural killer |
| PA | Pulmonary artery |

| | |
|---|---|
| PCR | Polymerase chain reaction |
| PI3Kγ | Phosphatidyl inositol 3 kinase gamma |
| PLN | Phospholamban |
| PTPRC | Protein tyrosine phosphatase receptor type C |
| r | Reverse |
| RA | Right atrium |
| RNA | Ribonucleic acid |
| RPM | Revolutions per minute |
| RT-mix | Reverse transcription master mixture |
| RT-PCR | Reverse transcription polymerase chain reaction |
| RV | Right ventricle |
| s | Second |
| SBT | Sequence-based typing |
| siRNA | small interfering ribonucleic acid |
| SLA | Swine leucocyte antigen |
| SNP | Single nucleotide polymorphism |
| SSP | Sequencing specific primer |
| SVC | Superior vena cava |
| SYBR | SYBR green |
| T | Thymine |
| TAE | Tris-acetate buffer |
| TBP | TATA- box binding protein |
| TCR | T cell receptor |
| TGFβ | Transforming growth factor beta |
| Th1 | Type 1 T helper cells |
| Th2 | Type 2 T helper cells |
| TNFα | Tumor necrosis factor alpha |
| UNG | Uracil N-glycosylase |
| VCAM | Vascular cell adhesion antigen |
| WT | Wild type |
| W/V | Weight by volume |
| YWHAZ | Tryptophan 5-monooxygenase activation protein zeta |
| µl | microliter |

| | |
|---|---|
| µg | microgram |
| °C | Degree Celsius |

# I. INTRODUCTION

Heart transplantation, also known as cardiac transplantation, is a surgical procedure of replacing a failing heart with a healthy donor heart. It is a terminal choice of treatment in end-stage heart failure patients. Cardiovascular diseases (CVD) are one of the major concerns in the health of the public, being the leading cause of worldwide death (Yang et al., 2020). Living organs from pigs can be a potential source to cope with the existing challenge of organ shortage (Boneva et al., 2001).

The compound interaction of clinical and immunological components governs graft survival in cardiac allotransplantation. Major histocompatibility complex matching is one of the key and critical determinants for graft survival. MHC molecules play a fundamental role in identifying antigens via antigen-presenting cells (APC), and mismatches in MHC alleles trigger both antibody-mediated and cellular rejection (Nakamura et al., 2019). In the "two-signal" model for lymphocyte activation, the first signal is given by the interaction between TCR with MHC on APC, and the second signal, the co-stimulatory signal, is derived from the interaction between CD28 and CTLA-4 on T-cell with B-1 (CD80) and B-7 (CD86) proteins on APC. Charpentier, 2012 described that belatacept has been used to block the co-stimulation signals and prevent rejection. Inhibition of T-cell activation by preventing the co-stimulatory pathways has been demonstrated to prevent organ rejection (Ville et al., 2015).

Bähr et al. (2016) developed the pig line CAG-LEA29Y, which expresses biologically active immunosuppressive protein LEA29Y, also known as belatacept. The ubiquitous expression of LEA29Y across the porcine organs or tissues and the adequate local transgene expression in the transplantation region protect the organ against rejection by human T-cells (Bähr et al., 2016). Thus, synthesizing such T-cell blocking agents in CAG-LEA29Y pigs supports CAG-LEA29 pigs as an attractive source to test local co-stimulation blockade in transplantation settings.

The intra-abdominal heterotopic cardiac allotransplantation in pigs allows a detailed monitoring for grafts while avoiding the need for the transplanted graft to be supported by systemic circulation (Mendiola Pla et al., 2022). This model allows us to assess the impacts of therapeutic interventions and immunopathology

on the rejection of grafts. This model does not require the allograft to support the systemic blood circulation of the recipient; hence, it becomes more beneficial than the orthotopic model (Kadner et al., 2000). The non-working but metabolically operative allograft has minimal possible side effects of systemic delivery (Cullen et al., 2021). The establishment of heterotopic abdominal heart transplantation of the CAG-LEA29Y pigs is a useful approach for testing the role of LEA29Y, i.e., belatacept in local co-stimulation blockade in graft survival and for testing the influence of MHC-matching between the donor and the recipient on the graft survival.

# II. REVIEW OF THE LITERATURE

## 1. Immunobiological barriers of cardiac transplantation

Cardiac transplantation is the end-stage treatment for heart failure. Advancements in genetic engineering and immunosuppressive therapies have significantly reduced hyperacute and acute humoral graft rejection; however, life-threatening complications from chronic diseases continue to pose challenges (Meier-Kriesche et al., 2004)

### 1.1. Hyperacute rejection

Hyperacute rejection is the most initial immunological barrier in transplantation between different species like pigs, NHPs, and humans. Preformed antibodies in the recipient against the alpha 1,3 Gal antigen present in porcine endothelial cells initiate a classical complement cascade causing the formation of membrane attack complex (MAC), leading to pathophysiological damage to endothelium, arterioles, and capillaries (Hryhorowicz et al., 2017). The pattern of response is equivalent to rejection of graft by the recipient in allotransplantation due to ABO blood group incompatibility (Stussi et al., 2006). This type of rejection typically develops in hours following transplantation, triggered by the edema and thrombosis, ultimately leading to complete graft loss in 24 hours (Hryhorowicz et al., 2017). After the role of Gal antigen in hyperacute rejection was discovered, the first α1,3GT / GGTA1 knockout pigs were generated (Phelps et al., 2003; Tseng et al., 2005). Using CRISPR/Cas9 to eliminate genes that are responsible for the synthesis of xenoantigens and to insert expression cassettes for human complement pathway regulatory proteins (CRPs) like CD46, CD55, and CD59 has improved the interaction of graft and recipient to prevent hyperacute rejection (Hryhorowicz et al., 2017).

### 1.2. Acute humoral rejection

Acute humoral rejection resembles hyperacute rejection, but it occurs over a longer span, which typically develops several days to a month following transplantation (Hryhorowicz et al., 2017). The antibodies from the recipient bind to vascular endothelium that initiate a complement cascade, and evoke inflammation and coagulation (Saadi et al., 2004). Saadi et al. defined acute humoral rejection as acute vascular rejection involving IgG immunoglobulins.

GTKO pigs expressing CRPs have prevented the rejection (Hara et al., 2008)

### 1.3. Acute cellular rejection

Acute cellular rejection occurs when the recipient's immune system activates T-cells to respond against the transplanted graft (Costanzo-Nordin, 1992; Ingulli, 2010). The immune system of the recipient is triggered by the antigens present in the transplanted graft, causing T cell activation and subsequent attack on the graft by the T cells (Costanzo-Nordin, 1992; Ingulli, 2010). In allotransplantation, strong cellular graft rejection happens early as a result of T-cell response. Allorecognition can take place either through direct pathway or indirect pathway. The major histocompatibility complex (MHC) adheres foreign antigens to T cell receptors (TCR) on T-cells, and the awareness of foreign MHC triggers the attack by T-cells (Ingulli, 2010)

### 1.4. Chronic rejection

Chronic rejection of graft occurs in a few months to years after the transplantation (Hryhorowicz et al., 2017). It is resulted from the combined impact of T cell and antigen-antibody complexes. It leads to damage to the vascular endothelium, ultimately resulting in graft failure, even though the exact mechanism for the rejection is yet not known (Hryhorowicz et al., 2017).

### 1.5. Coagulation dysfunction

Even if the graft rejection is turned off after transplantation, thrombotic microangiopathy or clotting in the graft blood vessels is noticed as a result of the aggregation of antibodies and complement on endothelial cells (Bühler et al., 2000; Houser et al., 2004). Coagulation dysfunction was elevated with elevating level of immunosuppression (Byrne et al., 2006)

## 2. Pig as a cardiac allotransplantation model

Mendiola et al. stated that pigs, as large animal models in heterotopic abdominal cardiac allotransplantation settings, provided a worthy approach to acquiring the impact of allograft procedures along with the immunopathology of rejection of the graft. In the heterotopic abdominal model, the donor heart does not support the recipient's circulatory system. Thus, this allows a longer duration of endurance of the graft to study and improve outcomes and remove the detrimental responses from recipients (Mendiola Pla et al., 2022). The resemblance of the anatomy and

physiology of swine hearts with human hearts provided a foundation for to use of genetically engineered strains of pigs to puzzle out technical issues of clinical transplantations and check the accessibility to a tolerance of transplantation in allograft settings (Kenmochi et al., 1994).

## 2.1. Porcine heterotopic abdominal cardiac transplantation

Heterotopic abdominal heart transplantation (HHTx) is a surgical technique in which the heart from a donor is transplanted into the abdomen of the recipient and integrated with the native circulatory system. Meanwhile, the native heart remains in its original space. HHTx provides a longer duration of endurance of the graft to study and improve outcomes and remove the detrimental responses from recipients without compromising the haemodynamics and circulation of the recipient (Mendiola Pla et al., 2022). HHTx utilizes a safe, non-toxic immunosuppressive approach to facilitate easy and continuous assessment of graft performance while maintaining immune suppression. However, the positioning of the transplanted heart in the abdominal cavity, which is very distinct from its natural location in the chest, can potentially alter how the heart's ventricles function together, due to changes in mechanical support provided by the pericardium and the pericardial fluid (Santamore & Dell'Italia, 1998).

### 2.1.1. Traditional non-volume-loaded HHTx

The traditional unloaded HHTx involves end-to-end anastomosis of the ascending aorta (AscA) of the donor graft is connected to the abdominal aorta (AbdA) of the recipient while the connection pulmonary artery (PA) of the donor graft is linked to the recipient's inferior vena cava (IVC) (Fu et al., 2016). In this setup (Fig. 1), The left ventricle remains inactive, as right ventricle is responsible for collecting venous blood and directing it into the recipient's circulatory system.

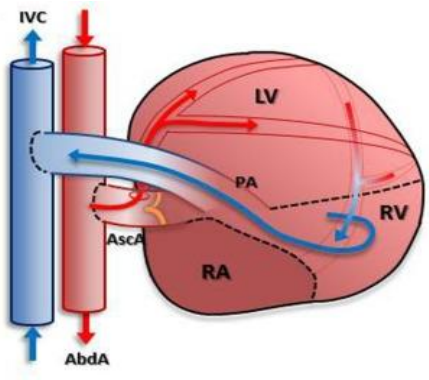


**Fig. 1: Diagrammatic representation of non-volume-loaded HHTx** (Fu et al., 2016)

### 2.1.2. Volume-loaded HHTx

Volume-loaded HHTx has anastomosis of the donor's ascending aorta (AscA) to the recipient's abdominal aorta (AbdA) (Flécher et al., 2013). In this setup, the pulmonary artery (PA) of the donor is connected to the left atrium (LA) of the donor and the donor's superior vena cava (SVC) is connected to the recipient's inferior vena cava (IVC) (Flécher et al., 2013). In volume-loaded HHTx (Fig. 2), the left ventricle receives volume-loading, which helps to preserve its structure and function.

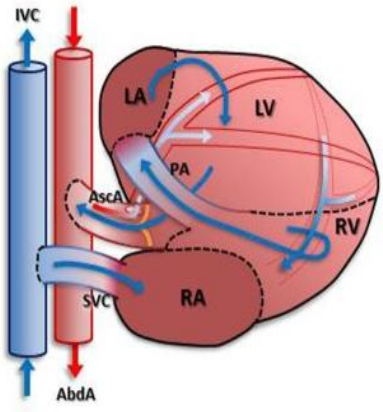


**Fig. 2: Diagrammatic representation of volume-loaded HHTx** (Fu et al., 2016)

## 3. Inflammatory response after transplantation

Inflammation in the transplanted graft generates acute and chronic rejections and reduces the chances of survival of the transplanted graft in the host. Cessation in the blood perfusion in the graft organ and sudden restoration of blood supply in the graft develops ischemia-reperfusion injury (IRI) in the graft that aids in graft necrosis. IRI induces the production of immune ligands damage-associated

molecular patterns (DAMPs), leading to sterile inflammation (Braza et al., 2016). DAMPs are released endogenously and innately and turn on graft cells, such as immune cells and endothelial cells (Mori et al., 2014). Immune cells like dendritic cells and macrophages, when activated, promote the production of chemokines that ultimately assist the intake of the immune cells from the host into the graft. The influx of immune cells from the host, like macrophages and dendritic cells, into the graft aggravates graft inflammation (Braza et al., 2016). At the same instance, a spike of adhesion molecules like vascular cell adhesion proteins like VCAM), which increases the entrance of neutrophils inside the graft, and also, lymphocyte function-associated antigen (LFA-1) that upregulates the adhesion of neutrophils in the blood vasculature of the graft (Li et al., 2012; Pittman & Kubes, 2013).

As soon as the initial phase of inducing inflammation in the graft is completed, the immune cells of the host regress back from the graft to the host and revert the immune cells to lymph nodes to set up an adaptive immune response against the donor (Kirk, 2003; Zhuang & Lakkis, 2015). The failure of the graft is dependent on the inflammatory response (Ezzelarab et al., 2015). Cytokines, also known as chemokines that are produced by the immune cells (neutrophils/ macrophages), act as the mediators for inflammation (Fig. 3). Thus, cytokines are responsible and determinant factors for the rejection of the graft. The difference in the cytokines and cell markers can be quantified via the analysis of gene expression of the cytokines and cell markers.

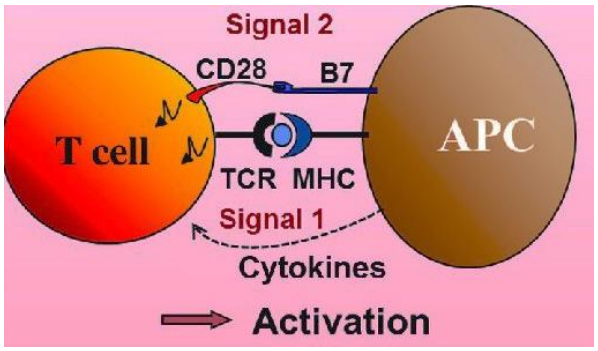


**Fig. 3: Two signal model of co-stimulation signal model for inflammatory response** (Mir, 2015)

## 4. T cell-mediated rejection in allotransplantation

T-cells are major contributors to induce cell-mediated rejection in cardiac allotransplantation (Pietra et al., 2000). The recipient's immune reaction against

the donor graft can result in graft failure. Antigens from the donors are recognized via two major pathways: direct and indirect pathways (Carnel et al., 2023). Acute rejection of allografts is mediated via direct and indirect T-cell reactions, whereas chronic rejection of allografts results from the attribution of indirect pathways of T-cell reaction (Siu et al., 2018).

TCR-allo-MHC interactions lead to the stimulation of T-cells. The immune response against the cardiac allograft is dependent on the CD4 T cells' activity (Pietra et al., 2000). CD4 T-cells themselves can enhance acute rejection of cardiac allograft through their interaction with the MHC complex (Nozaki et al., 2008). During graft rejection through the indirect pathway, CD4 T cells act to enhance and amplify both antibody-mediated immunity and cytotoxic actions of CD8 T cells against the graft (Siu et al., 2018). Both CD4 and CD8 T cells enhance the immune response against the graft via cytotoxicity delivered via the release of cytokines (Srivastava & Ernst, 2013).

### 4.1. Antigen recognition

T-cell receptors (TCRs) initiate antigen recognition and trigger T-cell activation (Carnel et al., 2023). MHC molecules have a fundamental role in the immune response by identifying antigens via APCs like macrophages to ensure that T-cells recognize and react to those antigens as a part of the targeted immune response (Fig. 4). Antigens from the donors are recognized via two major pathways: direct and indirect pathways (Carnel et al., 2023). In the direct pathway, T-cells interact with intact graft MHC alloantigen on the exterior surface of donor cells, in contrast to the indirect pathway, where T-cells interact with graft antigens that have already been processed and presented by the host's antigen-presenting cells (APC) (Carnel et al., 2023). In the direct pathway, graft-derived MHC cells from the donor migrate to the lymph node of the recipient and present the MHC antigens from the donor to the T-cells (Billingham, 1971; Steinmuller, 1980). Meanwhile, during the indirect pathway, a mechanism of self-restricted identification by T cell takes place as the alloantigens, specifically MHC antigens from the graft, are incorporated, processed, and introduced by host APC (specifically dendritic cells) to host MHC (Siu et al., 2018).

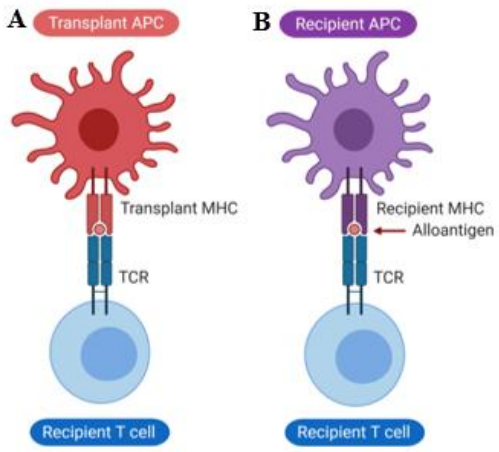


**Fig. 4: Antigen recognition (A)Direct allorecognition (B)Indirect allorecognition** (Demkes et al., 2021)

### 4.2. Co-stimulatory signals

Once an antigen is identified, a secondary signal, co-stimulation from APC, is necessary to initiate a full immune response (Magee et al., 2012) . In the "two-signal" model for lymphocyte activation, the first signal is given by the interaction between TCR with MHC on APC, and the second signal, the co-stimulatory signal, is derived from the interaction between CD28 and CTLA-4 on T-cell with B-1 (CD80) and B-7 (CD86) proteins on APC. Without this secondary signal, the lymphocyte would undergo apoptosis or anergic response as shown in Fig. 5 (Bretscher, 1999; Sharpe & Freeman, 2002). CD28 is expressed in all CD4 T cell populations and half of the CD8 T cell populations.

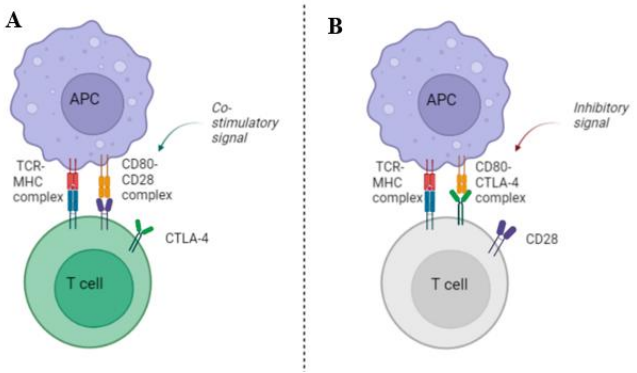


**Fig. 5: Co-stimulatory signals from APC (A) Activation T cells (B) Inactivated T cells** (Apol et al., 2023)

### 4.3. Co-stimulation as a target of immunosuppression

Co-stimulation is a secondary signal after antigen recognition, essential for

activating an immune response (Magee et al., 2012). In the "two-signal" model for lymphocyte activation, the primary signal is given by the interaction between TCR with MHC on APC, and the second signal, the co-stimulatory signal (Manikwar et al., 2012), is derived from the interaction between CD28 and CTLA-4 on T-cell with B-1 (CD80) and B-7 (CD86) proteins on APC. CD28 is a co-stimulatory receptor expressed in T cells (Riha & Rudd, 2010). CD28 is expressed in all CD4 T cell populations and half of the CD8 T cell populations. CD28 has crucial role in activation of T-cell. CD28 expressed on T lymphocytes binds on ligands CD80 and CD86 on APC that escorts to T cell activation. Cytotoxic T lymphocyte antigen-4 (CTLA-4) is concurrently induced on T cells to prevent excessive immune response via feedback mechanism and directing the displacement of CD28, hence downregulating further T cell activation (Hossen et al., 2023). Belatacept demonstrates higher binding affinity to CD80 and CD86 resulting reduced dissociations for CD80 and CD86. Compared to CTLA-4 or abatacept, belatacept demonstrates approximately four times greater affinity for CD68 and about twice the affinity for CD80 (Esensten et al., 2016).

### 4.4. Cytokine secretion and response

The activated T-cells produce cytokines that induce the immune response against the graft. Both CD4 along with CD8 T cells enhance immune response against the graft via cytotoxicity delivered via the release of cytokines (Srivastava & Ernst, 2013). Direct pathway of alloantigen recognition establishes an immunological synapse that serves two major functions, acts as a region for triggering antigen-specific cytotoxic T lymphocytes (CTLs) activation and acts as a facilitator the secretion of cytolytic molecules to destroy the grafts (Breart et al., 2008; Pietra et al., 2000). Immunological synapses spark the activation of cytokine-producing CD4 and CD8 T cells resulting the multidirectional emission of cytokines (Huse et al., 2006). The cytokines that have been synthesized will indeed act again on cells with the peptide-MHC complexes to deliver T-cell activation signal (Egen et al., 2011; Huse et al., 2006). These cytokines are able to spread through tissue and stimulate the bystander cells, which in turn activate the antigen-specific T-cells (Müller et al., 2012; Perona-Wright et al., 2010).

### 4.5. Proliferation and differentiation

At the final stage, T-cells go through proliferation and differentiation. The activated T cells expand and modify as T helper cells and cytotoxic T cells.

## 5. Complement factor and T-cell interaction during alloimmune inflammation

Complement factor and T-cell signaling participate in transplant-mediated injury. The interaction between complement factors and T-cell is responsible to regulate T-helper cells' immune response for inflammation, impairment of microvasculature and remodeling with fibrous tissue (Khan & Shamma, 2019). During the process of allotransplantation rejection, T-regulatory cells cohere to activated complement factors C3aR and C5aR (Khan & Shamma, 2019). Interaction of C3 molecule with TCRs or receptors in APC mediates the proliferation and differentiation of T-cells.

During the complement cascade, C3a convertase breaks C3 molecule into C3a and C3b among which C3a interacts with T and B cells, macrophages, mast cells and basophils. This interaction elevates the specific binding of C3a and C5a on T cells with the C3a and C5a receptors on APCs and macrophages. Afterwards, there is the activation of APCs with PI3Kγ/AKT resulting the downregulation of cAMP/phosphokinase in contrast to the activation of NF-κB pathways (Li et al., 2008; Peng et al., 2009) for secretion of cytokines. Subsequently, there is an acceleration in CD80/CD86 co-stimulation to multiply IFNγ-secreting T helper1 cells (Lalli et al., 2008; Li et al., 2008; Liu et al., 2008; Strainic et al., 2008). When C3a and C5a receptors on Tcells are involved, it activates PI3Kγ and leads to AKT phosphorylation, which subsequently impacts Bcl2 gene (BCL2 Apoptosis Regulator), helping to inhibit apoptosis of T-cells, thereby promoting the proliferation of T-cell (Lalli et al., 2008)

C3a is essential to generate an immune response to a specific antigen via CD4+ and CD8+ T-cells, either by direct or indirect pathway, as shown in Fig. 6 (Bode et al., 2012). Calcium influx was not detected in C3aR-deficient T-cells, whereas a transient calcium response occurred in C3aR-expressing CD4+ and CD8+ T cells following C3a stimulation, indicating that C3a specially activates T cells through its receptor (Werfel et al., 2000). It has been demonstrated that C3 fragments has role to induce the T-cells via APC in a mouse bone marrow

transplantation model (Ma et al., 2012) and in murine kidney allografts, inhibition of C5a led to prolonged graft endurance and noticeable reduction in the invasion of macrophages and monocytes (Gueler et al., 2008).

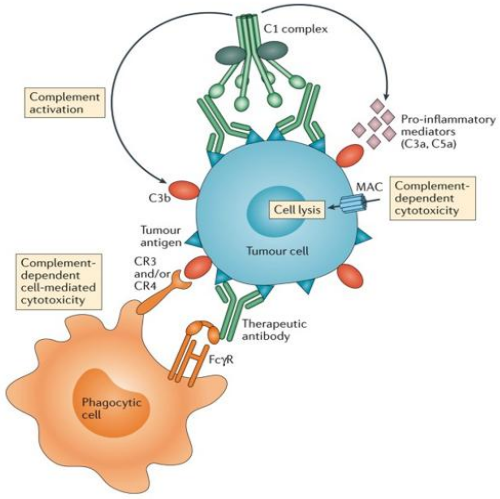


**Fig. 6: Complemented mediated T-cell cytotoxicity** (Reis et al., 2018)

## 6. Major histocompatibility Complex (MHC)

MHC is highly polygenic and polymorphic, a cluster of genes that codes the glycoproteins on the cell surface as an essential entity for adaptive immunity for self-recognition. MHC molecules have a fundamental role in the immune response by identifying antigens via APCs like macrophages allowing T-cells to detect and respond specifically to those antigens (Carnel et al., 2023). MHC region carries a cluster of genes provided that an individual has their own set of MHC genes due to the polygenic nature of MHC. Also, the polymorphic nature of MHC is attributed to numerous non-identical varieties and alleles within a herd that impact the T-cell antigen recognition mechanism (Sommer, 2005).

### 6.1. History of MHC

Gorer and Snell discovered MHC in 1936 (Nakamura et al., 2019). Snell et al. described MHC as self or non-self-recognition that relied on the genetic makeup (Snell, 1978). The patients with a history of frequent transfusions of blood reported antibodies in the patient's serum that were later identified as human MHC, i.e., Human leukocyte antigen (HLA) (Marchal et al., 1962). MHC matching was developed to enable the matching of the donor and recipient in the

mid to late 1960s (Nakamura et al., 2019). Sequencing-based typing (SBT), sequence-specific primers (SSP), and next-generation sequencing (NGS) have been used for MHC typing (Bentley et al., 2009; Gabriel et al., 2014).

### 6.2. Role of MHC in transplantation settings

With the discovery of MHC in 1936, the prospects for heart transplantation have broadened. MHC matching has been identified as a quick bypass to eliminate rejection (Nakamura et al., 2019). MHC-matching between the donor and the recipient has a critical and dominant role in the success of transplantation. The mismatches of the MHC alleles trigger both antibody-mediated and cellular rejection. Allogenic recognition of an allograft can be triggered by both APC derived from the donor and the recipient.

MHC molecules have a fundamental role in the immune response by identifying antigens via APCs like macrophages to ensure that T-cells recognize and react to those antigens as a part of the targeted immune response.

#### 6.2.1. MHC in cellular rejection

T lymphocytes are essential mediators in the process of cellular rejection (Ingulli, 2010). Allograft rejection is initiated by CD4+ T cell recognition, which activates the binding of CD8+ T cells through attachment with CD8 TCR and MHC class I (Nakamura et al., 2019). Alloreactive cytotoxic T cells reject the allografts. Antigens from the donors are recognized via two major pathways: direct and indirect pathways (Carnel et al., 2023). In the direct pathway, T-cells interact with intact graft MHC alloantigen on the exterior surface of donor cells, in contrast to the indirect pathway where T-cells interact with graft antigens that have been already processed and presented by the host's antigen-presenting cells (APC) (Carnel et al., 2023). Through the direct pathway, donor-derived MHC molecules travel to the recipient's lymph node, where they present donor antigens directly to the recipient's T cells (Billingham, 1971; Steinmuller, 1980). In contrast, the indirect pathway, a self-restricted recognition, particularly MHC molecules from the graft are internalized, processed and presented by the recipient's APC (specifically dendritic cells) on their own MHC (Siu et al., 2018).

A transplantation model with the knockdown of MHC expression using small interfering RNAs (siRNAs) might be a strategy to devitalize cellular rejection (Cui et al., 2017). Delayed-type hypersensitivity (DTH) triggered by CD4+ T cells

with the aid of IFNG activates macrophages, resulting in DTH-mediated rejection (Yamada et al., 2007). Natural killer cells, neutrophils, and myeloid-derived suppressor cells have also been reported to be involved in cellular rejection (Nakamura et al., 2019).

### 6.2.2. MHC in antibody-mediated rejection

Alloantigens are presented to CD4+ T cells by B cells via the indirect pathway of antigen recognition in a self-MHC-restricted manner (Nakamura et al., 2019). This antibody-mediated rejection contributes to the development of long-lasting plasma cells (Ballet et al., 2009). Donor-specific antibodies (DSA) are important in graft rejection among the variety of alloreactive antibodies.

## 6.3. Swine Leukocyte Antigen (SLA)

Swine leukocyte antigen is the major histocompatibility complex of the pig and is structurally equivalent to human leukocyte antigen (HLA). The SLA genes are located on chromosome 7 and are organized into two major groups: SLA class I and SLA class II (Techakriengkrai et al., 2021). SLA class I includes the genes SLA1, SLA2 and SLA3, whereas SLA class II comprises of genes such as SLA-DR, SLA-DQ, and SLA-DRB1. All the nucleated cell surfaces express SLA1, SLA2, and SLA3 whereas, APC surfaces express SLA-DR and SLA-DQ (Lunney et al., 2009). SLA has a critical role in immune responses. The peptide-binding groove in SLA is formed by exon 2 and 3 in SLA class I and exon 2 in SLA class II (Hammer et al., 2020)

### 6.3.1. SLA class I

SLA1 class I have a heterodimeric structure with beta-2 (β2) microglobulin (B2M) and heavy alpha chains, alpha 1 (α1), alpha 2 (α2) and alpha 3 (α3). Alpha 1 and alpha 2 domains form the binding groove of SLA as shown in Fig. 7 (Wieczorek et al., 2017). SLA1 and SLA2 genes are reported to have 90 and 96 alleles, respectively (Maccari et al., 2017; Ballingall et al., 2018). Cleft for peptide-binding is formed by alpha 1 and alpha 2 chains where the peptides of antigens are presented to CD8+ T cells and the two alpha chains, alpha 1 and alpha 2, are encoded by exon 2 and exon 3, respectively (Gao et al., 2017). Thus, the polymorphism in alpha 1 and alpha 2 is responsible for variation in response to allograft in regard to the interaction between the antigens from the graft.

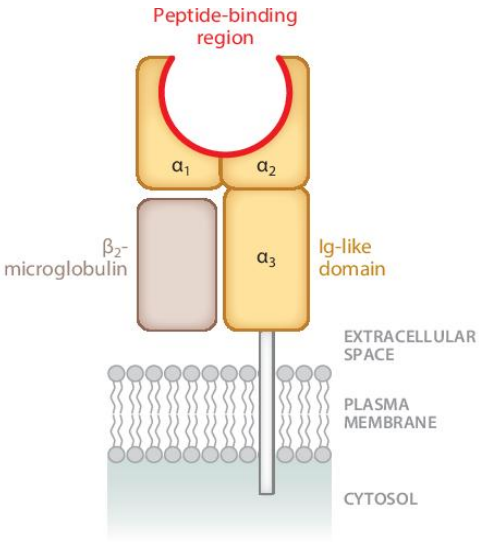


**Fig. 7: Model structure of SLA class I protein** (Hammer et al., 2020)

### 6.3.2. SLA class II

SLA class II represents swine MHC genes expressed on APCs (Lunney et al., 2009). As illustrated in Fig. 8, SLA II is composed of two distinct chains forming a heterodimer, with the apha chain containing alpha 1 (α1) and alpha 2 (α2) domains, and the beta chains comprising beta 1 (β1) and beta 2 (β2). The cleft for peptide binding is formed by alpha 1 and beta 1 domains, where the peptides of antigens are presented to CD4+ T cells (Techakriengkrai et al., 2021). Genes coding for alpha 1 domain in SLA-DR and SLA-DQ are inscribed in exon 2 (Hammer et al., 2020). SLA-DRB1 and SLA-DQB1 possess extremely polymorphic loci in contrast to SLA-DQA, which has a lower ratio of polymorphism (Hammer et al., 2020; Lunney et al., 2009). The SLA class II region shows significant genetic diversity, particularly in SLA-DQB1, SLA-DRB1 and SLA-DQA with 53, 99 and 26 allelic variants reported respectively (Ballingall et al., 2018; Maccari et al., 2017).

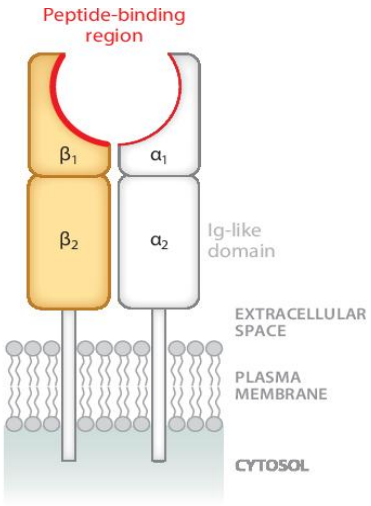


**Fig. 8: Model structure of SLA class II protein** (Hammer et al., 2020)

### 6.4. Interaction of SLA with T-cells

SLA molecules have a fundamental role in the immune response by identifying antigens via APCs like macrophages to ensure that T-cells recognize and react to those antigens as part of the targeted immune response. Antigens from the donors are recognized via two major pathways: direct and indirect pathways (Carnel et al., 2023). T cells recognize intact MHC alloantigens presented on the surface of donor cells in the direct pathway, whereas in the indirect pathway, T-cells respond to graft-derived antigens that are processed and displayed by the host's antigen-presenting cells (APCs) (Carnel et al., 2023). In the direct pathway, graft-derived MHC cells migrate to the recipient's lymph node and present the MHC antigens from the donor to the T cells (Billingham, 1971; Steinmuller, 1980). In contrast, the indirect pathway involves self-restricted recognition, where graft-derived alloantigen, primarily MHC molecules, are internalized, processed and the presented by the recipient's APC , such as dendritic cells, on hostg's own MHC molecules (Siu et al., 2018).

### 6.5. Influence of SLA on transplants

SLA is a highly polymorphic MHC. Polymorphism in SLA highly influences immune response to infectious diseases and transplantation (Gao et al., 2017). Screening of variations in SLA is a critical factor in the immune response of swine towards antigen recognition. 192 SLA class I alleles and 145 SLA class II alleles have been specified in the Immuno Polymorphism Database (IDP)-MHC (Gao et al., 2017). Glycoproteins synthesized by SLA class I and class II present antigenic peptides to T cells, which trigger adaptive immune responses (Hammer

et al., 2021). SLA class I molecules have a role in the activation and proliferation of T-cells by directly presenting the antigens or contribute to antibody-mediated rejection via antibodies produced against the SLA.

## 7. Research on LEA29Y pigs

In 2016, Bahr et al. developed a genetically modified transgenic pig, CAG-LEA29Y, to overcome immunological barriers in organ transplantation. To achieve ubiquitous expression of LEA29Y (belatacept), they utilized the CAG promoter, a chicken β-actin core promoter, and a genomic element from the rabbit *HBB* gene. As a result, the transgenic pigs expressed human CTLA4-Ig derivative LEA29Y in serum and multiple organs(Bähr et al., 2016). Despite some impact on the pigs' immune system, the transgene was stably inherited across generations and remained expressed until sexual maturity.

Belatacept, also known as LEA29Y, differs from the native CTLA4-Ig protein by two amino acid substitutions: glutamic acid and tyrosine replace leucine and alanine at positions 104 and 29, respectively(Larsen et al., 2005).

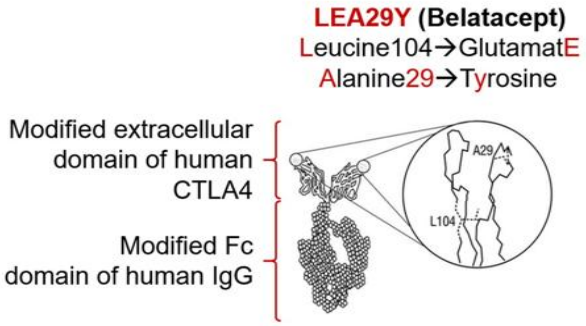


**Fig 9: Structure of LEA29Y** (Latek et al., 2009)

## 8. CAG-LEA29Y pigs as an intra-abdominal heterotopic cardiac allotransplantation model

A genetically modified pig line CAG-LEA29Y has been established which is able to synthesize biologically active LEA29Y that is also known as belatacept (Bähr et al., 2016). Eisenberg, 2014 states that LEA29Y also known as belatacept, is a fusion protein made by combining the extracellular domain of CTLA4 and Fc of IgG1. CTLA4 is an inhibitory receptor located intracellularly in resting T cell and has higher affinity to CD80/CD86 than CD28 on APC thus blocking co-

stimulation pathway of T-cell activation (van der Zwan et al., 2020). The ubiquitous expression of LEA29Y across the porcine organs or tissues and the adequate local transgene expression in the transplantation region protect the organ against rejection by human T-cells (Bähr et al., 2016). Thus, the synthesis of such T cell blocking agents in CAG-LEA29Y pigs supports it as an attractive source of organs for transplantation.

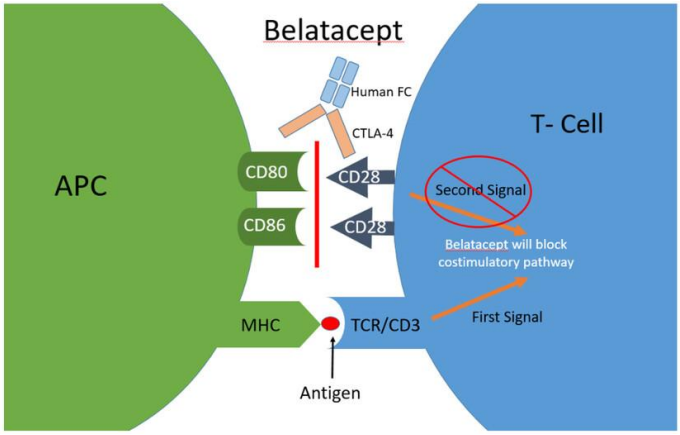


**Fig. 10: Mechanism of action of belatacept / LEA29Y** (adapted from Kidney News 14, 8)

Mendiola Pla et al. developed an intra-abdominal heterotopic cardiac allotransplantation porcine model to establish a robust and replicable approach for long-term graft evaluation. This model facilitates the assessment of therapeutic interventions and immunopathological mechanisms underlying graft rejection. Unlike the orthotopic model, it does not require the allograft to support systemic circulation, making it more advantageous(Kadner et al., 2000). Additionally, the non-functional but metabolically active allograft minimizes systemic side effects of therapeutic delivery(Cullen et al., 2021).

Mendiola Pla et al. emphasized that using pigs as a large animal model for heterotopic abdominal cardiac allotransplantation provides valuable insights into allograft procedures and rejection mechanisms. Since this model does not necessitate maintaining recipient circulation, it allows for prolonged graft survival, enabling researchers to optimize outcomes and mitigate adverse immune responses(Mendiola Pla et al., 2022). The anatomical and physiological similarities between swine and human hearts further support using genetically engineered pigs to address technical challenges in clinical transplantation and

explore tolerance mechanisms in allograft settings(Kenmochi et al., 1994)

Porcine allogeneic heterotopic abdominal cardiac transplantations (HHTx) were performed by Dr. Andrea Bähr (Klinikum rechts der Isar) and Dr. Sebastian Michel (Department of Cardiac Surgery, University Clinic Munich) with the use of wild type (WT) and CAG-LEA29Y pigs. It was performed to understand the graft protection provided by LEA29Y against T cell-mediated rejection. The level of rejection in the immunomodulated heart transplantation setting of the pig model was evaluated with the measure of gene expression of the cytokines and immune cell markers associated with rejection. The clinical outcomes and molecular and histological findings were analyzed with respect to the SLA mismatch among the donor-recipient pair of HHTx.

# III. ANIMALS, MATERIALS AND METHODS

## 1. Animals

In this project, LEA29Y pigs expressing CTLA4-Ig derivative were mated with wildtype pigs (WT) at Chair of Molecular Animal Breeding and Biotechnology, LMU Munich. The offsprings from the breeding, LEA29Y pigs and WT controls were used as heart transplantation model to investigate the success of local T cell co-stimulation blockade in isolated manner. The experiments were carried out at the Center for Innovative Medical Model (CIMM). Only female pigs were subjected as a recipient meanwhile pigs of both sexes were subjected as donors for abdominal allogenic heart transplantation (HHTx) settings. LEA29Y donor heart or WT donor heart was transplantated to WT female recipient in HHTx. The approximate ratio of donor to recipient weight was maintained to 1:3. The animals were fed the commercially available pig meal with enrichment nutrients and provided with surplus amount of water supplied by the tap in the stable.

All the experiments were carried out under the guidance of German Animal Welfare Act and the approval of government of Upper Bavaria (ROB 55.2-2532.Vet_02-16-212)

## 2. Materials

### 2.1. Devices

| | |
|---|---|
| Accu-jet™ pro pipette controller | Brand, Wertheim |
| Analytik Jena US UVP GelStudio Plus | Thermo Fisher Scientific, USA |
| Angiomat Illumena contrast agent pump | Liebel-Flarsheim Company LLC, France |
| RC 400 electric knife | BOWA-electronic GmbH & Co. KG, Gomaringen |
| Autoclav Varioklav 400 | H+P Labortechnik, Oberschleißheim |
| BioMat2 microbiological safety cabinet | Contained Air Solutions, UK |
| Benchtop 96 Tube working rack | Stratagene, USA |
| CardioMessenger Smart | Biotronik, Berlin |

| | |
|---|---|
| CARESCAPE Monitor B450 | GE, USA |
| Centrifuge 5417 | Eppendorf, Hamburg |
| Centrifuge 5424 | Eppendorf, Hamburg |
| Centrifuge 5804 R | Eppendorf, Hamburg |
| Centrifuge 5910 R | Eppendorf, Hamburg |
| Centrifuge Rotina 380 R | Hettich Lab Technology |
| Chyo Petit Balance MK-2000B | YMC CO, Japan |
| CoolCell® container | BioCision, USA |
| Daewoo KOC-154K microwave | Daewoo, South Korea |
| EPIQ 7G Ultrasound machine | Philips, Netherlands |
| FiveEasy pH meter F20 | Mettler-Toledo, USA |
| Grant JB Nova 5 water bath | Grant Instruments Ltd, UK |
| Heating plate with magnetic stirrer RH basic | IKA-Werke, Staufen im Breisgau |
| Heraeus Megafuge 16R | Thermo Fisher Scientific, USA |
| HLC Cooling-ThermoMixer MKR 13 | Ditabis, Pforzheim ino Lab® |
| pH meter 7110 | WTW, Weilheim |
| Labcycler thermocycler | SensoQuest GmbH, Göttingen |
| Laboratory Centrifuge 4-15C | SIGMA-ALDRICH CHEMIE GmbH, Steinheim |
| Lamina flow HB 2448K | Heraeus, Hanau |
| LIFEPAK 20 | Stryker Corporation, USA |
| Light Cycler 96® qPCR | Roche Diagnostics, Switzerland |
| LogiCal® Pressure Transducer | Smiths Medical, Inc, USA |
| Multipipette E3 | Eppendorf, Hamburg |
| Multitip pipette (300 µl) | Eppendorf, Hamburg |

| | |
|---|---|
| MyLab X8 ultrasound machine | Esaote, Italy |
| Neptune ventilator | Medec, Belgium |
| Owl™ gel electrophoresis systems (EasyCast™ B1A and B2mini, A2) | Thermo Fisher Scientific, USA |
| PC-EKG 2000 | EIKEMEYER®, Tuttlingen |
| Pipettes (1000 µl, 200 µl, 20 µl, 10 µl, 2 µl) | Gilson Inc, USA |
| Polymax 2040 shaker | Heidolph Instruments, Schwabach |
| Power Pac 300 gel electrophoresis unit | Bio-Rad Laboratories, Munich |
| Primus Ventilator | Drägerwerk AG & Co. KGaA, Lübeck |
| Rotilabo® mini centrifuge | Carl Roth, Karlsruhe |
| Select Vortexer | Select BioProducts, USA |
| SimpliNano™ spectrophotometer | Biochrom GmbH, Berlin |
| Spectrafuge 24D Microcentrifuge | Labnet International, USA |
| Thermo-Shaker TS-100 | BioSan, Lativa |
| Ultrasound probe P 1-5, P 2-9 | Esaote, Italy |
| Ultrasound probe X5-1 | Philips, Netherlands |
| Ultrasound table | EIKEMEYER®, Tuttlingen |
| Vismo patient monitor | Nihon Kohden, Japan |
| Ziehm Vision RFD mobile C-arm X-ray | Ziehm Imaging, Nuremberg |

## 2.2. Consumables

| | |
|---|---|
| Angiodyn Hahnbank-Baugruppe 3-Fach OFF | B. Braun Melsungen AG, Melsungen |
| Cellstar® serological pipettes (5 ml, 10 ml, 25 ml) | Greiner BioOne, Austria |
| Cellstar® tubes (15 and 50 ml) | Greiner BioOne, Austria |

| | |
|---|---|
| Discofix® Hahnbank | B.Braun Melsungen AG, Melsungen |
| Immuno plates maxisorp C96 | Thermo Fisher Scientific, USA |
| Intrafix® SafeSet | B. Braun Melsungen AG, Melsungen |
| Individual reaction tubes 1.2 ml | STARLAB, Hamburg |
| LogiCal® Pressure Monitoring Kit | Smiths Medical, Inc, USA |
| Microplate U-bottom 96 well | Eppendorf, Hamburg |
| Monocryl™ Plus | Ethicon, Inc., USA |
| Monovette® (K3 EDTA, Serum, Lithium-Heparin Gel+) | Sarstedt AG & Co. KG, Nümbrecht |
| NitriSense nitrile gloves | Süd-Laborbedarf, Gauting |
| Parafilm® M | Carl Roth, Karlsruhe |
| PCR reaction tubes (0.2 ml) | Brand, Wertheim |
| Petri dish 94×16 | Greiner BioOne, Austria |
| Pipette tips | Eppendorf, Hamburg |
| Pipette tips with filter | Greiner BioOne, Austria |
| Pressure transducer | Smiths Medical, Inc, USA |
| Prolene™ 3-0 | Ethicon, Inc., USA |
| Qualitative filter paper | VWR, USA |
| Safe-Lock reaction tubes (1.5 ml, 2 ml | Eppendorf, Hamburg |
| Silk | RESORBA® Medical GmbH, Nuremberg |
| Staple | Henry Schein, Munich |

| | |
|---|---|
| Tesa tape 4541 50 m x 50 mm | Tesa SE, Norderstedt |
| Tesa tape 4651 50 m x 50 mm | Tesa SE, Norderstedt |
| Vasofix® Braunüle® | B. Braun Melsungen AG, Melsungen |

## 2.3. Drugs

| | |
|---|---|
| Adrenaline | InfectoPharm Arzneimittel u. Consilium GmbH, Heppen-heim |
| Amiodarone | Ratiopharm GmbH, Ulm |
| Atropine sulfate | B. Braun Melsungen AG, Melsungen |
| Azaperone | Elanco GmbH, Cuxhaven |
| Cefuroxim 750 mg | Dr. Friedrich Eberth Arzneimittel GmbH, Ursen sollen |
| Fentanyl | Eurovet Animal Health BV, AE Bladel |
| Heparine | B. Braun Melsungen AG, Melsungen |
| KCl | B. Braun Melsungen AG, Melsungen |
| Ketamine | CP-Pharma Handelsgesell-schaft mbH, Burgdorf |
| Magnesiumsulfate 50% | Inresa Arzneimittel GmbH, Freiburg |
| Midazolame 15 mg | Hexal AG, Holzkirchen |
| NaCl | B. Braun Melsungen AG, Melsungen |
| Propofol 20 mg/ml | B. Braun Melsungen AG, Melsungen |

| | |
|---|---|
| Ringer-Lactate | B.BraunMelsungenAG, Melsungen |
| Tauro Lock™ HEP500 | TauroPharm GmbH, Waldbüttelbrunn |

## 2.4. Chemicals and reagents

| | |
|---|---|
| Invitrogen™ TRIzol™ LS Reagent | Invitrogen, USA |
| iPrOH (Isopropanol) | Carl Roth, Karlsruhe |
| Ethanol Rotripuran 99.8% P.a | Carl Roth, Karlsruhe |
| Ethanol puriss 99.8% P.a | Sigma, |
| Ethanol euro 99% 5L | VWR Chemicals, |
| Trichormethane /Chloroform 2.5L-M | Sigma, |
| Universal Agarose | Bio&SELL, Nuremberg |
| Agarose Standard | Carl Roth, |
| dNTP mix (100mM) | Agilent Technologies, USA |
| dNTPs (dATP, dCTP, dGTP, dTTP) | ThermoFisher Scientific, USA |
| EDTA (Ethylenediaminetetraacetic acid) | Carl Roth, Karlsruhe |
| GelRed® Nucleic Acid Gel Stain | Biotium, USA |
| Gene Ruler™ 1kb DNA ladder | ThermoFisher Scientific, USA |
| Bromphenolblue | Carl Roth, Karlsruhe |
| Herculase II Reaction Buffer | Agilent Technologies, USA |
| Q-Solution | Agilent Technologies, USA |
| Sequencing buffer | Applied Biosystems, USA |
| NaOH (Sodium hydroxide 2N) | Roth, Karlsruhe |
| PBS (Phosphate buffered saline) | Sigma Aldrich, USA |

## 2.5. Kits

| | |
|---|---|
| Dneasy Blood and Tissue DNA isolation kit | Qiagen |
| BioSell Double Pure Kombi Kit | Bio&Sell GmbH, Nürnberg |

## 2.6. Enzymes

| | |
|---|---|
| BigDye® Terminator v3.1 | Applied Biosystems, USA |
| Fast Start SYBR® Green Master | Roche, Switzerland |
| Herculase II Fusion DNA Polymerase | Agilent Technologies, USA |
| Proteinase K | Agilent Technologies, USA |
| RNAse A | ThermoFisher Scientific, USA |
| SuperScript$^{TM}$ III Reverse Transcriptase | ThermoFisher Scientific, USA |

## 2.7. Softwares

| | |
|---|---|
| BioEdit Sequence Alignment Editor 7.0.5.3 | Informer Technologies Inc., USA |
| Endnote20 | Clarivate Analytics, UK |
| FinchTV 1.4.0 | Geospiza Inc., USA |
| IBM SPSS Version 29.0 | IBM SPSS Statistics, USA |
| Light Cycler 96® Software 1.1.0.1320 | Roche Diagnostics Internat., Switzerland |
| Microsoft Office 2016 | Microsoft Corporation, USA |
| Prism 10.4.1 | GraphPad Software, USA |
| QuPath 0.5.1 | University of Edinburgh, Scotland |
| RefFinder | East Carolina University, USA |
| Vision Works® Acquisition and Analysis 9.0 | Analytic Jena GmbH, Jena |

## 2.8. Oligonucleotides

| | |
|---|---|
| ABOint7f | 5′-AAT GTC CTT ATG CTG GCC TGG-3′ |
| ABOint7r | 5′-AAC AAC ACA CTC CTG AAC AAC AGA-3′ |
| ABOex8f | 5′-CGC CAG TCC TTC ACC TAC GAA C-3′ |
| ABOex8r | 5′-CGG TTC CGA ATC TCT GCG TG-3′ |
| ACTBf1 | 5′-AGC GCA AGT ACT CCG TGT G-3′ |

| | |
|---|---|
| ACTBr1 | 5′-CGG ACT CAT CGT ACT CCT GCT T-3′ |
| bgA1f | 5′-CTG GAG ACA GCG GAG AAA TAC-3′ |
| bgAO2f | 5′- CCT GTG CTG CTG TTC GTT TC-3′ |
| bgA3f | 5′-TGT CCC CGG AGT ACC TAT GG-3′ |
| bgA4f | 5′-CCC GAC AGA TGA GGA CAA ATA C-3′ |
| bgO1f | 5′-CGG GTC AGT CGT GTT ATG TAT T-3′ |
| bgAO2f | 5′-CCT GTG CTG CTG TTC GTT TC-3′ |
| bgO3f | 5′-GCC TAA GTC TAC CCC TGT GC-3′ |
| bgO4f | 5′-TGA CTT TCT GTG GTC AGC TTA T-3′ |
| bgA1r | 5′-GCT TGC TGG CAC CAA ATA AA-3′ |
| bgA2r | 5′-GCG GAT CAT CTC CAT TCG GT-3′ |
| bgA3r | 5′-GAA AGC AAA GCC ACA GTC GG-3′ |
| bgA4r | 5′-GAG GAG GCT GTC TTC ATG ATT T-3′ |
| bgO1r | 5′-TGT GGT GTA GGT TGC AGA TG-3′ |
| bgO2r | 5′-CAC AAC GAG AAC TCC GGG AA-3′ |
| bgO3r | 5′-GGG AAC TCC AGT GTG TCA GG-3′ |
| bgO4r | 5′-GCA ACC TCA TGG TTC CTA GT-3′ |
| CAGf | 5′-CTC TGC TAA CCA TGT TCA TG-3′ |
| CD45qf4 | 5′-CTG ATG AAC GTG GAG CCT ATC-3′ |
| CD45qr4 | 5′-ACC CTG CAT CTC CGT TTA TAT C-3′ |
| CD68qf1 | 5′-CTC CAA GCC CAG ATT CAG ATT-3′ |
| CD68qr1 | 5′-CAG CCA TGT AGT TCA GGT AGA C-3′ |
| CD172a_q10F | 5′-ATG CAG ACC TGA ACC TGC C-3′ |
| CD172a_q10R | 5′-ATA CTC CGT GTG GTC GTT GG-3′ |
| CD172a_q11F | 5′-TGC TGA CCT GGA TAT GGT GC-3′ |

| | |
|---|---|
| CD172a_q11R | 5′-CAT ACT CCG AGC AGG ATG GC-3′ |
| CYBBf1 | 5′-AGG CAG ACT CAA GGC ATT CAA-3′ |
| CYBBr1 | 5′-GCG CAG ACC CAA GAA GTT TT-3′ |
| FP | 5′-GAG TTC CCC TTG TGG CTC AGT-3′ |
| GAPDHq1f | 5′-CAG AAC ATC ATC CCT GCT TC-3′ |
| GAPDHq1r | 5′-GCT TCA CCA CCT TCT TGA TG-3′ |
| IFNGqf1 | 5′-CAT TCA AAG GAG CAT GGA TGT G-3′ |
| IFNGqr1 | 5′-AGT TTC CCA GAG CTA CCA TTT AG-3′ |
| IFNGqf1 | 5′-GGC CAT TCA AAG GAG CAT GGA-3′ |
| IFNGqr2 | 5′-GAT GGC TTT GCG CTG GAT CT-3′ |
| IFNGqf3 | 5′-TCC AGC GCA AAG CCA TCA G-3′ |
| IFNGqr3 | 5′-CTC TGG CCT TGG AAC ATA GTC T-3′ |
| IFNGqf4 | 5′-GGT TCC TAA ATG GTA GCT CTG G-3′ |
| IFNGqr4 | 5′-CTG ACT TCT CTT CCG CTT TCT TA-3′ |
| IL1aqf3 | 5′-AGC CCA GAT CAG CAA CAT AC-3′ |
| IL1aqr3 | 5′-CAC TGC CTC ATC CAG GTT ATT-3′ |
| IL1Bf2 | 5′-GTC CTC TGT CCT TGG CAC C-3′ |
| IL1Br2 | 5′-GGC ACA CTC ACC CCA AAG AA-3′ |
| IL6qf1 | 5′-ACC GGT CTT GTG GAG TTT CA-3′ |
| IL6qr1 | 5′-ATC TGC ACA GCC TCG ACA TT-3′ |
| IL6qf2 | 5′- TGA GAA AGG AGA TGT GTG AGA AG-3′ |
| IL6qr2 | 5′-TCT CCT GAT TGA ACC CAG ATT G-3′ |
| IL6qf3 | 5′- AGA CGG ATG CTT CCA ATC TG-3′ |
| IL6qr3 | 5′-TCT CAT ACT CTT TCT GGA GGT AGT-3′ |
| IL6qf4 | 5′-GGA GAC CTG CTT GAT GAG AAT C-3′ |

| | |
|---|---|
| IL6qr4 | 5′-CAG CCT CGA CAT TTC CCT TAT-3′ |
| IL6_q10F | 5′-GTG ATG CCA CCT CAG ACA AA-3′ |
| IL6_q10R | 5′-GCC ATT TTT GGA AGG TTC AG-3′ |
| IL6_q11F | 5′-CCA ATC TGG GTT CAA TCA GG-3′ |
| IL6_q11R | 5′-CAG GGT CTG GAT CAG TGC TT-3′ |
| IL6 q12f | 5′-GGA GAC CTG CTT GAT GAG AAT C-3′ |
| IL6 q12r | 5′-TTTC TGG AGG TAG TCC AGG TAT-3′ |
| IL10qf1 | 5′-CGG CGC TGT CAT CAA TTT CT-3′ |
| IL10qr1 | 5′-GAG CTT GCT AAA GGC ACT CTT C-3′ |
| IL10qf2 | 5′-ATC AAG GAG CAC GTG AAC TC-3′ |
| IL10qr2 | 5′-CTT CAT CGT CAT GTA GGC TTC T-3′ |
| IL10qf3 | 5′-GGG AGG ATA TCA AGG AGC ACG-3′ |
| IL10qr3 | 5′-CCC TAG AAT GCT TCA GTT CTT CCT-3′ |
| IL10qf4 | 5′-GTA ATG CCG AAG GCA GAG AG-3′ |
| IL10qr4 | 5′-TCA CAG GGC AGA AAT TGA TGA-3′ |
| IL18f1 | 5′-ACG ATG AAG ACC TGG AAT CGG-3′ |
| IL18r1 | 5′-AAA CAC GGC TTG ATG TCC CT-3′ |
| LEAr | 5′-GGC TTT GTC TTG GCA TTA TG-3′ |
| NLRP3_q10F | 5′-CAA AAA CTG GGG TTG GTG AA-3′ |
| NLRP3_q10R | 5′-GTG CAA CAG TCC CTC ACA GA-3′ |
| O2f | 5′-CCA TGG ATA ATC CTA CCT GCT C-3′ |
| O3f | 5′-TGT TGA GCC ATC TTT GTA TCC C-3′ |
| O2r | 5′-TAG GAA CCA TGA GGT TGC AG-3′ |
| O3r | 5′-CAT GAG GTT GCA GGT TCG AT-3′ |
| O1r | 5′-GTG GTT AAC GAA TCC GAC TAG G-3′ |

| | |
|---|---|
| RP | 5′-TTG CCT AAG TCT ACC CCT GTG C-3′ |
| SRPAqf3 | 5′-CAG GTC CGG AGG AAG TGA AC-3′ |
| SRPAqr3 | 5′-ACC CTC ACT CTT GAG TCC CA-3′ |
| SLA13_f1 | 5′-GAC TCC GAG GCT GAG GAT CA-3′ |
| SLA123_r1 | 5′-CGC TTC TTC CTC CAG ATC ACA A-3′ |
| SLA123_r2 | 5′-ACG AGA ACC AGG CCA ACA AT-3′ |
| SLA1_f1 | 5′-CTC CAC CCA CCC GGC TCT GCT-3′ |
| SLA1_r1 | 5′-CTC ACA CTC TAG GAC CCT TGG TA-3′ |
| SLA1_f2 | 5′-AGG CTG AGG ATC ATG GGG CCT G-3′ |
| SLA1_r2 | 5′-GCA GTT GTC TCA CAC TCT AGG AC-3′ |
| SLA1_q1R | 5′-GCT GCC AGG TCA GGG AGA T-3′ |
| SLA1_q2F | 5′-GAT GAG GCG GAG CAG TG-3′ |
| SLA1_q2R | 5′-GGG TCA CAT GTG TCT TTG GA-3′ |
| SLA1_q3F | 5′-GAG CTA CCT GCA GGG CCT-3′ |
| SLA1_q3R | 5′-GCT GCC AGG TCA GGG AGA T-3′ |
| SLA1_q4F | 5′-AGC TAC CTG CAG GGC CT-3′ |
| SLA1_q4R | 5′-GGC GGG TCA CAT GTG TCT TT-3′ |
| SLA1 fx 1 | 5′-ACG ACG GCG CCG ATT ACA TC-3′ |
| SLA2_f1 | 5′-CCC TCA AGC CAT CCT CAT TCT-3′ |
| SLA2_r1 | 5′-CGT GAA CAA ATC TGT GTC ACT-3′ |
| SLA2_f2 | 5′-GAC ACA GAA TCT CCG CAG ATT-3′ |
| SLA2_r2 | 5′-GCT CAT AGG GAC ACA GAC ACA T-3′ |
| SLA 2_f3 | 5′-ATC TCC GCA GAT TCC AAA GAT G-3′ |
| SLA2_q1F | 5′-CGA TGT GGC GGA GCA GGA-3′ |
| SLA2_q1R | 5′-CAT GTG TCT TTG GAG GCT CTG-3′ |

| | |
|---|---|
| SLA2_q2R | 5′-GTC TCC ACC AGC TCC ATG TC-3′ |
| SLA2_q3F | 5′-GAG CTA CCT GGA GGG CAC-3′ |
| SLA2_q3R | 5′-CATGTGTCTTTGGAGGCTCTG-3′ |
| SLA2 fx1 | 5′-GGC TGC TAC TTG GGA CCA GA-3′ |
| SLA2 fx 2 | 5′-CTT CTA CCC TAA GGA GAT CTC CCT-3′ |
| SLA2 fx 3 | 5′-GCT GGA GTT GTG ATC TGG AGG AAG-3′ |
| SLA3_f1 | 5′-GGA CCC TGG CCC TGA CTG GTA C-3′ |
| SLA3_r1 | 5′-CAC ACT CTA GGA TCC TTG GTG AG-3′ |
| SLA3_f2 | 5′-CTC TCC ATC CAT TCG CCT CGA-3′ |
| SLA3_r2 | 5′-CCT TGG TGA GGG ACA CAT GAG-3′ |
| SLA3_q1F | 5′-GAT GCG GCG GAG CAA AT-3′ |
| SLA3_q1R | 5′-CAT GTG TCT TTG GAG GCT CTG-3′ |
| SLA3_q2F | 5′-CGA TGC GGC GGA GCA AAT-3′ |
| SLA3_q2R | 5′-GTC TCC ACC AGC TCC ATG TC-3′ |
| SLA3_q3F | 5′-GCT ACC TGG AGG GCG C-3′ |
| SLA3_q3R | 5′-ACA TGT GTC TTT GGA GGC TCT G-3′ |
| SLA3_q4F | 5′-AAG CTA CCT GGA GGG CGC-3′ |
| SLA3_q4R | 5′-TGT GTC TTT GGA GGC TCT GC-3′ |
| SLA3-r3 | 5′-CCT TGG TGA GGG ACA CAT CAG-3′ |
| SLA3 fx 1 | 5′-AGC AGG AGG GGC AGG AGT-3′ |
| SLA3 fx 2 | 5′-ATT ACA TCG CCC TGA ACG AGG-3′ |
| SLA3 rx1 | 5′-GTA GCT CTG CTC CTC TCC AGG-3′ |
| SLA DRB1_f1 | 5′-ACA CCC CAC CGC ATT TC-3′ |
| SLA DRB1_r1 | 5′-AGA GCA GAC CAG GAG GTT-3′ |
| SLA DRB1_f2 | 5′-GTG CTG AGC CCT CCC TTG-3′ |

| | |
|---|---|
| SLA DRB1_r2 | 5′-GTA GAA CCC GGT CAC AGA GC-3′ |
| SLA DRB1_f3 | 5′-GGA CAC CCC ACC GCA TTT-3′ |
| SLA DRB1_r3 | 5′-ACA GAG CAG ACC AGG AGG TT-3′ |
| SLA DQA_f1 | 5′-GCC TGT GGA GGT GAA GAC AT-3′ |
| SLA DQA_r1 | 5′-ACA GAG TGC CCG TTC TTC AA-3′ |
| SLA DQA _f2 | 5′-GTG GAG GTG AAG ACA TTG CG-3′ |
| SLA DQA _r2 | 5′-GAC AGA GTG CCC GTT CTT CA-3′ |
| SLA DQA _r3 | 5′-GAG TGC CCG TTC TTC AAC CA-3′ |
| SLA DQB_f1 | 5′-ATG TCT GGG ATG GTG GCT CTG-3′ |
| SLA DQB_r1 | 5′-AGA TTC ATC TCT AGC ATC AC-3′ |
| SLA DQB _f2 | 5′-CCT TGA CGG TGA TGC TGG T-3′ |
| SLA DQB _r2 | 5′-TCT GCC TTG GAT GGG GAG AT-3′ |
| SLA DQB_f3 | 5′-CTT TGG ACA GCG GCC TTG A-3′ |
| SLA DQB _r3 | 5′-TCT GCC TTG GAT GGG GAG A-3′ |
| TBPf | 5′-GAT GGA CGT TCG GTT TAG G-3′ |
| TBPr | 5′-AGC AGC ACA GTA CGA GCA A-3′ |
| TGFB1f3 | 5′-CCT GGG CTG GAA GTG GAT TC-3′ |
| TGFB1r3 | 5′-CCG GGT TGT GCT GGT TGT A-3′ |
| TNFf2 | 5′-CCC CTT GAG CAT CAA CCC TC-3′ |
| TNFr2 | 5′-ATT GGC ATA CCC ACT CTG CC-3′ |
| YWHAZr | 5′-GCA TTA TTA GCG TGC TGT CTT-3′ |
| YWHAZf | 5′-ATG CAA CCA ACA CAT CCT ATC-3′ |

# 3. Methods

## 3.1. Animal Experiments

### 3.1.1. Genotyping of experimental animals

In order to select the correct animals for the experimental groups, offspring from LEA29Y x WT matings were genotyped for the presence of the LEA29Y transgene. Genomic DNA was isolated from biopies from ear, taken shortly after birth, using the DNeasy® Blood Tissue Kit (Qiagen) following the manufacturer´s instructions. The concentration of extracted DNA was measured in a spectrophotometer to equilibrate it to 20 ng/µl and used as template for genotyping PCRs. Previously identified DNA of WT and LEA29Y pigs served as controls. The established primers CAGf and LEAr for specific transgene detection were mixed with the other reagents to a volume of 20 µl on ice in 0.2 ml reaction tubes. For a non- template control, master mix was left without DNA. The compositions of the master mix as well as the cycler protocol can be found in Tab. 1, 2, 3 and 4. To check the presence and size of the PCR product, electrophoresis on 1% (1 g Agarose/ 100 ml 1x TAE buffer) agarose gel was subsequently performed. 2.5 µl of a 1:250 mixture of GelRed® and bromophenol blue was added to the samples before pipetting these and 6 µl of GeneRuler™ DNA ladder into the gel slots. The electrophoresis chamber was filled with 1x TAE buffer and connected to an electrical voltage. The resulting DNA fragments could then be visualized under UV light as bands.

| Reagent | Amount (µl) |
|---|---|
| $H_2O$ | 14 |
| 10 × Buffer | 2 |
| dNTP (2mM) | 2 |
| CAGf | 0.4 |
| LEAr | 0.4 |
| HST-TAQ | 0.2 |
| Template | 1 |
| Total | 20 |

**Tab. 1: Master mix of PCR for genotyping**

| Step | Temperature | Duration | Repetitions |
|---|---|---|---|
| Denaturation | 95°C | 5 min | |
| Denaturation | 94°C | 30s | 35x |
| Annealing | 56°C | 30s | |
| Elongation | 72°C | 45s | |
| Final Elongation | 72°C | 5min | |
| Termination | 4°C | 5min | |

**Tab. 2: Cycler protocol for PCR for genotyping**

| Reagent | Amount (µl) |
|---|---|
| H2O | 13.7 |
| 10 × Buffer | 2 |
| dNTP (2mM) | 2 |
| GGTA22f | 0.3 |
| GGTA21r | 0.3 |
| neopf | 0.5 |
| HST-TAQ | 0.2 |
| Template | 1 |
| Total | 20 |

**Tab. 3 : Master mix for PCR for genotyping**

| Step | Temperature | Duration | Repetitions |
|---|---|---|---|
| Denaturation | 95°C | 5 min | |
| Denaturation | 95°C | 30s | 40x |
| Annealing | 60°C | 30s | |
| Elongation | 72°C | 1min | |
| Final Elongation | 72°C | 10min | |
| Termination | 4°C | 5min | |

**Tab. 4 : Cycler protocol for PCR for genotyping**

### 3.1.2. Experimental Setup and groups

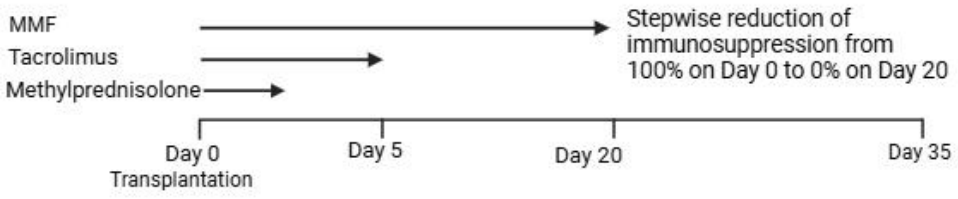


**Fig. 11: Additional immuno-suppression applied to transplanted recipients and gradually phased out**

Methylprednisolone was intravenously supplied to the animal via a vein catheter in the ear and locked by TauroLock™. Tacrolimus capsules were hidden in food and bananas, and double gloves were worn to ensure the provider did not come in contact

with the tacrolimus. The MMF was provided by mixing it with a very small volume of juice and feed.

CAG-LEA29 donor animals and WT recipient animals were utilized for the experiments. Three WT and three LEA animals were used as controls. The clinical outcomes of the transplantations are summarized in Tab. 5.

| Donor | Recipient | Number of experiments | Outcome |
|---|---|---|---|
| WT | WT | 5 | Rejection |
| LEA29Y | WT | 1 | Intraoperative technical failure |
| LEA29Y | WT | 3 | Postoperative technical failure |
| LEA29Y | WT | 5 | Rejection |
| LEA29Y | WT | 3 | Survival |

**Tab. 5: Clinical outcomes of the heterotopic abdominal heart transplantation**

Despite having the initial number of LEA29Y-WT transplantations as 16, five of these LEA29Y-WT transplantations, i.e., 10431, 12921, 12951, 11826 and 10898, were not incorporated in the processing of the sample and the study, as these animals died either during the experiment or died due to technical failure after transplantation or the quality of the cDNA was not satisfactory even after multiple trails. Thus, five WT-WT transplants, eleven LEA29Y-WT transplants, three WT, and three LEA29Y control animals' samples were processed and analyzed.

### 3.1.3. Anesthesia

The pigs for the surgeries were fasted overnight for 12 hours before sedating. Pigs were sedated intramuscularly with Ketamine and Azaperone at the rate of 20 mg/kg and 0.02 mg/kg, respectively. An intravenous bolus of Propofol was administered at the rate of 2mg/kg via the ear vein catheterization placed in the ear vein of the sedated pig. The endotracheal tube was inserted into the trachea and connected to a volume-controlled ventilator (Dräger; Medec) to maintain the ventilation. The animal was infused with Ringer's lactate, Gelafundin 4%, and glucose. The animal was continuously anesthetized by infusion of propofol and Fentanyl at the rate of 10 mg/kg/h and 4µg/kg/hr, respectively. The physiological parameters were monitored by pulse oximeter and invasive blood pressure measurement (CARESCAPE Monitor, GE; Vismo Monitor, Nihon Kohden) during the entire intervention.

### 3.1.4. Porcine Heterotopic Heart Transplantation

Heterotopic abdominal heart transplantation (HHTx) with a two-anastomosis system was performed where a graft from a donor was coupled parallelly in the abdomen to the recipient's heart. HHTx of LEA29Y and wildtype control hearts was performed into German landrace wildtype recipients, with the vena cava inferior anastomosed to the pulmonary artery and the aorta connected to the bulbous aortic of the graft (Langendorff-mode).

#### 3.1.4.1. Explanation of the heart from the donor

After the medial thoracotomy of the donor animal, a purse string was positioned in the ascending aorta to place the cardioplegia cannula. The animal was heparinized at the rate of 500 IU/kg in order to prevent any blood clots. Immediately, the pharmacological arrest of the heart was initiated by a retrograde aortic infusion of ice-cold cardioplegic solution (CUSTODIOL). The cardioplegic solution, which has potassium citrate with high concentration, prevents any action potential conductivity, thus assisting in diastolic cardiac arrest. After cardiectomy, the donor heart was placed in cardioplegic solution for preservation until transplantation.

#### 3.1.4.2. Implantation of the heart into the abdomen of the recipient

The recipient was prepared with a midline incision on the abdomen. The inferior vena cava and the abdominal aorta were exposed. The heart of the donor was placed in the abdomen of the recipient, and the ascending aorta from the donor was anastomosed with the recipient's abdominal aorta, inferior vena cava of the recipient was anastomosed with the pulmonary artery of the donor as shown in Fig. 12. The sutures were checked for bleeding from the anastomosis and the abdomen was closed again.

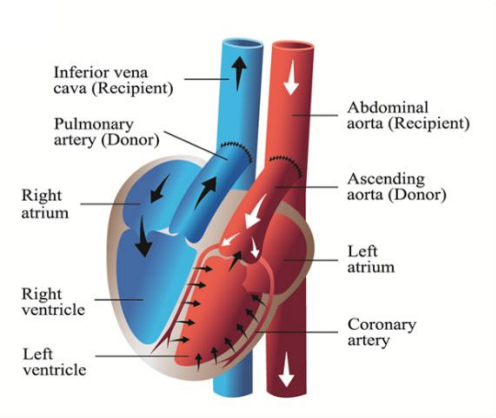


**Fig. 12: Vessel anastomoses in unloaded heterotopic abdominal heart transplantation** (adapted from Mohiuddin et al., 2015)

### 3.1.5. Perioperative treatment and immunosuppression

The immunosuppressive regimen included methylprednisolone (Urbasone), Mycophenolate mofetil (MMF/Cellcept), and Tacrolimus. The methylprednisolone was intravenously supplied to the animal via a vein catheter in the ear on day zero and day one at the dosage of 250mg and 125mg, respectively. Tacrolimus was fed at the rate of 0.2mg/kg until day five, and the capsules were hidden in food and bananas by wearing double gloves to ensure that the provider did not come in contact with the tacrolimus. The MMF was medicated at the dose of a twice daily dose of 20mg/kg orally and was provided by mixing it with a very small volume of juice and feeding until day 20. The protocol for immunosuppression was followed as mentioned in Tab. 6.

| Medication | Dose | Mode | Days |
|---|---|---|---|
| Methylprednisolone (Urbasone) | 250mg | Intravenous | Day 0 |
| | 125mg | Intravenous | Day 1 |
| Tacrolimus | 0.2mg/kg | Oral | Day 0-5 |
| Mycophenolate (MMF) | 2x20mg/kg | Oral | Day 0-20 |

**Tab. 6: Dose of medication and regime after the transplantation**

Gradual waning of the pharmacological immunosuppression with corticosteroids, tacrolimus, and MMF over the time of 21 days was applied to test self-sufficient graft protection by LEA29Y. The clinical outcomes of the HHTx are summarized in Tab. 7.

| Donor | Recipient | Number of experiments | Outcome |
|---|---|---|---|
| WT | WT | 5 | Rejection |
| LEA29Y | WT | 1 | Intraoperative technical failure |
| LEA29Y | WT | 3 | Postoperative technical failure |
| LEA29Y | WT | 5 | Rejection |
| LEA29Y | WT | 3 | Survival |
| | | | |

**Tab. 7: Clinical outcomes of the heterotopic abdominal heart transplantation**

### 3.1.6. Euthanasia, tissue collection and storing

At the end of the experiment, the animals were euthanized with 60ml of potassium chloride (KCl) intracardially after inducing the animal into deep anesthesia with fentanyl and propofol. The transplanted heart from the abdomen region was immediately explanted. The heart was weighed, and systemic tissue sampling was performed, as described below. The left atrium, left ventricle, right atrium, and ventricle were sliced into 5x5 mm squares and immediately placed for snap-freezing on aluminum foil over dry ice. These slices were later stored at -80°C. Three non-transplanted wild type (WT) and three non-transplanted CAG-LEA29Y (LEA) animals were euthanized and sampled as a negative control.

The right atrium, right ventricle, left atrium, left ventricle, liver, and spleen from seventeen transplanted animals and six control animals were collected.

## 3.2. Histological analysis

The tissue of each transplant pig's left and right ventricles was examined histologically and graded for the level of rejection of the heart tissues. Hematoxylin and eosin staining were performed to gain knowledge of the graft's rejection level in the transplanted heart by the time of explantation. The histological images were described via the standards of the International Society for Heart and Lung Transplantation (Stewart et al., 2005).

### 3.2.1. Tissue fixation and slice preparation

The tissue samples after the euthanasia were instantly shifted to a 4% formalin solution. The samples were then fixed for 24-32 hours and later were processed in the Excelsior AS as shown in Tab. 8.

| Procedure | Reagent | Time |
|---|---|---|
| Dehydration | EtOH 70%<br>EtOH 90%<br>EtOH 90%<br>EtOH 100% | 2 x 1.5 h<br>1.5 h<br>1 h<br>2 x 1 h |
| Intermedium | Xylol | 3 x 1 h |
| Infiltration | Paraffin<br>Paraffin | 2 x 1.75 h<br>2 h |

**Tab. 8: Tissue embedding in Excelsior AS**

For further paraffin embedding, the TES 99 embedding system was used to cut the samples into 1 μm thick paraffin sections using Microm HM 325 microtome by Mr. Maximilian Moraw. Later the sections were mounted on Star Frost® slices and stored at 37°C until staining. Almost all of the LEA29Y transplanted animals' tissue slices used for histological analysis were already fixed and prepared by Mr. Max Moraw.

### 3.2.2. Hematoxylin and Eosin Staining (HE Staining)

The HHTx samples were processed with the protocol displayed in Tab. 9.

| Procedure | Reagent | Time |
|---|---|---|
| Deparaffination | Xylene | 20 min |
| Rehydration | 2x EtOH 100%<br>2x EtOH 96%<br>EtOH 70% | 2 min each |
| Staining | Mayer´s Hemalum | 5 min |
| Rinsing | Floating warm tap water | 4 min |
| Differentiation | 0.5% HCl- EtOH | Dip 1-3 times, briefly |
| Rinsing | Floating warm tap water | 5 min |
| Counterstaining | 1% Eosin | 2 min |
| Washing | Aqua bidest. | 2 min |
| Dehydration | EtOH 70%<br>2x EtOH 96%<br>2x EtOH 100% | 2 min each |
| Clearing | Ascending alcohol series,<br>Xylene | 5 min |
| Mounting | Histokit | Cover with histokit |

**Tab. 9: Standard protocol for HE staining**

### 3.2.3. Analysis of HE staining

The HE stainings for the LA and RV were done for five WT-WT transplantations, eleven LEA29Y-WT transplantations, three WT controls, and three LEA29Y controls. LEA29Y transplantation animals were done with the assistance of Ms Heinke Heymer (Klinikum rechts der Isar, Technical University of Munich, Germany). The pictures of the stained slides were processed at the Institute for Veterinary Pathology (LMU Munich, Germany). The processing and analysis of images was done with the help of QuPath 0.5.1 (University of Edinburgh, Scotland).

The images were described via the standards by the International Society for Heart and Lung Transplantation as shown in Fig. 13. (Stewart et al., 2005). The infiltration of immune cells is described as shown in Tab. 10.

| Grade of rejection | Description |
|---|---|
| Grade 0 R[a] | No rejection |
| Grade 1 R, mild | 1 focal region of damage of myocyte, either with interstitial or perivascular immune cell infiltration |
| Grade 2 R, moderate | Region of damage of myocyte associated with either two or more infiltration foci of immune cells |
| Grade 3 R, severe | Diffused infiltration of immune cells with myocyte damage in a multifocal pattern can also be associated together with hemorrhage, edema and vasculitis |

**Tab. 10: ISHLT Standardized Cardiac Biopsy Grading** (Stewart et al., 2005)

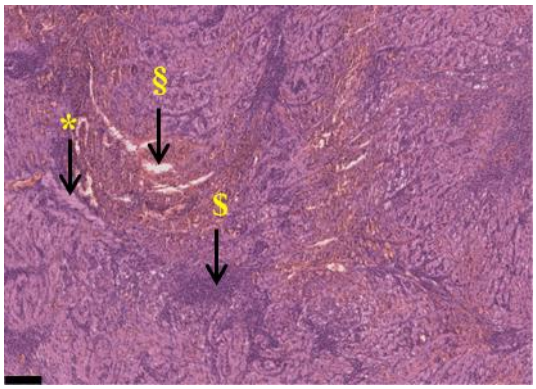


**Fig. 13: Representative sample for grading of rejection of HE stained slices on QuPath.** Examples of interstitial edema (asterisk), myocardial fibrosis (#) and foci of immune cell infiltration ($) are indicated.

### 3.3. Molecular analysis of gene expression

Transcript analysis of the HHTx graft samples was conducted to study the cellular and molecular responses of the graft donor transgenic animal and the immune responses from the recipient animal. The study and analysis of the cellular and molecular responses are essential for the long-term use of LEA29Y to regulate T cell-mediated rejection. The study of cytokine patterns assists in differentiating a non-rejected graft from a rejected one. Also, monitoring and evaluation of cytokines and cell markers expression during immune response directs the adjustment of immunosuppressive regiments and understanding the immune mechanism for graft rejection. The production of cytokines is fundamentally regulated transcriptionally. So, the assessment of cytokines' and cell markers' mRNA expression was conducted using real-time quantitative PCR (RT-PCR).

#### 3.3.1. Powderization

The samples at -80° were transferred in dry ice. The 2-liter styrofoam box was filled in half with liquid nitrogen, and a steel base and hammer were placed to cool in liquid nitrogen. The mortar and pestle were also placed in liquid nitrogen in a styrofoam box. The tissue samples were wrapped in frozen aluminum foils, placed in the steel base, and hit by a hammer until the tissue samples were crushed. The crushed tissue samples were transferred to a mortar pestle and further crushed into fine powder. The powder was then transferred to the 2ml Eppendorf tubes. The right atrium, right ventricle, left atrium, left ventricle, liver, and spleen from the transplanted animals were pulverized, so there was a total of 138 processed for pulverization.

#### 3.3.2. RNA extraction

RNA was extracted using TRIzol™ Reagent from the frozen left atrium, left ventricle, right atrium, right ventricle, spleen and liver samples. 138 samples were processed for RNA extraction as right atrium, right ventricle, left atrium and left ventricle, liver and spleen were processed from seventeen transplantion and six control animals.

##### 3.3.2.1. Homogenization and separation of phases

The RNA was extracted from the pulverized tissue by using TRIzol™ method. 50-100mg of tissue was mixed in 1 ml TRIzol™ and homogenized using a tissue homogenizer. The homogenizer lysted the tissue at the rate of 15000 rpm

(revolutions per minute). After the homogenization, the supernatant was transferred to a new tube and allowed for dissociation for five minutes. 0.2 ml of choloroform was added to the 1ml of supernatant and thoroughly mixed by shaking and then incubated for 2-3 minutes. The mixture was centrifuged at 12,000 x g for 15 minutes. The mixture was separated into a lower phenol-cholroform, an interphase and colourless upper aqueous phase with RNA as demonstrated in Fig. 14. The aqueous phase lying over was transferred to new tube by angling the tube at 45°.

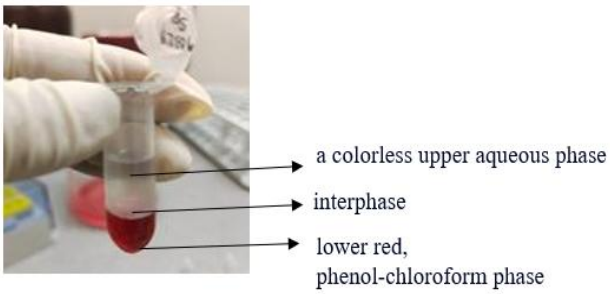


**Fig. 14: Trizol method for RNA extraction**

### 3.3.2.2. Precipitation

For the precipitation of the proteins, 0.5 ml of isopropanol is added to the aqueous phase for every 1 ml of TRIzol™ Reagent, and the mixture is strongly vortexed for the precipitation. The mixture is centrifuged at 4°C at 12000 x g to form a white-gel-like pellet at the bottom of the tube. The supernatant is discarded.

### 3.3.2.3. Washing of RNA

Afterward, we resuspended the white-gel-like pellet with 75 % ethanol for every 1 ml of TRIzol™. As per the protocol, the RNA could be stored at -20°C for one year or at least for one week at 4°C or can be further processed for RNA extraction. The mixture is slightly vortexed and centrifuged for 7500 x g at 4°C, the supernatant is discarded with a micropipette, and the RNA is air-dried for 5-10 minutes.

### 3.3.2.4. Solubilise the RNA

The RNase-free water is heated on a heat block at 55°C-60°C for 10-15 minutes. The RNA is resuspended in 20-50 μL of RNase-free water by pipetting up and down.

### 3.3.2.5. Quantitation and storage of isolated RNA

The quality and concentration of the synthesized RNA were examined using SimpliNano™ spectrophotometer (Biochrom GmbH, Berlin). The nanodrop functions on the principle of ultraviolet-visible spectrum (US-Vis) absorbance. 1µl of the RNA was pipetted into the well of Nanodrop. The concentration and A260/A280 ratio were acquired. RNA samples with an A260/A280 ratio reading of 1.9-2 passed the quality assurance test and, hence, were selected for further processing. The RNA samples with a concentration greater than 200ng/µl were further diluted with RNase-free water and stored in 1.5-2ml tubes at -80°C.

### 3.3.3. Reverse transcription/ cDNA synthesis

The diluted RNA was reverse-transcripted to cDNA using SuperScript™ Reverse Transcriptase from Thermofisher. 5 µl of the 200ng/µl RNA was used as a starting material for cDNA synthesis, so 1000ng of RNA was used as a standard amount for cDNA synthesis.

| | |
|---|---|
| RNA | 5 µl |
| DNase, RNase-free | 1.5 µl |
| DNase-buffer | 1.5 µl |
| $H_2O$ | 7 µl |
| Total volume | 15 µl |

**Tab. 11: Mixture for DNA digestion for cDNA synthesis**

The mixture of RNA, DNase, DNase buffer, and $H_2O$ were incubated at 37°C on a thermoshaker for 30 minutes for DNA digestion, as shown in Tab. 11. After the incubation, 1µl 50Mm EDTA was added to destroy the leftover DNase. The mixture is afterward incubated at 65°C for 30 minutes. The total volume of 16µl of the mixture was allocated as 12µl for cDNA synthesis, and the remaining 4µl was isolated to use as a control specifically to check any genomic DNA contamination. The following master mixture was prepared.

| | |
|---|---|
| dNTP | 1µl |
| Oligo dT | 1µl |

**Tab. 12: Mixture for cDNA synthesis**

2µl of the master mixture as shown in Tab. 12 was added to the 12µl of mixture allocated for cDNA preparation and incubated at 65°C for 5 minutes. The aliquots were immediately transferred on ice. A reverse-transcriptase mixture (RT-mix) was prepared as mentioned in Tab. 13.

| | |
|---|---|
| 5x buffer | 4 µl |
| DTT | 1 µl |
| SuperScript™ III Reverse Transcriptase | 1 µl |
| Total | 6 µl |

**Tab. 13: Master mixture for reverse transcription for cDNA synthesis**

6 µl RT-mix demonstrated in Tab. 13 was pipetted and mixed properly into the aliquot with the mixture of cDNA preparation, and this mixture with reverse transcriptase was incubated at 50°C for 1 hour and again incubated at 70°C for 15 minutes. Thus, the cDNA formed was stored at -20°C.

### 3.3.4. Quality check of samples

All the cDNAs were further tested for quality check by using real-time PCR. The quality cDNA sample was diluted into 5 different dilutions: 1:50, 1:100, 1:200, 1:400, and 1:800. The first dilution, 1:50, was freshly prepared, and other dilutions, 1:100, 1:200, 1:400, and 1:800 were consecutively made by serial dilutions. The composition of the master-mix is demonstrated in Tab. 14.

| Reagent | Amount |
|---|---|
| SYBR green | 6.25 µl |
| UNG | 0.075 µl |
| GAPqf1 (10 µM) | 0.3 µl |
| GAPqr1 (10 µM) | 0.3 µl |
| $H_2O$ | 3.075 µl |
| Template | 2.5 µl |
| Total | 12.5 µl |

**Tab. 14: Master mixture for quality check of cDNA**

The 10µl of the master mix was pipetted into the well of a 96-well plate. 2.5 µl of each dilution, i.e., 1:50, 1:100, 1:200, 1:400, and 1:800 cDNA dilutions, were consecutively pipetted into the wells in the rows. Each dilution was duplicated to prevent any errors. The 96-well plate was run in the real-time PCR machine at 63°C for 45 cycles. After the RT-PCR, the data regarding the amplification curve, standard curve, and Cq values were extracted. The Cq value of consecutive lower dilution was expected to be one cycle behind. If the slope and $R^2$ values of the sample were approximately around -3.2 and 0.99-1, the cDNA passed the quality test for the sample. The cDNA that did not pass the quality check was discarded, and the synthesis was repeated for the particular sample.

### 3.3.5. Primers design and optimization

The immune panel set up by by Florian Jaudas (Chair of Molecular Animal

Breeding and Biotechnology, LMU) and Miquel Cambra (Klinikum rechts der Isar, TUM), was again observed and checked for optimization. The optimization was done at different concentrations of primers and temperatures. The NCBI database designed and checked new primers for more immune panels.

#### 3.3.5.1 CYBB

Cytochrome B-245 beta chain (CYBB/ NOX2/ gp91-phox) is a cell marker that is a component of transmembrane ion transporter, which allows the oxidation of nicotinamide adenine dinucleotide phosphate (NADPH) to produce superoxide (Bassoy et al., 2021). Oxidative stress is developed by generating reactive oxygen species (ROS). Stimulation of the Tcell receptor (TCR) influences the production of a phagocytic NADPH (Jackson et al., 2004). The presence of foreign grafts is responsible for stimulating phagocytic cells and neutrophils. NAPDH oxidase regulates the phagocytic activity of immune cells and causes the burst in phagocytes and the destruction of foreign grafts.

#### 3.3.5.2. CD68

CD68, also known as lysosomal-associated membrane protein (LAMP), is a transmembrane glycosylated protein cell marker, primarily confined in endosomes and lysosomes (Gottfried et al., 2008). CD68 is highly expressed by monocytes and macrophages and thus plays a critical role in phagocytosis and allograft rejection (Zhang et al., 2022).

#### 3.3.5.3. CD45

Protein tyrosine phosphatase receptor type (PTPRC/CD45) is a transmembrane gatekeeper glycoprotein and a cell marker commonly expressed on the surface of hematopoietic and immunological cells except for non-nucleated erythrocytes (Ye et al., 2022). Rheinlander described CD45 as Leukocyte common antigen (Rheinländer et al., 2018). CD45 modulates the response to the survival of the graft as it regulates the endurance of lymphocytic cells, response via cytokines, and signalling of T-cell receptor(TCR) to the graft (Saunders & Johnson, 2010; Tchilian & Beverley, 2006). CD45 activates Src family kinase assisting T cell in detecting and responding to antigen/foreign graft. Meanwhile, presence of low-affinity antigen influences CD45 to have a suppressive role on TCR, thus standardizing graded signaling and sieving out weak signals(Courtney et al., 2019).

#### 3.3.5.4. IL1A

Interleukin-1 alpha (IL1A) is member of IL1 family. Neutrophils and macrophages manufacture IL1A. It is a powerful pro-inflammatory cytokine as it stimulates other inflammation-related genes. IL1A derived from the transplanted graft promotes T-cell mediated immunity and increases the recruitment of T-cell, thus activating the innate immune system against the transplanted graft.

#### 3.3.5.5. IL1B

Interleukin-1 beta (IL1B) is another pro-inflammatory cytokine member of IL1. This cytokine is synthesized by natural killer (NK) cells, neutrophils and macrophages. Cardiac allografts showed a remarkable amount of IL1B in comparison to controls (Seto et al., 2010). During the early phase of rejection, IL1B has a role switch on the synthesis of adhesion molecules from endothelial cells, thus assisting the adhesion of mononuclear adhesion and leakage (Hoffmann et al., 1993).

#### 3.3.5.6. IL18

Interleukin18 (IL18) is one of the proinflammatory cytokines from the IL1 family. IL18 is synthesized by dendritic cells and macrophages. Natural killer cells are stimulated by IL18 (Nakanishi, 2018). T helper 1 cell (Th1) and T helper 2 cell (Th2) mediated immunity are stimulated as a result of the production of IL18 (Zeiser et al., 2007).

#### 3.3.5.7. TGFB

TGFB is responsible for signaling T-cells during allotransplantation. TGFB has a role in recruiting leukocytes to the regions of injury in case of cell-mediated allotransplant rejection, whereas, in chronic rejection, TGFB elevates proteins.

#### 3.3.5.8. TNFA

TNFA is an essential pro-inflammatory cytokine and has a big role in innate immunity. Lymphocytes and macrophages synthesize TNFA. TNFA is a molecule responsible for the co-stimulation of T-cells and amplifies T-cell receptor (TCR) dependent activation of CD4+ and CD8+ (Mehta et al., 2018).

#### 3.3.5.9. IL6

Interleukin 6 is a member of the IL6 family. IL6 triggers endothelial cells to

enhance damage to the vascular endothelium and aggravate damage to the graft (Berger et al., 2024). It also stimulates T-cell activation and aids in the development and differentiation of T helper cells to assist in inflammation and rejection (Mehta et al., 2018). A pro-inflammatory condition is created in allografts by IL6 to encourage T-cell-mediated rejection (Jordan et al., 2017).

#### 3.3.5.10. IL10

IL10 is an anti-inflammatory cytokine produced by monocytes. IL10 suppresses T cell-mediated rejection and contributes to graft tolerance in transplantation.

#### 3.3.5.11. IFNG

Interferon-gamma (IFNG) blocks the formation of thrombi and prevents congestion and necrosis from maintaining the viability of the graft during acute rejection, whereas during chronic rejection, IFNG causes injury to the graft. It mostly activates the major histocompatibility complex (MHC) expression to elevate the antigenicity and reject the graft.

The panel for housekeeping genes and the immune panel for heart are tabulated in Tab. 15 and 16.

| | |
|---|---|
| GAPDH | GAPf1 / GAPqr1 |
| ACTB | ACTBf1 / ACTBr1 |
| TBP | TBPf / TBPr |
| YWHAZ | YWHAZf / YWHAZr |

**Tab. 15: Panel for housekeeping genes**

| | |
|---|---|
| IL1A | IL1Aqf3 / IL1Aqr3 |
| IL1B | IL1Bf2 / IL1Br2 |
| IL18 | IL18f1 / IL18r1 |
| TNFA | TNFAf2 / TNFAr2 |
| TGFB | TGFBf3 / TGFBr3 |
| CYBB | CYBBf1 / CYBBr1 |
| NLRP3 | NLRP3f2 / NLRP3r2 |
| CD45 | CD45qf4 / CD45qr3 |
| CD68 | CD68qf1 / CD68qr1 |
| CD172A | SRPAQRf3 / SRPAQR3 |
| IL6 | IL6f1 / IL6r1 |
| IL10 | IL10f1 / IL10r1 |
| IFNG | IFNGf3 / IFNGR3 |

**Tab. 16: Immune panel for heart**

### 3.3.6. Q-PCR

The cDNA samples of the left ventricle (LV), left atrium (LA), right ventricle (RA), and right atrium (RA) from five WT-WT transplantation animals, eleven LEA29Y- WT animals, three WT control animals, and three WT control animals were opted for running immune panel assays for 11 genes and four housekeeping genes. 92 samples from these animals were utilized to operate the immune panel assays. The Master Mix (MM) of each gene was prepared depending on the optimized conditions and are demonstrated in Tab. 17 to 31.

| Reagent | Amount |
|---|---|
| SYBR green | 6.25 |
| UNG | 0.075 |
| GAPqf1 (10 µM) | 0.3 |
| GAPr1 (10 µM) | 0.3 |
| $H_2O$ | 3.075 |
| Template | 2.5 |
| MM-x-fold | |

**Tab. 17: Master Mix for GAPDH**

| Reagent | Amount |
|---|---|
| SYBR green | 6.25 |
| UNG | 0.075 |
| ACTBf1 (10 µM) | 0.5 |
| ACTBr1 (10 µM) | 0.5 |
| $H_2O$ | 2.675 |
| Template | 2.5 |
| MM-x-fold | |

**Tab. 18: Master Mix for ACTB**

| Reagent | Amount |
|---|---|
| SYBR green | 6.25 |
| UNG | 0.075 |
| YWHAZf (10 µM) | 0.3 |
| YWHAZr (10 µM) | 0.3 |
| $H_2O$ | 3.075 |
| Template | 2.5 |
| MM-x-fold | |

**Tab. 19: Master Mix for YWHAZ**

| Reagent | Amount |
|---|---|
| SYBR green | 6.25 |
| UNG | 0.075 |
| TBPf (10 µM) | 0.7 |
| TBPr (10 µM) | 0.7 |
| $H_2O$ | 2.275 |
| Template | 2.5 |
| MM-x-fold | |

**Tab. 20: Master Mix for TBP**

| Reagent | Amount |
|---|---|
| SYBR green | 6.25 |
| UNG | 0.075 |
| CYBBf1 (10 µM) | 0.3 |
| CYBBr1 (10 µM) | 0.3 |
| $H_2O$ | 3.075 |
| Template | 2.5 |
| MM-x-fold | |

**Tab. 21: Master Mix for CYBB**

| Reagent | Amount |
|---|---|
| SYBR green | 6.25 |
| UNG | 0.075 |
| CD68qf1(10 µM) | 0.5 |
| CD68qr1(10 µM) | 0.5 |
| $H_2O$ | 2.675 |
| Template | 2.5 |
| MM-x-fold | |

**Tab. 22: Master Mix for CD68**

| Reagent | Amount |
|---|---|
| SYBR green | 6.25 |
| UNG | 0.075 |
| IL1Aqf3 (10 µM) | 0.7 |
| IL1Aqr3 (10 µM) | 0.7 |
| $H_2O$ | 2.275 |
| Template | 2.5 |
| MM-x-fold | |

**Tab. 23: Master Mix for IL1A**

| Reagent | Amount |
|---|---|
| SYBR green | 6.25 |
| UNG | 0.075 |
| IL18f1 (10 µM) | 0.7 |
| IL18r1 (10 µM) | 0.7 |
| $H_2O$ | 2.275 |
| Template | 2.5 |
| MM-x-fold | |

**Tab. 24: Master Mix for IL18**

| Reagent | Amount |
|---|---|
| SYBR green | 6.25 |
| UNG | 0.075 |
| IL6f (10 µM) | 0.3 |
| IL6r (10 µM) | 0.3 |
| $H_2O$ | 3.075 |
| Template | 2.5 |
| MM-x-fold | |

**Tab. 25: Master Mix for IL6**

| Reagent | Amount |
|---|---|
| SYBR green | 6.25 |
| UNG | 0.075 |
| IL10f (10 µM) | 0.5 |
| IL10r (10 µM) | 0.5 |
| $H_2O$ | 2.675 |
| Template | 2.5 |
| MM-x-fold | |

**Tab. 26: Master Mix for IL10**

| Reagent | Amount |
|---|---|
| SYBR green | 6.25 |
| UNG | 0.075 |
| IL1Bf2 (10 µM) | 0.3 |
| IL1Br2 (10 µM) | 0.3 |
| $H_2O$ | 3.075 |
| Template | 2.5 |
| MM-x-fold | |

**Tab. 27: Master Mix for IL1B**

| Reagent | Amount |
|---|---|
| SYBR green | 6.25 |
| UNG | 0.075 |
| TGFB1f3 (10 µM) | 0.5 |
| TGFB1r3 (10 µM) | 0.5 |
| $H_2O$ | 2.675 |
| Template | 2.5 |
| MM-x-fold | |

**Tab. 28: Master Mix for TGFB**

| Reagent | Amount |
|---|---|
| SYBR green | 6.25 |
| UNG | 0.075 |
| TNFAf2 (10 µM) | 1.5 |
| TNFAr2 (10 µM) | 0.7 |
| $H_2O$ | 1.475 |
| Template | 2.5 |
| MM-x-fold | |

**Tab. 29: Master Mix for TNFA**

| Reagent | Amount |
|---|---|
| SYBR green | 6.25 |
| UNG | 0.075 |
| IFNG (10 µM) | 0.5 |
| IFNG (10 µM) | 0.5 |
| $H_2O$ | 2.675 |
| Template | 2.5 |
| MM-x-fold | |

**Tab. 30: Master Mix for IFNG**

| Reagent | Amount |
|---|---|
| SYBR green | 6.25 |
| UNG | 0.075 |
| CD45qf4 (10 µM) | 0.5 |
| CD45qr3 (10 µM) | 0.5 |
| $H_2O$ | 2.675 |
| Template | 2.5 |
| MM-x-fold | |

**Tab. 31: Master Mix for CD45**

Each sample was diluted in the concentration 1:200. Each dilution was pipetted into duplicate wells along 96 well plates. The RT-PCR was done using Light Cycler 96® (Roche Diagnostic, Switzerland). The annealing temperature for each of the genes from the immune panel was adjusted as per the optimized annealing temperature for 40 cycles.

### 3.3.7. Analysis of the gene expression of transplanted hearts

Left atrium (LA), left ventricle (LV), right atrium (RA), and right ventricle (RV) from five WT-WT transplantations, eleven LEA29Y-WT transplantations as well as three WT and three LEA29Y nontransplanted hearts were analyzed. Though, initially, 16 LEA29Y-WT transplants were performed, five transplantation animals, 10431, 12921, 12951, 11826 and 10898 were not incorporated in the study as the animals either died during the experiment or died due to technical failure or the standard quality of cDNA was not attained even after multiple synthesis. Four samples from each animal were assimilated from each animal were analyzed for the study.

The primary data from qPCR, quantification cycle (Cq), or threshold cycle (Ct) was received via Light Cycler 96® Software 1.1.0.1320 (Roche Diagnostics Internat., Switzerland). MS Excel was used to normalize the Cq values of the gene. The stability of housekeeping genes was analyzed with Reffinder. Housekeeping genes TBP and GAPDH were comparatively more stable than YWHAZ and

ACTB (Fig. 15). Therefore, TBP and GAPDH were used to normalize the transplantation values' Cq values.

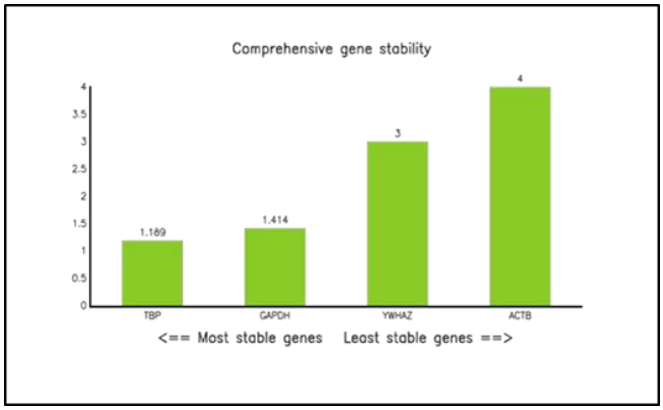


**Fig. 15: Stability check of housekeeping genes**

The normalized data from the MS-Excel were plotted in Prism 10 (GraphPad Software, USA) to demonstrate the gene expression of the cytokines and cell markers in the graft's LA, LV, RA, and RV from the transplanted animals.

### 3.3.8. Statistical analysis

An unpaired two-tailed T-test was performed in IBM SPSS Statistics Version 29.0 (USA) for statistical analysis. The effects were considered significant at $p < 0.05$ (*), highly significant at $p < 0.01$ (**), or significant at $p < 0.001$ (***).

## 3.4. Molecular analysis for Swine Leukocyte Antigen (SLA) typing

SLA is a highly polygenic and polymorphic cluster of pig genes that codes the glycoproteins on the cell surface as an essential entity for adaptive immunity for self-recognition. SLA-matching between the donor and the recipient has a critical and dominant role in the success of transplantation. The mismatches of the SLA alleles trigger both antibody-mediated and cellular rejection. SLA matching between the donor and the recipient is essential to ensure minimum graft rejection.

### 3.4.1. Design of primer

The SLA1, SLA2 and SLA3 primers were designed using Primer3Plus, NCBI, and IDT oligoanalyzer™ Tool as shown in Fig. 16. The primer design was focused on exon 2 and exon 3 for SLA class I genes and exon 2 for SLA class II genes. The polymorphism in these genes is crucial for studying graft rejection in transplantation.

Each SLA gene has variants, so the primer design had to be done so that the primer did not fall in the polymorphic region or specific position with SNP. Therefore, the frame for primer designing was very small and also the different variants of the gene had to be taken into consideration while designing the primers.

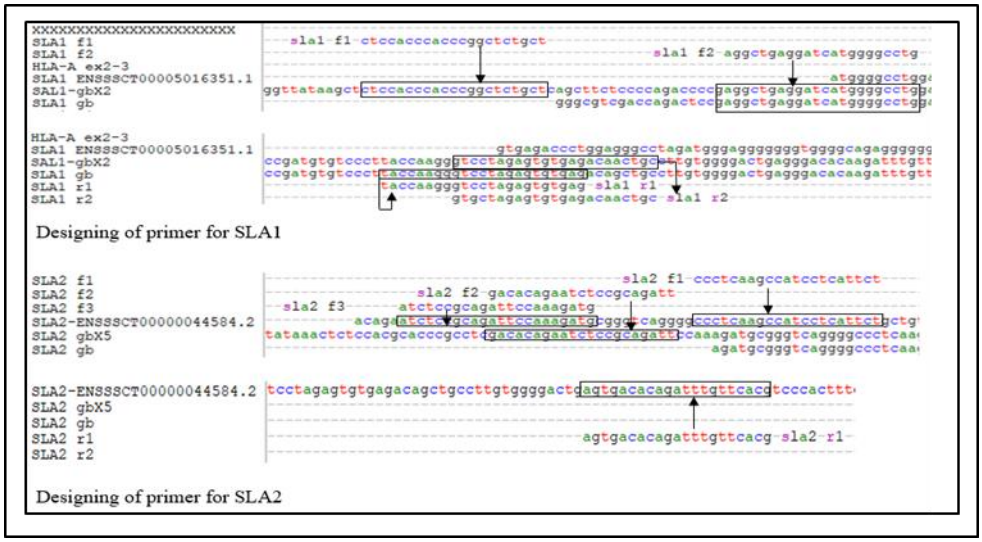


**Fig. 16: Primer designing for SLA class I**

Three different primer pairs were designed for the three classical SLA class I loci (SLA1, SLA2 and SLA3) and SLA class II loci (SLA DRB1, SLA DQA, SLA DQB). The primer combinations for SLA typing had to amplify all the alleles of

the three classical SLA class I loci (SLA1, SLA3, SLA2) and the three classical SLA class II loci (DQB1, DRB1, DQA).

### 3.4.2. Designing of inner primers

For locating the overall SNPs in exon 2-3 in SLA class I gene (SLA1, SLA2 and SLA3), the forward and the reverse primers were not enough to have a clean chromatograph of the targeted sequence. Therefore, inner primers were designed as demonstrated in Fig. 17. The use of inner primers aided in for sequencing the target exon in the gene.

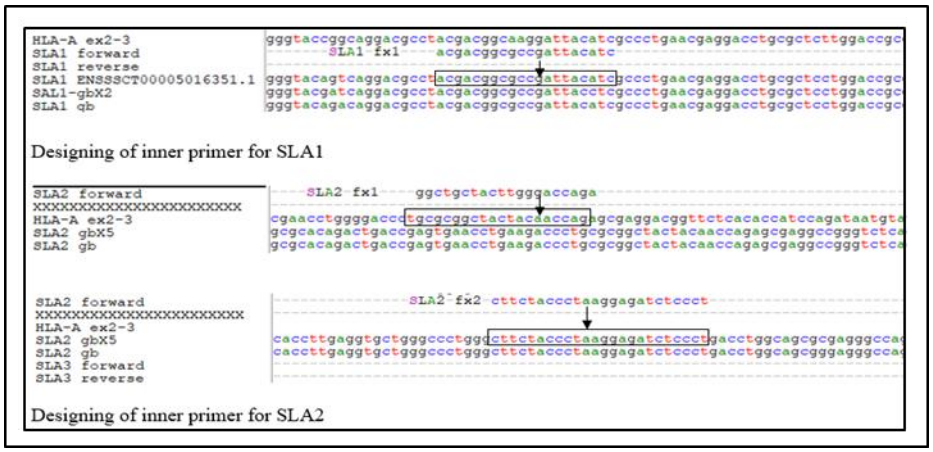


**Fig. 17: Primer designing for inner primer for SLA class I**

### 3.4.3. Selection and optimization of primer combination

After the identification of the primer pairs, the primer pairs were subsequently processed for end-point PCR. The cDNA used for optimizing the SLA-typing was diluted to 1:10. For the PCR reactions, master Mix (MM) was prepared on ice as demonstrated in Tab. 32 and 33. The cycler protocol can be found in Tab. 34 and 35 and 36.

| Reagent | Amount |
|---|---|
| $H_2O$ | 14 µl |
| Q-solution | 4 µl |
| 5x buffer | 2 µl |
| Dntp | 2 µl |
| Forward primer | 0.4 µl |
| Reverse primer | 0.4 µl |
| Hercules | 0.2 µl |
| Template | 1 µl |
| Total | 25 µl |

**Tab. 32: Master mix of PCR fo SLA class I**

| Reagent | Amount |
|---|---|
| $H_2O$ | 11.5 µl |
| Q-solution | 4 µl |
| 5x buffer | 5 µl |
| dNTP | 2.5 µl |
| Forward primer | 0.4 µl |
| Reverse primer | 0.4 µl |
| Hercules | 0.2 µl |
| Template | 1 µl |
| Total | 25 µl |

**Tab. 33: Master mix of PCR for SLA class II**

| Step | Temperature | Duration | Repetitions |
|---|---|---|---|
| Denaturation | 95°C | 5 min | |
| Denaturation | 94°C | 30s | 35x |
| Annealing | 63°C | 30s | |
| Elongation | 72°C | 1min 30s | |
| Final Elongation | 72°C | 5min | |
| Termination | 4°C | 5min | |

**Tab. 34: Cycler Protocol for PCR for SLA1 from SLA class I**

| Step | Temperature | Duration | Repetitions |
|---|---|---|---|
| Denaturation | 95°C | 5 min | |
| Denaturation | 94°C | 30s | 35x |
| Annealing | 61°C | 30s | |
| Elongation | 72°C | 1min 30s | |
| Final Elongation | 72°C | 5min | |
| Termination | 4°C | 5min | |

**Tab. 35: Cycler Protocol for PCR for SLA2 from SLA class I**

| Step | Temperature | Duration | Repetitions |
|---|---|---|---|
| Denaturation | 95°C | 5 min | |
| Denaturation | 94°C | 30s | 35x |
| Annealing | 60°C | 30s | |
| Elongation | 72°C | 45s | |
| Final Elongation | 72°C | 5min | |
| Termination | 4°C | 5min | |

**Tab. 36: Cycler Protocol for PCR for SLA class II** (SLA_DRB1, SLA_DQA, SLA_DQB1)

Gel electrophoresis for PCR products was performed in 2% (w/v) agarose, 1X TAE with a voltage of 80-120 Volts for 30-45 minutes. The primer pair combinations that generated clear, positive signals on PCR gel-based visualization demonstrating successful target amplification were selected for further optimization.

The experimental design for optimization included multiple combinations of annealing temperatures and elongation time. The fine-tuning of the PCR processes

explores the numerous PCR parameters. During the optimization, we needed to evaluate the diverse reaction conditions that could provide a clean chromatograph sequence of the target exon we were interested in. Thus, the PCRs for SLA class I and SLA class II were optimized as in Tab. 34, 35 and 36.

### 3.4.4. PCR-gel cleanup

After the PCR and gel electrophoresis were performed, the PCR gel was excised to place the slices in 1.5ml of the reaction tubes and subsequently processed for nucleic acid purification. The PCR-gel cleanup was done with the Bio and Sell Double Pure Kombi kit.

Each gel slice not more than 300 mg was incubated at 50$^{o}$C with 650 µl of Gel Solubilizer for 10 minutes on a shaking thermal platform. The samples were alternately vortexed 3-4 times during the period of incubation. 50 µl of Binding Optimizer was pipetted into the suspension and mixed by vortexing. The suspension was applied to the spin filter loaded over a 2ml receiver tube, closed, and centrifuged at 11,000 x g (approximately 11,000 rpm) for 1 minute. The filtrate was discarded, but the spin filter was reused to load 700 µl of Washing Solution MT, closed, and centrifuged at 11,000 x g for 1 minute. Again, the same process was repeated after discarding the filtrate. Afterward, to eliminate the traces of ethanol, the tube was centrifuged for 2 minutes at the maximum speed. The spin filter was placed back into a new 1.5 ml elution tube, and 10-20 µl of elution buffer (pre-warmed at 50°C) was added, incubated for 2 minutes at room temperature, and centrifuged at 11,000 x g for 1 minute. The quality and concentration of the DNA were examined using SimpliNano™ spectrophotometer (Biochrom GmbH, Berlin). The DNAs were then stored at 4$^{o}$C-8$^{o}$C.

### 3.4.5. Sequencing cycle

The preparation of mastermix and the cycler protocol for the sequencing cycle were performed as shown in Tab. 37 and 38.

| Reagent | Amount |
|---|---|
| 5x sequencing buffer | 4 µl |
| Big dye | 1 µl |
| Forward primer | 1 µl |
| $H_2O$ | 2 µl |
| template | 2 µl |

**Tab. 37: Master mix for sequencing reaction**

| | | | |
|---|---|---|---|
| Denaturation | 95°C | 1 min | |
| Denaturation | 95°C | 5s | 40 x |
| Annealing | 54°C | 10s | |
| Elongation | 60°C | 4 min | |
| Termination | 4°C | 5 min | |

**Tab. 38: Cycler protocol for sequencing**

### 3.4.6. Clean

125mM of EDTA was prepared (0.5ml+3ml distilled water). 2.5 µl of 125mM was added to the cap of samples to be sequenced and briefly spinned. 30 µl of 100% ethanol was pipetted into new 1.5 ml tubes, and all the contents from the PCR tubes were pipetted into the 1.5 ml tubes. The mixture was incubated on ice for 15 minutes and centrifuged at 13,000 rpm for 30 minutes at 4°C. While centrifuging, the hinged cap was placed facing outside the centrifuge so that the pellet could form towards the wall of the tube. The supernatant was removed and the pellet was resuspended in 150 µl of 70% ethanol after brief vortexing. Further centrifugation was done at 13,000 rpm for 2.5 minutes. The supernatant was again removed and allowed to dry with the lid open for 6 minutes. Afterward, 20 µl of H2O was added, briefly shaken, spun down, and transferred to the plate.

Once all the samples were loaded on the plate, 10 µl of formamide was added on top before sending sample for the run for base sequence determination.

### 3.4.7. Run

The samples were afterwards sequenced at Sequencing Service of LMU Biozentrum, Martinsreid.

### 3.4.8. Analysis of sequences of transplanted animal

The SLA profiling of the donor and recipient animal of the heterotopic abdominal heart transplantation experiments was conducted to assess the immunological compatibility between the graft donor and recipient. The differences and the

variability between the donor and the recipient could potentially have triggered a rejection response to the transplanted graft. The refined, optimized protocols for SLA profiling of SLA class I (SLA-1 and SLA-2) and SLA class II (SLA-DRB1, SLA-DQA, SLA-DQB) were implemented for both the donor and the recipient. The protocols targeted the amplification of exon 2-3 for SLA class I and exon 2 for SLA class II genes to locate the SNP.

The cDNA of the donor animals' left ventricle (LV) samples of the donor animals' spleen and liver samples were utilized as a sample source for the donor and recipient animals, respectively, for SLA profiling. The cDNA of LV from the donor and cDNA of the spleen and liver from the recipient were amplified with the refined PCR protocols for SLA class I and SLA class II profiling. Gel electrophoresis was conducted in 2% (w/v) agarose, and the bands were excised. The PCR-gel cleanup was done with the Bio and Sell Double Pure Kombi kit. The cleanup product was further processed for sequencing. The final sequencing was done at the Sequencing Service of LMU Biozentrum, Martinsreid. The sequencing chromatograph acquired from the LMU Biozentrum was displayed using Flinch TV 1.4.0 (Geospiza Inc., USA). The SLA1, SLA2, SLA-DRB1, SLA-DQA, and SLA-DQB sequences from all the optimized primer combinations were arranged and aligned along with Bioedit. Exon 2-3 for SLA1, SLA2, and exon 2 for SLA-DRB1, SLA-DQA, and SLA-DQB were traced in the aligned sequences. The sequences of graft donor and recipient animals from the experiments were compared to locate the SNP along the position of exon 2-3 in SLA1 and SLA2 and exon 2 in SLA-DRB1, SLA-DQA, and SLA-DQB. A comprehensive list was compiled, chronologically locating the precise locus of all the SNPs between each combination of donor and recipient animals from the experiments. The loci having SNPs were nomenclatured using the IUPAC standard protocol for nucleic acids as shown in Tab. 39.

| Symbol | Translation |
|---|---|
| R | A+G |
| Y | C+T |
| M | A+C |
| K | G+T |
| S | C+G |
| W | A+T |

**Tab. 39: IUPAC code for nucleic acid specification** (Johnson, 2010)

The codons from the incorporating SNPs in exon 2 and 3 in SLA1 and SLA2 and exon 2 in SLA-DRB1, SLA-DQB, and SLA-DQA were individually translated to amino acids (codon chart). The amino acid variation due to the presence of SNPs in specific locations was compiled in a table. After the clear amino acid variations between donor and recipient, the interaction between the amino acids was scored. The scoring was done was performed based on Tab. 40.

| Animal | Amino acid | Score of the interaction |
|---|---|---|
| Donor | A/A | 0 |
| Recipient | A/B | |

| Animal | Amino acid | Score of the interaction |
|---|---|---|
| Donor | A/B | 1 |
| Recipient | A/A | |

| Animal | Amino acid | Score of the interaction |
|---|---|---|
| Donor | A/A | 0 |
| Recipient | A/A | |

| Animal | Amino acid | Score of the interaction |
|---|---|---|
| Donor | A/A | 1 |
| Recipient | B/B | |

**Tab. 40: Scoring for interactions between amino acids**

The interaction between the donor and recipient amino acids was scored based on amino acids presented from the donor to the recipient. In the case of allelic expression of amino acid A/A by the donor and A/B by the recipient, the donor expresses the amino acid A while the recipient expresses amino acids A and B. Amino acid A from the donor was not foreign to the recipient, which expresses

amino acid A simultaneously along with amino acid B. Thus, the interaction between donor and recipient was scored 0. In the case of allelic expression of amino acid A/B by the donor and A/A by the recipient, the donor expresses the amino acids A and B. In contrast, the recipient expresses amino acid A. Amino acid B from the donor was foreign to the recipient, so the interaction between donor and recipient was scored as 1. Similarly, there was no foreign amino acid from donor to recipient in the allelic expression of amino acid A/A by both donor and recipient, so the interaction was scored as 0. However, in the allelic expression of A/A by the donor and B/B by the recipient, the amino acid A expressed by the donor is foreign to the recipient so the interaction is scored as 1. The cumulative score of the impact of the interaction between the donor and the recipient's amino acids due to variations in SLA1, SLA2, SLA-DRB1, SLA-DQA, and SLA-DQA was summed up.

The cumulative scoring of the amino acid interaction between donor-recipient pairs was plotted in the bar graph along with the degree of rejection of graft. The graphs were plotted for each of the SLA gene, i.e., SLA1, SLA2, SLA-DRB1, SLA-DQA, SLA-DQB1 and cumultative score of the 5 genes.

# IV. RESULTS

## 1. Heterotopic abdominal heart transplantation model

### 1.1. Breeding Program

Donor and recipient animals were produced by conventional breeding using LEA29Y transgenic pigs and unrelated WT mating partner at Center of Innovative Medical Models. In total, for the project, 14 LEA29Y litters were produced with a total number 38 offsprings (Tab. 41). 14 animals showed LEA29Y genotype (Fig. 18). From these animals, 19 were used as donors and 19 animals as recipients (Tab. 41).

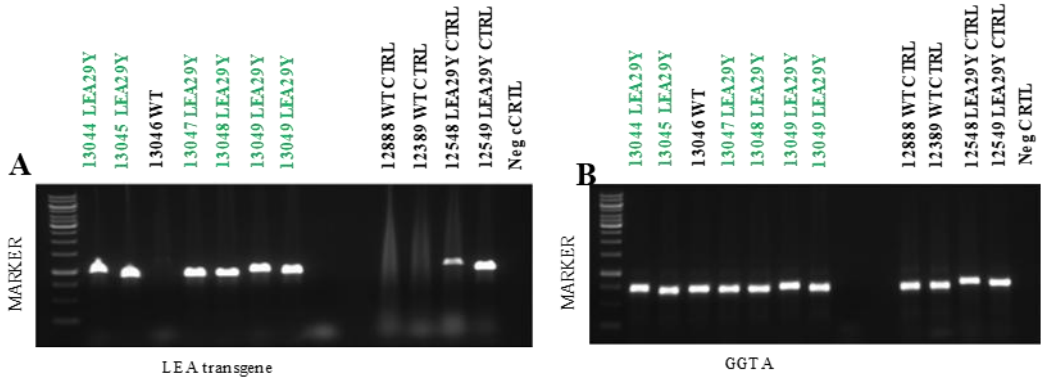


**Fig. 18: Genotyping of LEA29Y litters. Genomic DNA of all offspring was used in end-point PCR with primers specific for the LEA29Y transgene** (A) and primers for the GGTA gene to check for DNA quality (B). Verified WT and LEA29Y samples from previous litters were used as controls. LEA29Y-transgenic animals are highlighted in green.

**Tab. 41 : Breeding of experimental animals.**

| Sow | Boar | Parturition date | Total piglets | LEA29Y | Donor | Recipient |
|---|---|---|---|---|---|---|
| 12095 WT | 11452 LEA29Y | 1.07.2022 | 6 | 5 | 13044(LEA29Y) 13045(LEA29Y) | 0 |
| 10190 WT | 10147 LEA29Y | 31.10.2019 | 13 | 8 | 10702(LEA29Y) 10708(LEA29Y) 10704(LEA29Y) | 0 |
| 10082 WT | 10147 LEA29Y | 22.06.2019 | 6 | 4 | 10518(LEA29Y) 10519(LEA29Y) 10520(LEA29Y) | 0 |
| 10077 WT | 10147 LEA29Y | 21.03.2020 | 11 | 5 | 10963(LEA29Y) 10964(LEA29Y) 10965(LEA29Y) | |
| 135 WT | 10957 LEA29Y | 14.05.2021 | 13 | 8 | 11873(LEA29Y) 11871(LEA29Y) 11868(LEA29Y) 11875(WT) | |
| 68 WT | 10047 IndCas9 | 2.02.2019 | 10 | | | 10323(WT) 10324(WT) 10325(WT) |
| 10082 WT | 10110 CAG-Irfp | 29.01.2019 | 13 | | | 10297 (WT) |
| 10131 WT | 10090 WT | 29.03.2019 | 5 | | 10373(WT) 10374(WT) 10372(WT) | |
| 43 WT | 10105 CAG- Irfp | 26.03.2019 | 14 | | 10358(WT) | |
| 10006 WT | 10131 WT | 19.05.2019 | 10 | | | 10432(WT) 10434(WT) 10437(WT) |
| 10129 C94Y | 10182 WT | 30.08.2019 | 5 | | | 10566(WT) |
| 10007 WT | 10136 INsGFP#2760 | 8.09.2019 | 10 | | | 10574(WT) 10577(WT) |
| 10331 DMD+/- | 10131 WT | 28.01.2020 | 14 | | | 10884(WT) |
| 10311 CFTR+/- | 10306 CFTR+/- | 20.02.2020 | 9 | | | 10896(WT) 10898(WT) |
| 140 WT | 10957 LEA29Y | 12.04.2021 | 8 | | | 11823(WT) 11824(WT) 11827(WT) 11826(WT) |
| 11810 PLN | 10771 WT | 9.04.2022 | 11 | | | 12921(WT) |
| 11628 GHR+/- | 11626 GHR+/- | 27.04.2022 | 6 | | | 12951(WT) |

### 1.2. Summary of the total heterotopic abdominal heart transplantation

A total number of 16 transplantation experiments was performed by Dr. Andrea Bähr and team (Tab. 42). This included the transplantation of eleven LEA29Y transgenic hearts and five WT hearts. According to standard operating protocol, a follow-up of up to five weeks was performed with additional immunosuppression given for the majority of the period. In all cases, the last two weeks of follow up were without additional immunosupresison to investigate the protective capacity of LEA29Y expression on the graft. For details of the immunosuppression protocol, see Material and Methods (Fig. 11)

**Tab. 42: Experimental animals use in HHTx**

| Recipient | Donor | Date of transplantation |
|---|---|---|
| 10323 (WT) | 10373 (WT) | 6.05.2019 |
| 10324 (WT) | 10374 (WT) | 07.05.2019 |
| 10325 (WT) | 10358 (WT) | 13.05.2019 |
| 10297 (WT) | 10372 (WT) | 14.05.2019 |
| 11827 (WT) | 11875 (WT) | 01.07.2021 |
| 10432 (WT) | 10518 (CAG-LEA29Y) | 28.08.2019 |
| 10434 (WT) | 10519 (CAG-LEA29Y) | 02.09.2019 |
| 10437 (WT) | 10520 (CAG-LEA29Y) | 03.09.2019 |
| 10566 (WT) | 10702 (CAG-LEA29Y) | 19.11.2019 |
| 10574 (WT) | 10708 (CAG-LEA29Y) | 20.11.2019 |
| 10577 (WT) | 10704 (CAG-LEA29Y) | 22.11.2019 |
| 10884 (WT) | 10963 (CAG-LEA29Y) | 04.05.2020 |
| 10896 (WT) | 10964 (CAG-LEA29Y) | 05.05.2020 |
| 11823 (WT) | 11873 (CAG-LEA29Y) | 02.07.2021 |
| 11824 (WT) | 11871 (CAG-LEA29Y) | 29.06.2021 |
| 12917 (WT) | 13044 (CAG-LEA29Y) | 13.07.2022 |

We observed heterogeneous clinical outcomes trajectories across the study cohort of HHTx. All of the five WT transplants were completely rejected. Meanwhile, LEA29Y transplants demonstrated considerable clinical outcomes variability, where eight of these transplants were rejected, while three of these transplants, i.e., 10434, 10884, and 10896, survived by the time of explantation. 10434, explanted on the 32nd day after transplantation, was still beating during the time of explantation. 10884, explanted on the 30th day, was initially beating

independently after implantation, but during the time of explantation, it was slightly beating with hardened and inelastic ventricular thickening without hemorrhages. 10886 was initially beating independently after implantation, while during the time of explantation, it had minimal movement in the heart with a coarse-elastic and enlarged appearance with hemorrhages.

**Tab. 43: Clinical outcomes in HHTx**

| Donor | Recipient | Number of experiments | Outcome |
|---|---|---|---|
| WT | WT | 5 | Rejection |
| LEA29Y | WT | 1 | Intraoperative technical failure |
| LEA29Y | WT | 3 | Postoperative technical failure |
| LEA29Y | WT | 5 | Rejection |
| LEA29Y | WT | 3 | Survival |

After the euthanasia, the transplanted cardiac graft was explanted and systematic tissue sampling was conducted. The left atrium, left ventricle, right atrium and right ventricle from the transplanted graft heart were sectioned into 5 x 5mm specimens, which were immediately snap-frozen on aluminium foil placed over dry ice and subsequently stored at -80°C. These tissue samples were deployed for qPCR for the analysis of gene expression profiles of the immune panels for rejection in the transplanted cardiac grafts.

The tissues samples for tissue fixation were instantly shifted to a 4% formalin solution, fixed for 24-32 hours and later processed in Excelsior AS. For detailed process of tissue fixation and slice preparation, see materials and methods (Tab. 8). These samples were employed for histological analysis for grading of rejection of transplanted graft.

The snap frozen liver and spleen samples from the recipients from HHTx as well as LA, LV, RA, RV from the donor animals were utilized for assessment of swine leukocyte antigen (SLA) mismatching.

## 2. Local histological assessment

The tissue of each transplant pig's left and right ventricles was examined histologically and graded for the level of rejection of the heart tissues. Hematoxylin and eosin staining were performed to gain knowledge of the graft's rejection level in the transplanted heart by the time of explantation. The histological images were described via the standards of the International Society for Heart and Lung Transplantation (Stewart et al., 2005).

### 2.1. Rejection grading

Rejection grading was done by HE stainings of fixed tissue, according to the ISHLT Standard Cardiac Biopsy Grading (Stewart et al., 2005).

**Tab. 44: Grading of rejection of transplanted hearts**.

| | Sample number | Degree of rejection |
|---|---|---|
| WT-WT transplants | 10323 LV | 3R |
| | 10324 LV | 3R |
| | 10325 LV | 3R |
| | 10297 LV | 3R |
| | 11827 LV | 2R |
| LEA-WT non-survival transplants | 10432 LV | 3R |
| | 10437 LV | 3R |
| | 10566 LV | 3R |
| | 10577 LV | 3R |
| | 11824 LV | 3R |
| | 11823 LV | 3R |
| | 12917 LV | 3R |
| | 10574 LV | 1R |
| LEA-WT survival transplants | 10886 LV | 1R |
| | 10884 LV | 1R |
| | 10434 LV | 1R |

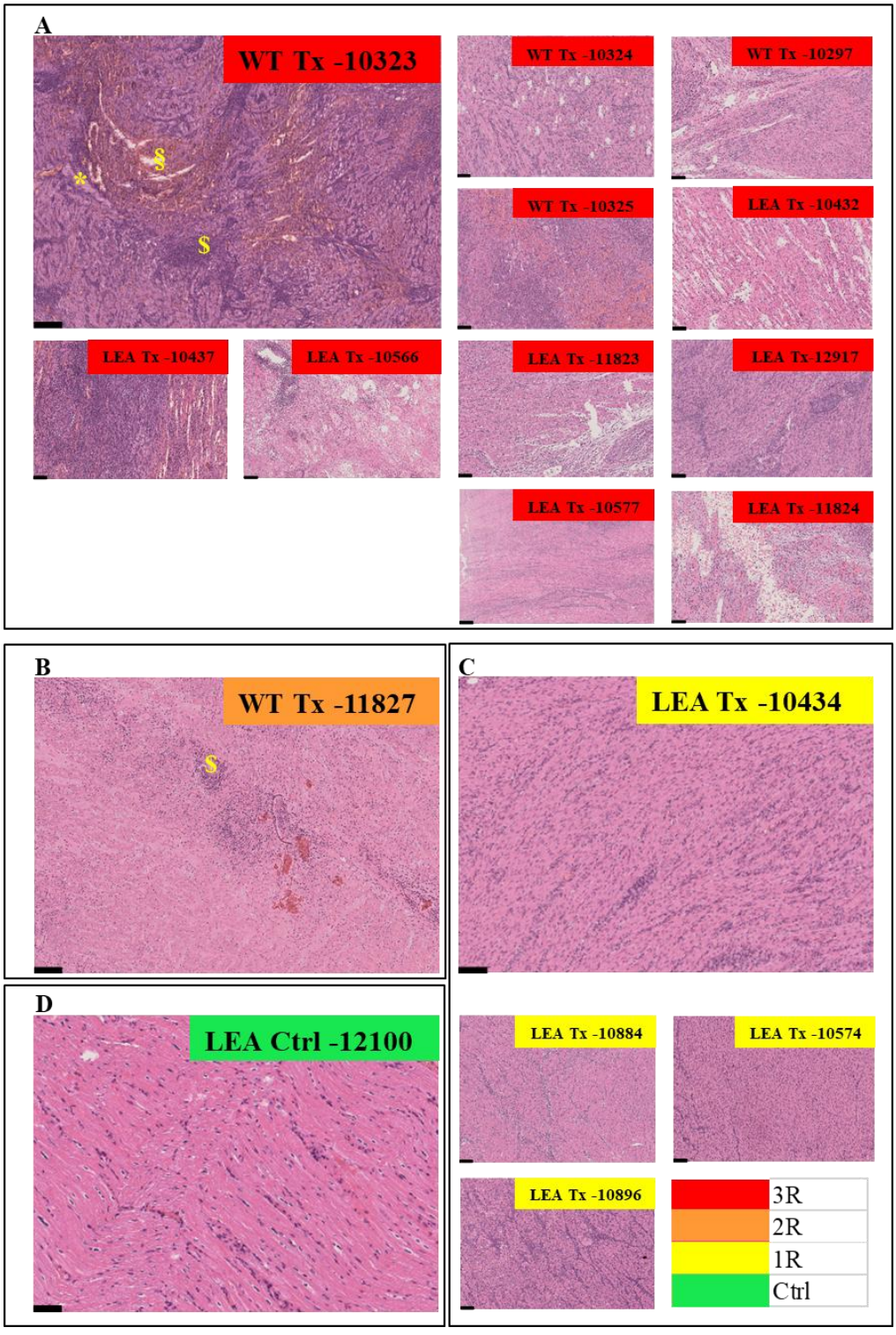


**Fig. 19: Overview of histological classification of LV samples from transplanted hearts.** Rejection grading was done by HE stainings of fixed tissue, according to the ISHLT Standard Cardiac Biopsy Grading (Stewart et al. 2005). Representative sample graded as (A) 3R rejection, (B) 2R rejection, (C) 1R rejection as well as (D) unaffected control tissue are highlighted. Scale bar indicates 100µm. Examples of interstitial edema (asterisk), myocardial fibrosis (#) and foci of immune cell infiltration ($) are indicated. Generalized diffuse immune cell infiltration characterizes 1R grade. Other samples are shown at a smaller magnification scale bar is 50µm.

# 3. Molecular analysis for gene expression

Transcript analysis of the HHTx graft samples was conducted to study the cellular and molecular responses of the graft. The assessment of cytokines' and cell markers' mRNA expression was conducted using real-time quantitative PCR (RT-PCR). QPCR has high sensitivity, high specificity, versatility, precision, reproducibility, a wide dynamic range, and an affordable operational cost. The immune panel previously established for lungs were extended for conducting qPCR assays for HHTx samples (Tab. 47). The study of immune markers assists in differentiating a non-rejected graft from a rejected one.

The cDNA synthesized from the graft tissue samples was subjected to qPCR assays targeting immune markers for rejection analysis. The rejection marker assay for the immune panel was optimized to meet the standard slope of -3.32 and coefficient of determination ($R^2$) between 0.99 – 1.00. 132 cDNA samples from LA, LV, RA and RV were subjected to the qPCR assay of rejection markers (Tab. 46). All the cDNA samples were standardized to meet the quality standards.

## 3.1. Quality check of the cDNA

All the cDNA samples were standardized to meet the quality standards. Quality of cDNA was monitored with house-keeping gene GAPDH, with serially diluted cDNA of 1:50, 1:100, 1:200, 1:400 and 1:800 concentrations (Tab. 17 in materials and methods). The cDNA that exhibited the slope of -3.32 and a coefficient of determination ($R^2$) value between 0.99 and 1.0 were considered to have passed the quality control criteria (Tab. 45).

**Tab. 45: Quality check of representative cDNA**

| Animal | Slope | R^2 | | Animal | Slope | R^2 |
|---|---|---|---|---|---|---|
| 10577 LV | -3.59 | 0.99 | | 12917 LN | -3.58 | 1 |
| 10577 Sp | -3.08 | 0.99 | | 12917 LA | -3.21 | 1 |
| 10577 liv | -3.24 | 1 | | 10434 LV | -3.14 | 0.99 |
| 10297 LA | -3.25 | 1 | | 10297 LV | -3.25 | 0.99 |
| 10297 LV | -3.22 | 0.99 | | 10323 LA | -3.21 | 1 |
| 12100 LV | -3.21 | 1 | | 10323 LV | -3.26 | 0.99 |
| 12100 liv | -3.01 | 0.99 | | 10324 LA | -3.31 | 1 |
| 10297 LA | -3.35 | 0.99 | | 10324 LV | -3.54 | 1 |
| 12323 LV | -3.19 | 0.99 | | 10325 LA | -3.32 | 1 |
| 12323 liv | -3.42 | 0.99 | | 10325 LV | -3.30 | 1 |
| 12323 LA | -3.38 | 0.99 | | 10297 LA | -3.33 | 1 |
| 12323 LV | -3.41 | 0.99 | | 10297 LV | -3.29 | 0.99 |

The cDNA that met the quality assurance requirement passed the quality test. These cDNA samples were subsequently used as templates for RT-qPCR. An LV sample that was classified as highly rejected, i.e., 10297LV, was used as a template in order to optimize the qPCRs. High-quality cDNA ensures the integrity of transcripts and improved outcomes in experiments, assuring the precision of quantitative assays.

**Tab. 46: Samples processed from HHTx.**

| HHTx animals | Samples used | number of samples |
|---|---|---|
| 10323 (WT Tx) | LA, LV, RA, RV, liv, sp | 6 |
| 10324 (WT Tx) | LA, LV, RA, RV, liv, sp | 6 |
| 10325 (WT Tx) | LA, LV, RA, RV, liv, sp | 6 |
| 10297 (WT Tx) | LA, LV, RA, RV, liv, sp | 6 |
| 11827 (WT Tx) | LA, LV, RA, RV, liv, sp | 6 |
| 10432 (CAG-LEA29Y Tx) | LA, LV, RA, RV, liv, sp | 6 |
| 10434 (CAG-LEA29Y Tx) | LA, LV, RA, RV, liv, sp | 6 |
| 10437 (CAG-LEA29Y Tx) | LA, LV, RA, RV, liv, sp | 6 |
| 10566 (CAG-LEA29Y Tx) | LA, LV, RA, RV, liv, sp | 6 |
| 10574 (CAG-LEA29Y Tx) | LA, LV, RA, RV, liv, sp | 6 |
| 10577 (CAG-LEA29Y Tx) | LA, LV, RA, RV, liv, sp | 6 |
| 10884 (CAG-LEA29Y Tx) | LA, LV, RA, RV, liv, sp | 6 |
| 10896 (CAG-LEA29Y Tx) | LA, LV, RA, RV, liv, sp | 6 |
| 11823 (CAG-LEA29Y Tx) | LA, LV, RA, RV, liv, sp | 6 |
| 11824 (CAG-LEA29Y Tx) | LA, LV, RA, RV, liv, sp | 6 |
| 12917 (CAG-LEA29Y Tx) | LA, LV, RA, RV, liv, sp | 6 |
| 12100 (CAG-LEA29Y Ctrl) | LA, LV, RA, RV, liv, sp | 6 |
| 12321 (CAG-LEA29Y Ctrl) | LA, LV, RA, RV, liv, sp | 6 |
| 12325 (CAG-LEA29Y Ctrl) | LA, LV, RA, RV, liv, sp | 6 |
| 12322 (WT Ctrl) | LA, LV, RA, RV, liv, sp | 6 |
| 12323 (WT Ctrl) | LA, LV, RA, RV, liv, sp | 6 |
| 12324 (WT Ctrl) | LA, LV, RA, RV, liv, sp | 6 |
| Total | | 132 |

Tissue samples from the left atrium (LA), left ventricle (LV,) right atrium (RA), right ventricle (RV), liver (liv) and spleen (Sp) from the hearts of five WT transplants, eleven LEA transplants, three WT controls and three LEA controls.

## 3.2. Optimization of RT-PCR

A

| Gene Name | GAPDH | ACTB | TBP | YWHAZ | IL1A | IL18 | CYBB | CD68 |
|---|---|---|---|---|---|---|---|---|
| Slope | -3.3485 | -3.5146 | -3.6481 | -3.3219 | -3.1705 | -3.4458 | -3.3668 | -3.3585 |
| Efficiency | 1.99 | 1.93 | 1.88 | 2 | 2.07 | 1.95 | 1.98 | 1.98 |
| Error | 0.04 | 0.15 | 0.21 | 0.07 | 0.25 | 0.27 | 0.15 | 0.06 |
| R^2 | | 0.99 | 0.99 | 1 | 0.98 | 0.98 | 0.99 | 1 |
| Y-Intercept | 27.58 | 26.42 | 35.49 | 30.90 | 35.77 | 33.71 | 33.04 | 31.51 |

B

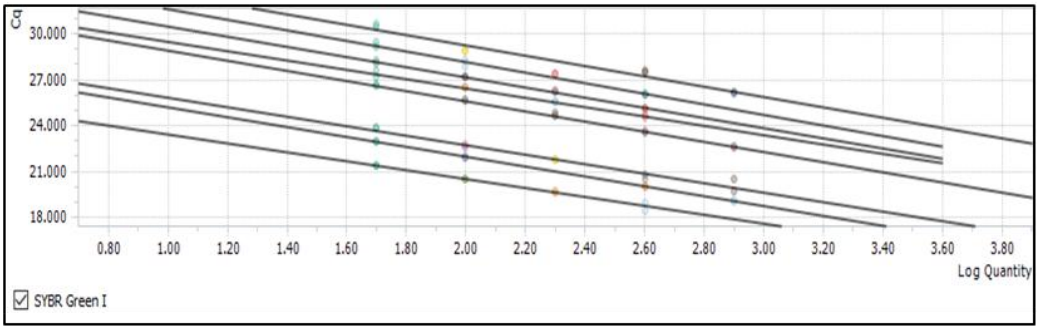


C

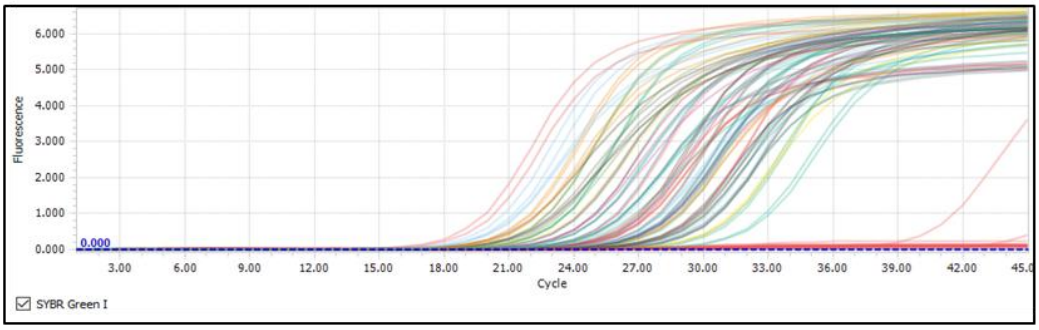


D

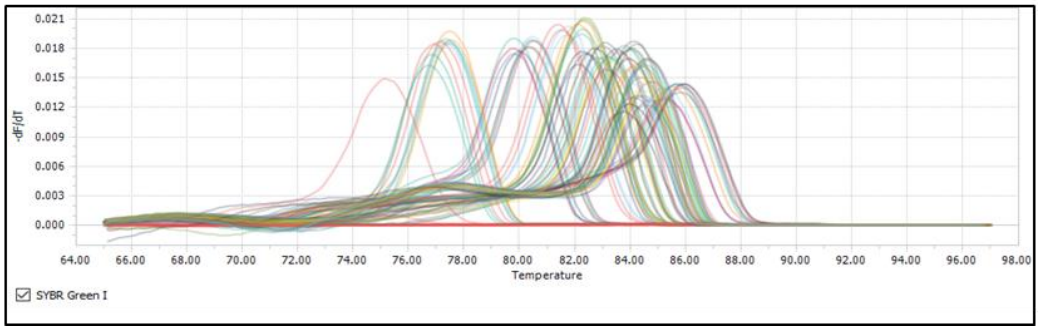


**Fig 20: Optimizing primers for cytokines.** Primer pair candidates were used at 63°C annealing temperature in qPCR in serial 2-fold dilutions, compared to establishe GAPDH HKG. (A) Slope and linearity of 1:50, 1:100, 1:200, 1:400, 1:800 dilution standard curves were determined for different primer concentrations. Graphical depiction (B), amplification plots (C) and melting curves (D) for GAPDH and cytokine standard curves.

The predesigned assay, previously validated for lung tissues by Florian Jaudas (Chair of Molecular Animal Breeding and Biotechnology, LMU) and Miquel Cambra (Klinikum rechts der Isar, TUM), was optimized using cDNA derived from cardiac tissue samples. All sets of assays were systematically optimized, adjusting parameters like primer concentrations, primer annealing temperature, and reaction components. Optimizing conditions were validated by melting curve, standard curve to ensure specificity and amplification efficiency.

### 3.3. Optimization of additional immune panel

Subsequent to the optimization of the pre-established immune panel for cardiac rejection markers, additional immune markers IL6, IL10 and IFNG were selected to establish a broad panel of immune markers. Following the multiple primer design for each immune marker, primer combination yielding the most robust amplicons were subsequently selected for further optimization under refined PCR conditions (Fig. 21).

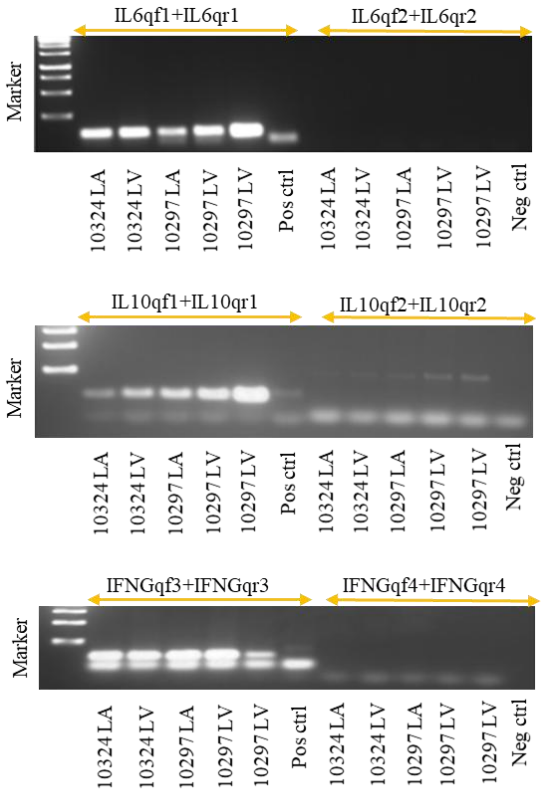


**Fig. 21: Testing primers for lowly expressed cytokines.** Several primer pairs were designed for IL6, IL10 and IFNG and tested in end-point PCR on cDNA from severely rejected tissue. Standard conditions were used to select the most promising primer pairs for further optimization in qPCR.

A

| Gene Name | GAPDH | IL6 | IL10 | IFNG | IFNG | IL6 | IL10 | IFNG |
|---|---|---|---|---|---|---|---|---|
| Slope | -3.3701 | -3.758 | -3.5456 | -3.6392 | -3.2588 | -3.4778 | -3.3346 | -2.9549 |
| Efficiency | 1.98 | 1.85 | 1.91 | 1.88 | 2.03 | 1.94 | 1.99 | 2.18 |
| Error | 0.09 | 0.94 | 0.46 | 0.27 | 0.36 | 0.68 | 0.79 | 0.23 |
| R^2 | 0.99 | 0.81 | 0.93 | 0.96 | 0.96 | 0.84 | 0.76 | 0.98 |
| Y-Intercept | 29.72 | 39.83 | 40.87 | 39.12 | 38.2 | 39.39 | 40.20 | 37.33 |

B

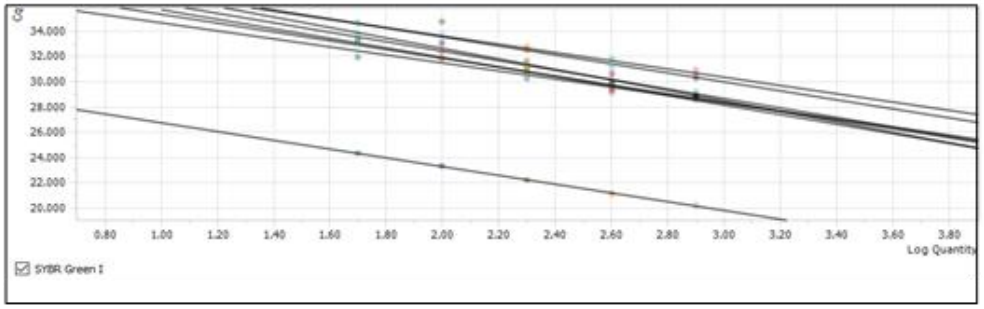


C

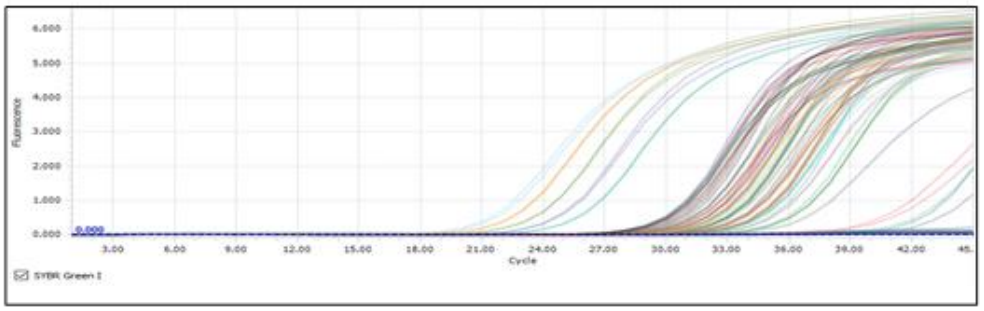


D

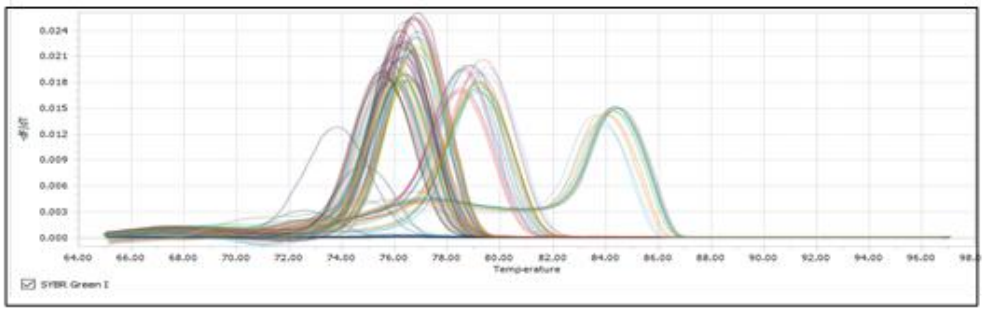


E

| | Slope | Cq | R^2 | temp | primer conc |
|---|---|---|---|---|---|
| IL6 | -3.1 | 28-34 | 0.97 | 63 | 0.5+0.5 |
| IL10 | -3.5 | 30-34 | 0.97 | 63 | 0.5+0.5 |
| IFNG | -2.9 | 28-33 | 0.98 | 63 | 0.5+0.5 |

**Fig. 22: Optimizing primers for lowly expressed cytokines**. Primer pair candidates were used at 60°C annealing temperature in qPCR in serial 2-fold dilutions, compared to establishe GAPDH HKG. (A) Slope and linearity of 1:50, 1:100, 1:200, 1:400, 1:800 dilution standard curves were determined for different primer concentrations. Graphical depiction (B), amplification plots (C) and melting curves (D) for GAPDH and cytokine standard curves. (E) Optimized primer concentrations and annealing temperatures for IL6, IL10, IFNG.

Optimization of the additional immune panels, IL6, IL10, and IFNG, was systematically conducted with various combinations of annealing temperature, primer combination, and reaction components (For details, see table for mastermix for qPCR in materials and methods). Validation of the optimized conditions was carried out with melting curve analysis and standard curve assessment. Optimal efficiency was confirmed by standard curve slope of -3.32 and coefficient of determination ($R^2$) in the range of 0.99-1.00.

### 3.4. Summary of optimization of immune panel

Following multiple attempts of optimization, both the immune panel with additional immune markers were optimized with subjected primer concentration and annealing temperature based on empirical evaluation of melting curve, standard curve slope assessment and coefficient of etermination. Optimal efficiency was confirmed by standard curve slope of -3.32 and coefficient of determination ($R^2$) in the range of 0.99-1.00.

**Tab. 47: Adapted conditions for immune panels.**

| House-keeping genes | Forward primer concentration | Reverse primer concentration | Annealing temperature | Number of Trials |
|---|---|---|---|---|
| ACTB | 0.5 | 0.5 | 63 °C | 4 |
| GAPDH | 0.3 | 0.3 | 63 °C | 3 |
| TBP | 0.7 | 0.7 | 63 °C | 4 |
| YWHAZ | 0.3 | 0.3 | 63 °C | 3 |
| Immune-related genes | Forward primer concentration | Reverse primer concentration | Annealing temperature | |
| IL-1α | 0.7 | 0.7 | 60 °C | 13 |
| IL-1β | 0.3 | 0.3 | 60 °C | 2 |
| IL-18 | 0.7 | 0.7 | 63 °C | 7 |
| TNF-α | 1 | 0.7 | 60 °C | 5 |
| TGFβ | 0.5 | 0.5 | 60 °C | 5 |
| CYBB | 0.3 | 0.3 | 63 °C | 7 |
| CD45 | 0.7 | 0.7 | 60 °C | 8 |
| CD68 | 0.5 | 0.5 | 63 °C | 3 |
| IL6 | 0.3 | 0.3 | 63 °C | 17 |
| IL10 | 0.5 | 0.5 | 63 °C | 19 |
| IFNG | 0.5 | 0.5 | 60 °C | 9 |

The optimized condition for the immune panel assays achieved by multiple trials with different combinations of annealing temperature and primer concentrations was subsequently applied to cDNA from HHTx heart samples.

The cDNA of WT transplant, i.e. 10297LV which was anticipated to exhibit

elevated rejection was employed for further primer optimization of IL6, IL0 and IFNG. Sample 10297 exhibited Cq values of 29, 28, and 28 for IL6, IL10, and IFNG, respectively. In contrast to other transplanted samples exhibited the Cq values ranging from 31 to 34 cycles for these cytokines, signifying lower transcript abundance of these cytokines in those tissues.

### 3.5. Gene expression of cytokines and cell markers in different heart locations

A total of 132 cardiac tissue samples representing LA, LV, RA and RV from HHTx were analysed to assess the gene expression profiles of immune markers associated with graft rejection. The samples obtained were from four groups: WT transplants, LEA transplants, WT control and LEA control animals (Tab. 42). The snap-frozen tissue was pulverized under liquid nitrogen and the futher processed (Fig. 23). The cDNA derived from HHTx were subjected to qPCR assays with the optimized parameters (Tab. 47). The immune gene panel for qPCR assasys comprised of markers for immune cell infiltration and cytokine response, including CYBB, CD68, CD45, IL1A, IL1B, TGFA, TNFA, IL6, IL10, and IFNG. GAPDH and TBP were included as reference housekeeping genes for normalization.

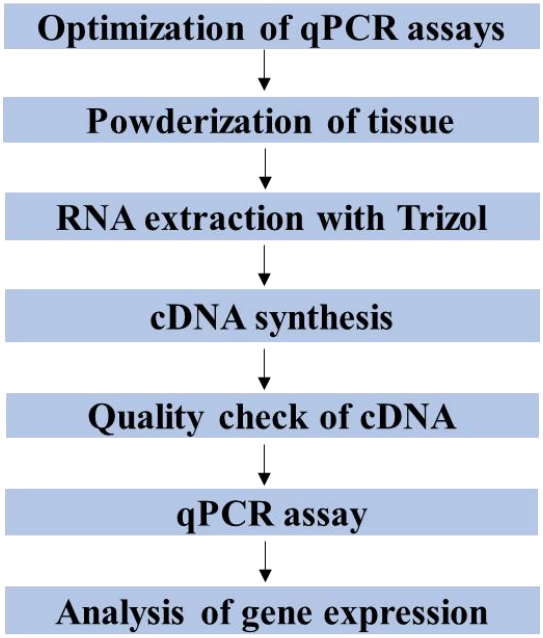


**Fig. 23: Workflow for gene expression of immune panels**

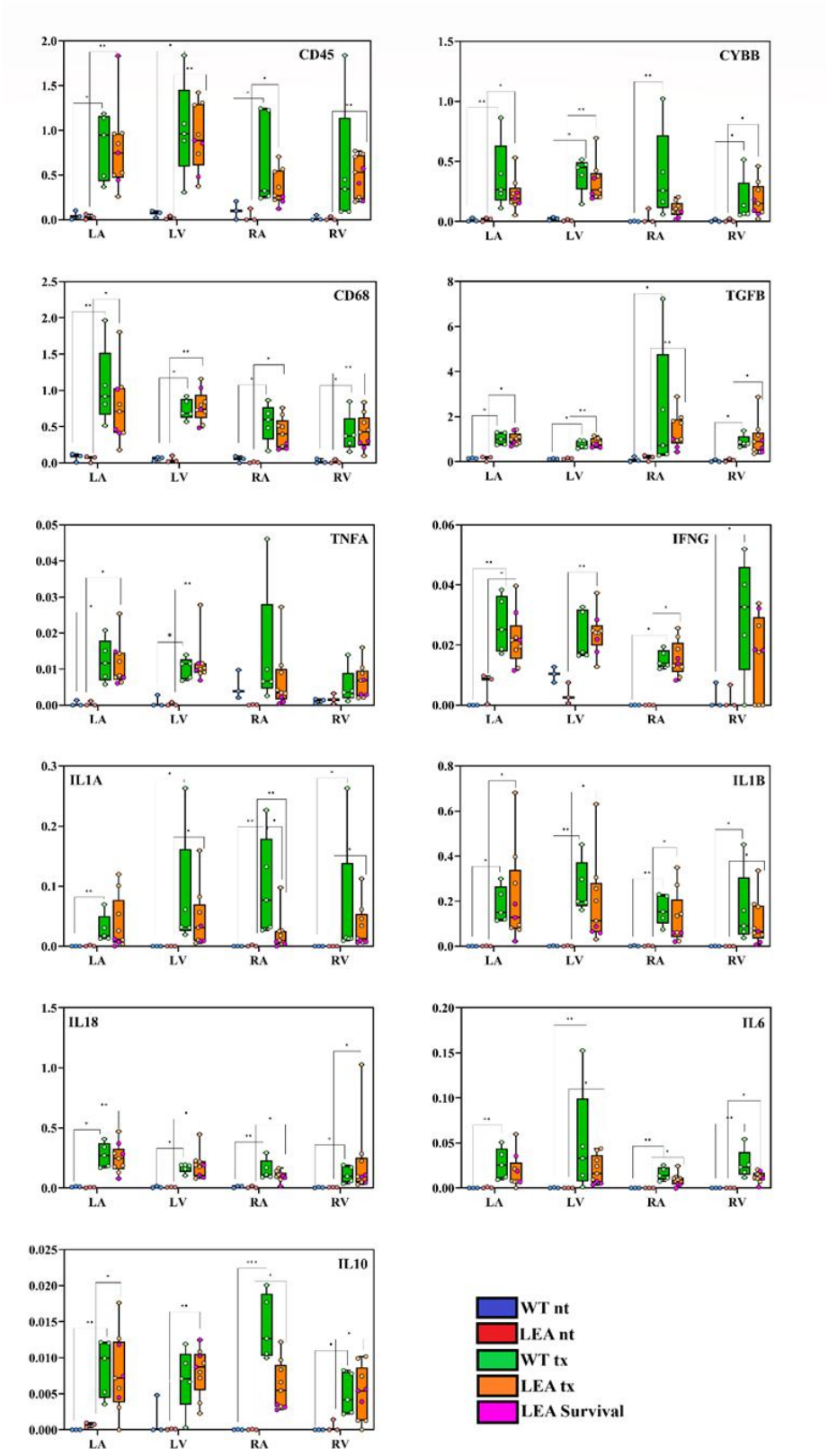


**Fig. 24: Gene expression of immune panel.** Relative expression levels of inflammatoy genes from immune panel assays were quantified using primary quantification cycle (Cq). Gene stability was assessed with RefFinder, and the housekeeping genes GAPDH and TBP to normalize Cq values for accurate gene expression analysis.

The preliminary analysis of the gene expression of the immune panel demonstrated a significant upregulation of cytokines and immune cell marker transcripts in cardiac allograft groups in contrast to the non-transplanted control groups. Both WT and LEA transplanted groups exhibited elevated gene expression profiles relative to their respective control counterparts. However, no statistically significant differences in gene expression were detected between the WT transplanted and the LEA transplanted groups, with the exception of IL1A expression in the RA, which was significantly different between these groups. The surviving grafts 10434, 10884 and 10886 exhibited lower gene expression for most of the cytokines and immune cell markers for rejection.

## 4. Molecular analysis for Swine Leukocyte Antigen (SLA) typing

Preliminary analysis of the immune gene expression panel revealed significant differences between transplanted and non-transplanted control groups. However, no statistically significant differences in gene expression were observed between the WT-transplanted and LEA29Y-transplanted cohorts. Mixed outcome was observed in LEA transplants. Extensive polymorphism of swine leukocyte antigen (SLA) genes exerts a major influence on immune responses in transplantation outcomes. So, mismatches in SLA alleles was assumed to be associated with the mixed outcome of LEA transplants.

Initially, the primers were designed for SLA I class (SLA-1, SLA-2) and SLA II class (SLA-DRB1, SLA-DQA, SLA-DQB) targeting exon 2 and 3 for SLA class I genes and exon 2 for SLA class II genes as these exons code the antigen binding domains and bear the major polymorphic regions critical for graft rejection mechanisms. For more details, see the materials and methods for primer designing. The selected primer combinations were validated to ensure amplifications at the targeted SLA loci, thereby allowing high-resolution SLA typing for both class I and class II (Fig. 26). The cDNA of heart tissues from the donor and the cDNA from the liver and spleen from the recipient were used for SLA typing to locate the SNP between the donor-recipient pairs of HHTx. A comprehensive list was compiled, chronologically locating the precise locus of all the SNPs between each combination of donor and recipient animals from the experiments (Tab. 49). The codons from the incorporating SNPs in exon 2 and 3 in SLA1 and SLA2 and exon 2 in SLA-DRB1, SLA-DQB, and SLA-DQA were individually translated to amino acids with IUPAC nomenclature. The amino acid variability between the donor-recipient pairs was estimated as per the workflow (Fig. 25).

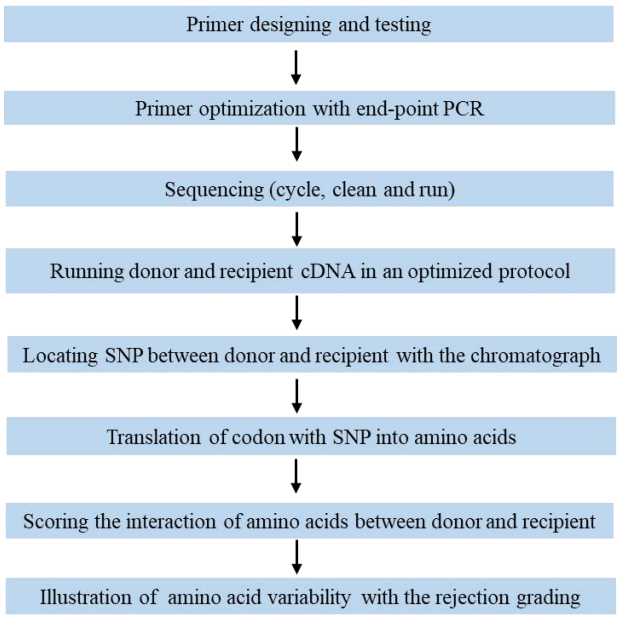


**Fig. 25: Workflow for SLA typing**

## 4.1. Loci of SLA genes in porcine

SLA I class (SLA1, SLA2) and SLA II class (SLA-DRB1, SLA-DQA, SLA-DQB) bear the major polymorphic regions critical for graft rejection mechanisms.

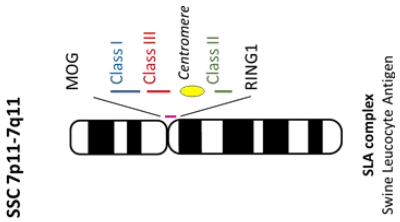


**Fig. 26: Representation of loci of SLA genes in swine** (adapted from Hammer, Ho et al. 2020)

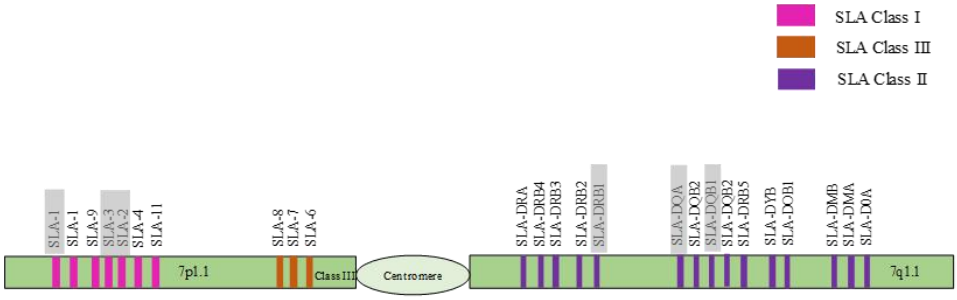


**Fig 27: Schematic representation of the SLA gene in the pig genome.** The SLA genes highlighted I grey were targeted to locate SNPs to track the mismatch between donor and recipient pairs in HHTx.

## 4.2. Selection and optimization of primer

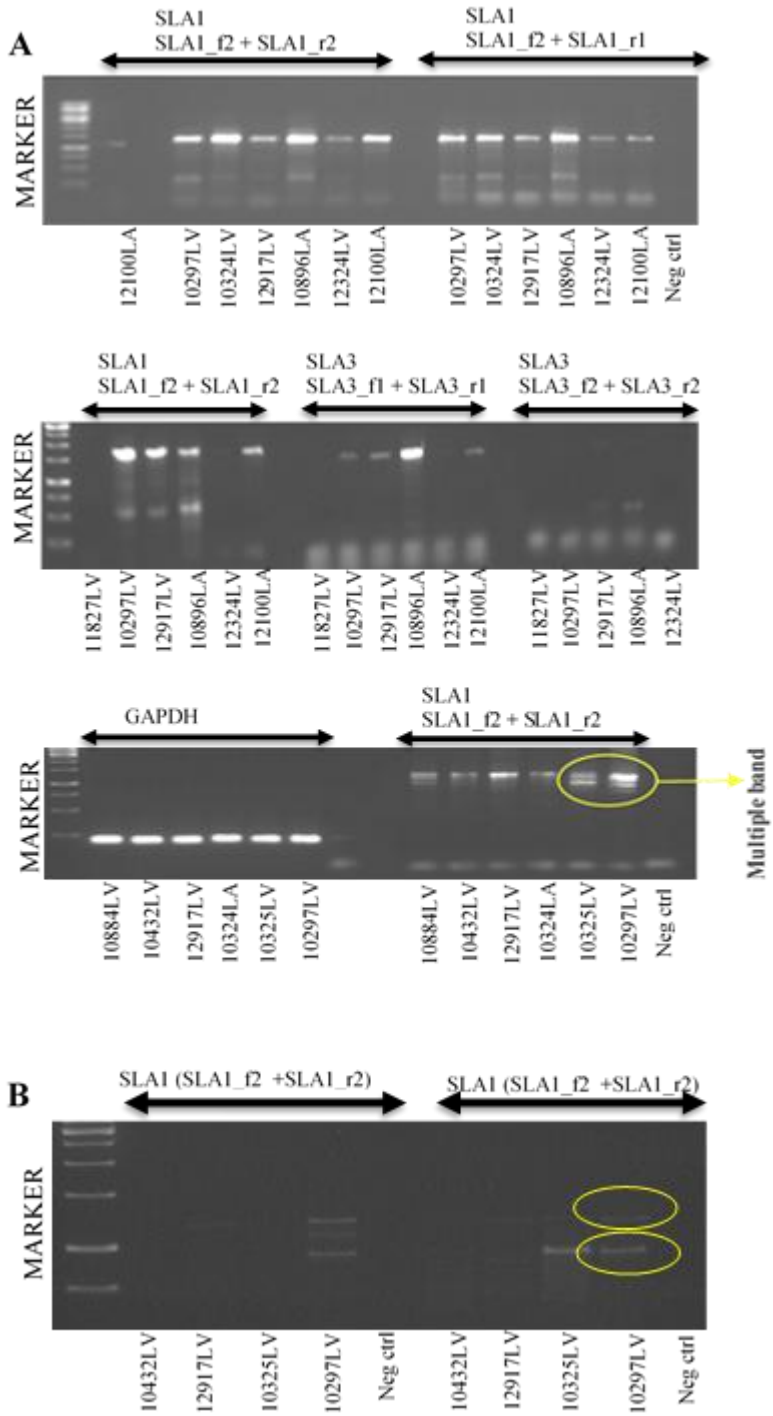


**Fig. 28: Optimization of SLA class I primers.** End point PCR for optimization of SLA class I primers (A) demonstrated double band formation. Thus, end-point PCR (B) at low voltage (10 V) overnight was executed to demonstrate the double band formation.

Multiple primer combinations targeting SLA class I (SLA1 and SLA2) were evaluated with endpoint PCR, and the most robust amplicons were subsequently selected for further optimization under refined PCR conditions (Fig. 28). Further optimization of the SLA primers was systematically conducted with various

combinations of annealing temperature, elongation time, primer concentration, and reaction components.

During the optimization process, endpoint PCR frequently resulted in the appearance of double bands (Fig. 28A and 28B). To resolve this, q-solution was incorporated into PCR reactions, which effectively resolved the issue of double band formation by enhancing amplication specificity and optimizing the melting behaviour of the template. However, a major technical challenge was encountered during sequencing with the selected primer combinations, as the resulting chromatograms exhibited substantial background noise (Fig. 29).

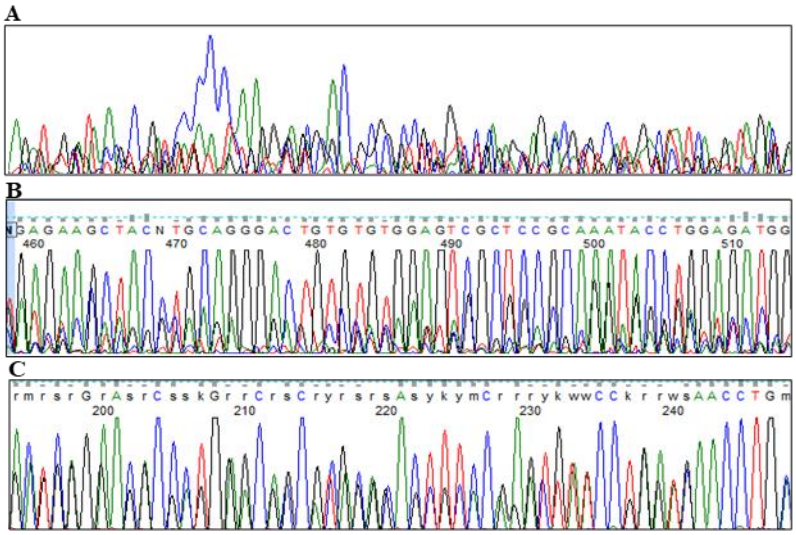


**Fig. 29: Challenges encountered during the optimization of SLA primers.** (A) Chromatogram of SLA1 amplicon (SLA1_f2+SLA1_r2) sequenced by SLA1_f2, (B) Chromatogram of SLA2 amplicon (SLA2_f1+SLA2_r2) sequenced by SLA2_r2

### 4.3. Primer Designing for inner primers

To obtain high-quality chromatograms suitable for single nucleotide polymorphism (SNP) detection, internal sequencing primers were specifically designed and implemented (Fig. 30). These primers enhanced sequencing specificity and resolution, thereby facilitating accurate identification and localization of SNPs within the target regions (Fig. 30).

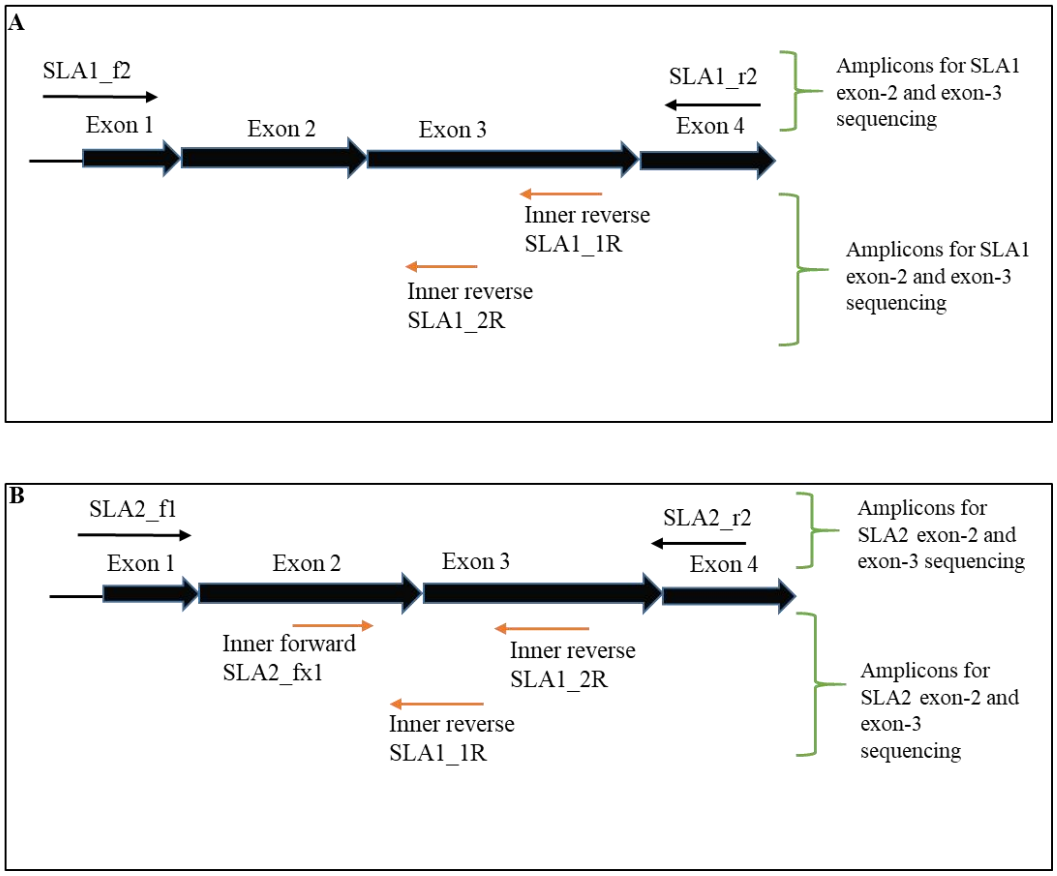


**Fig. 30: Alternative seqencing of SLA1 and SLA2 amplicon with inner primers.** (A) Inner primers for SLA1, (A) Inner primers for SLA2

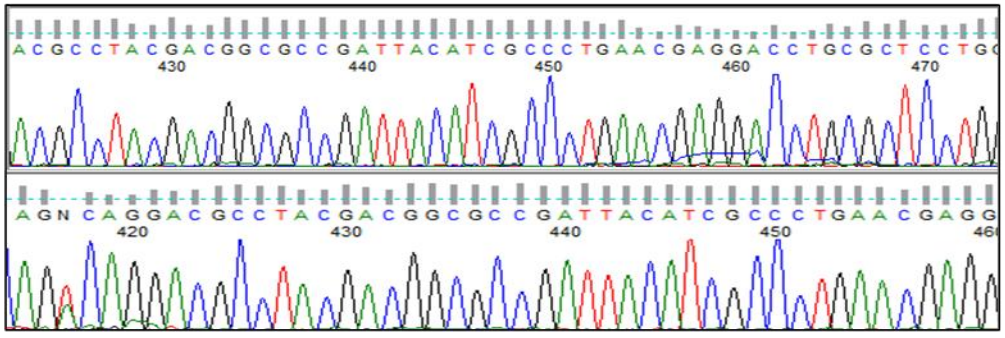

**Fig. 31: Chromatogram after sequencing of SLA inner primers.** (A) Chromatogram of SLA1 amplicon (SLA1_f2+SLA1_r2) sequenced by inner primer SLA1_1R, (B) Chromatogram of SLA2 amplicon (SLA2_f1+SLA2_r2) sequenced by inner primer SLA2_2R

### 4.4. Optimized conditions for the SLA class I genes

After resolving multiple technical challenges encountered during SLA typing, a standardized protocol for SLA class I (SLA1 and SLA2) typing was successfully established (Fig. 32).

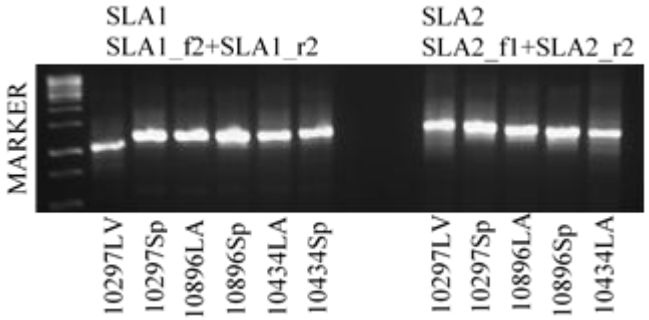


**Fig. 32: SLA typing following the resolution of technical artifacts during primer optimization.** Addition of q-solution effectively eliminated the formation of double bands, thereby improving the specificity of the amplification.

### 4.5. Selection and optimization of SLA class II primers

Multiple primer combinations targeting SLA class II (SLA-DRB1, SLA-DQA and SLA-DQB) were evaluated with endpoint PCR, and the most robust amplicons were subsequently selected for further optimization under refined PCR conditions (Fig. 33). Further optimization of the SLA primers was systematically conducted with various combinations of annealing temperature, elongation time, primer concentration, and reaction components.

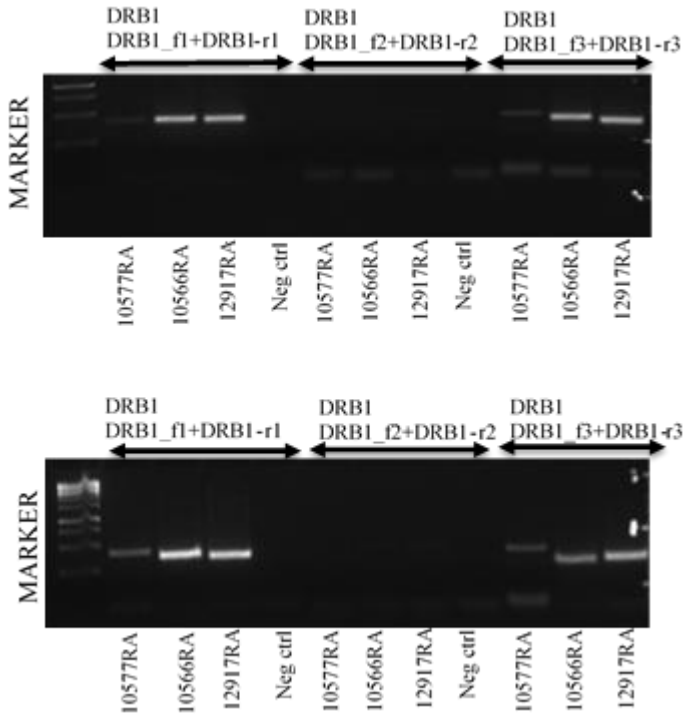


**Fig. 33: Primer optimization of SLA class II.** Primer optimization for SLA class II was performed by systematically varying annealing temperatures and primer concentrations to identify the optimal conditions for specific and efficient

amplification.

### 4.6. SLA typing for donors and recipients for HHTx

The SLA typing of donor and recipient animals from HHTx experiments was performed to evaluate immunological compatibility between graft donors and recipients. For SLA profiling, cDNA generated from LV and RA of donor animals and cDNA from spleen and liver tissues of recipient animals were employed as the template. Optimized protocols for SLA class I (SLA1 and SLA2) and SLA II profiling (SLA-DRB1, SLA-DQA, and SLA-DQB) were applied to both donor and recipient templates (Fig. 34). The amplicons from SLA typing were sequenced at the Sequencing Service at LMU Biozentrum, Martinsried. Thus, the exons 2 and 3 of SLA class I genes, and exon 2 in the SLA class II genes were sequenced and aligned in BioEdit.

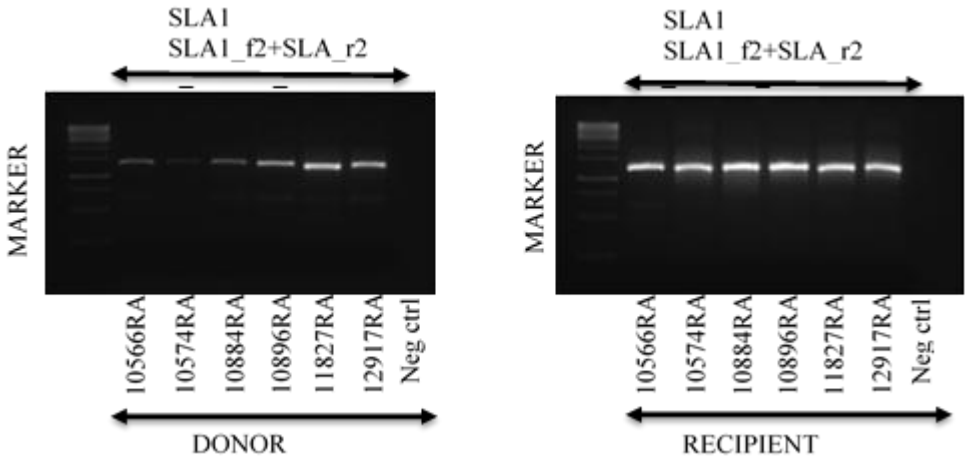


**Fig. 34: SLA genotyping of donor and recipient of HHTx.** cDNA from LA, LV, RA and RV from donor animals and cDNA from spleen and liver from recipient animals were used as template for SLA typing.

### 4.7. Locating SNPs between the donor and recipient pairs

The donor and recipient sequences from the HHTx experiments were aligned for the corresponding SLA genes (Fig. 35). The single nucleotide polymorphisms (SNPs) between the donor and recipient pairs were highlighted as in Fig. 35.

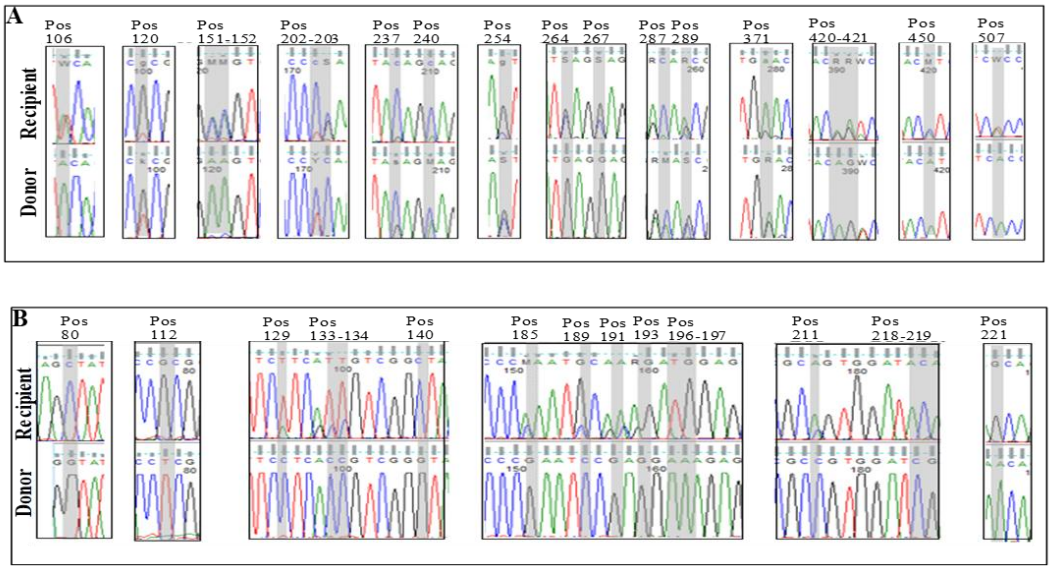


**Fig. 35: Illustration of SNPs identified between donor-recipient pairs in HHTx animals.** (A) shows SNPs distinguishing the donor and recipient, specifically indicating the SNP locations in SLA1 for recipient 10432 and donor 10518. Panel (B) displays the SNP locations in SLA2 for recipient 10884 and donor 10963

## 4.8. Variation of SNPs between donor-recipient pairs

A comprehensive list was compiled, chronologically locating the precise locus of all the SNPs between each combination of donor and recipient animals from the experiments (Tab. 48).

**Tab. 48: SNP variations between donor-recipient pairs in the SLA1 gene of HHTx animals**

| Animal | 106 | 118 | 130 | 137 | 138 | 143 | 147 | 150 | 151 | 152 | 202 | 203 |
|---|---|---|---|---|---|---|---|---|---|---|---|---|
| 10297 (WT) | A/T | C/T | G/G | C/G | C/T | C/T | A/A | G/G | C/A | C/A | C/T | C/G |
| 10372 (WT) | A/T | C/C | G/T | C/C | T/T | C/C | A/A | G/G | C/A | C/A | C/T | C/G |
| 10323 (WT) | A/A | C/C | G/T | C/C | T/T | C/C | A/A | G/G | C/A | C/A | C/T | C/G |
| 10373 (WT) | A/A | C/C | G/G | C/C | T/T | C/C | A/A | G/G | C/C | C/C | C/C | G/G |
| 10324 (WT) | A/A | C/C | G/T | C/C | T/T | C/C | A/A | G/G | C/A | C/A | C/T | C/G |

**Fig. 36: Haplotyping of pig MHC-I genes.** For all donor-recipient pairs, amplicons spanning exons 2 and 3 of the SLA1 (A) and SLA2 (B) genes were amplified and sequenced by internal primers and nucleotide constellations at polymorphic positions are indicated in color codes. Blue = any homozygous constellation in recipient and identical constellation in donor. Yellow: any non-matching homozygous constellation in donor. Blue/yellow: any heterozygous constellation. Color coding for donor recipient pairs corresponds to degree of rejection as defined in Fig. 19 (rejection grading of transplanted hearts). The genotype of the donor (WT or LEA29Y) is indicated.

A

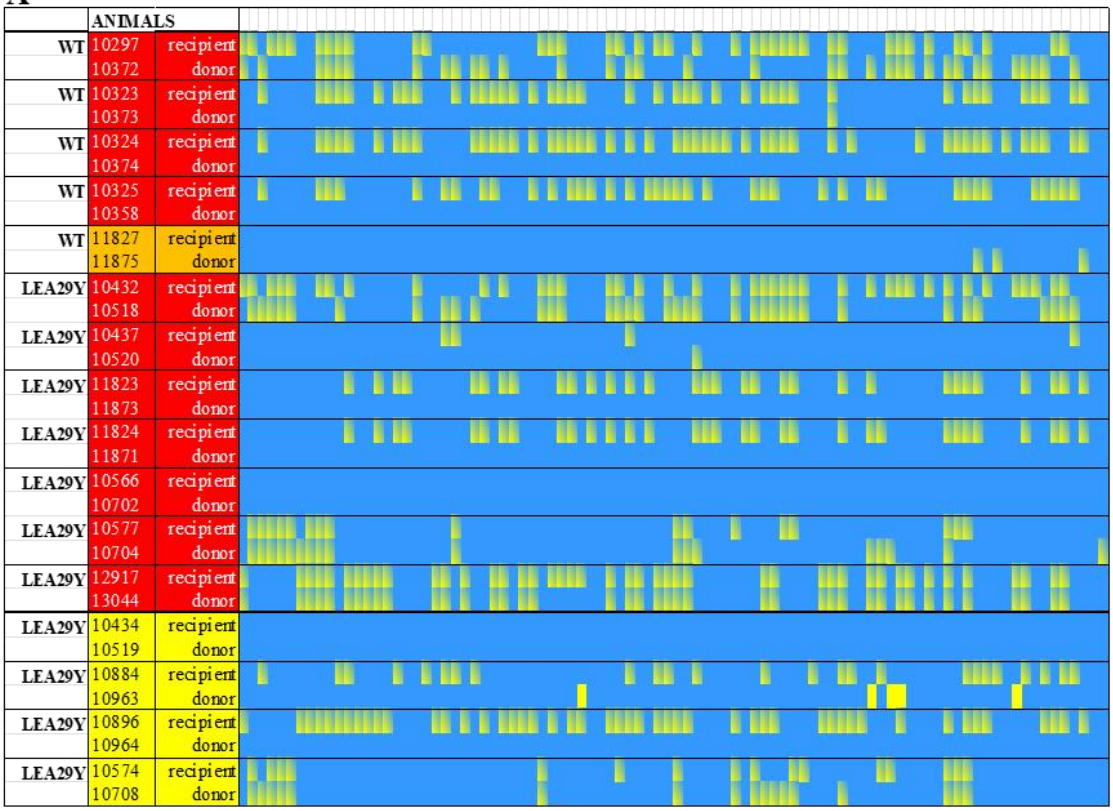

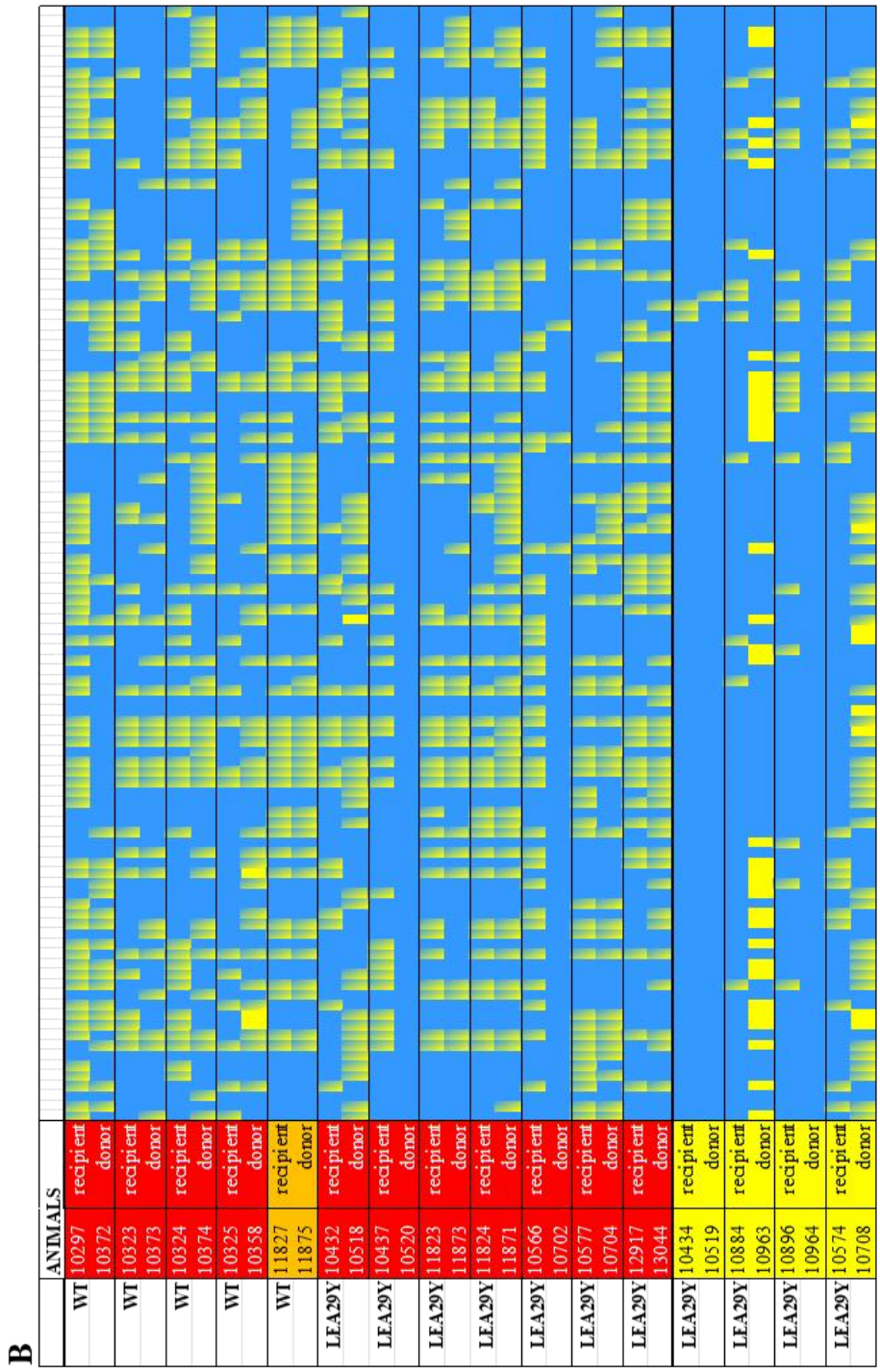
B
ANIMALS
WT 10297 recipient
10372 donor
WT 10323 recipient
10373 donor
WT 10324 recipient
10374 donor
WT 10325 recipient
10358 donor
WT 11827 recipient
11875 donor
LEA29Y 10432 recipient
10518 donor
LEA29Y 10437 recipient
10520 donor
LEA29Y 11823 recipient
11873 donor
LEA29Y 11824 recipient
11871 donor
LEA29Y 10566 recipient
10702 donor
LEA29Y 10577 recipient
10704 donor
LEA29Y 12917 recipient
13044 donor
LEA29Y 10434 recipient
10519 donor
LEA29Y 10884 recipient
10963 donor
LEA29Y 10896 recipient
10964 donor
LEA29Y 10574 recipient
10708 donor

**Fig. 37: Haplotyping of pig MHC-II genes.** For all donor-recipient pairs, amplicons spanning exons 2 in SLA-DQA (A), SLA-DQB1 (B), SLA-DRB1(C) genes were amplified and sequenced with amplification primers. Color coding of nucleotide constellations and donor-recipient pairs is as in Fig. 36.

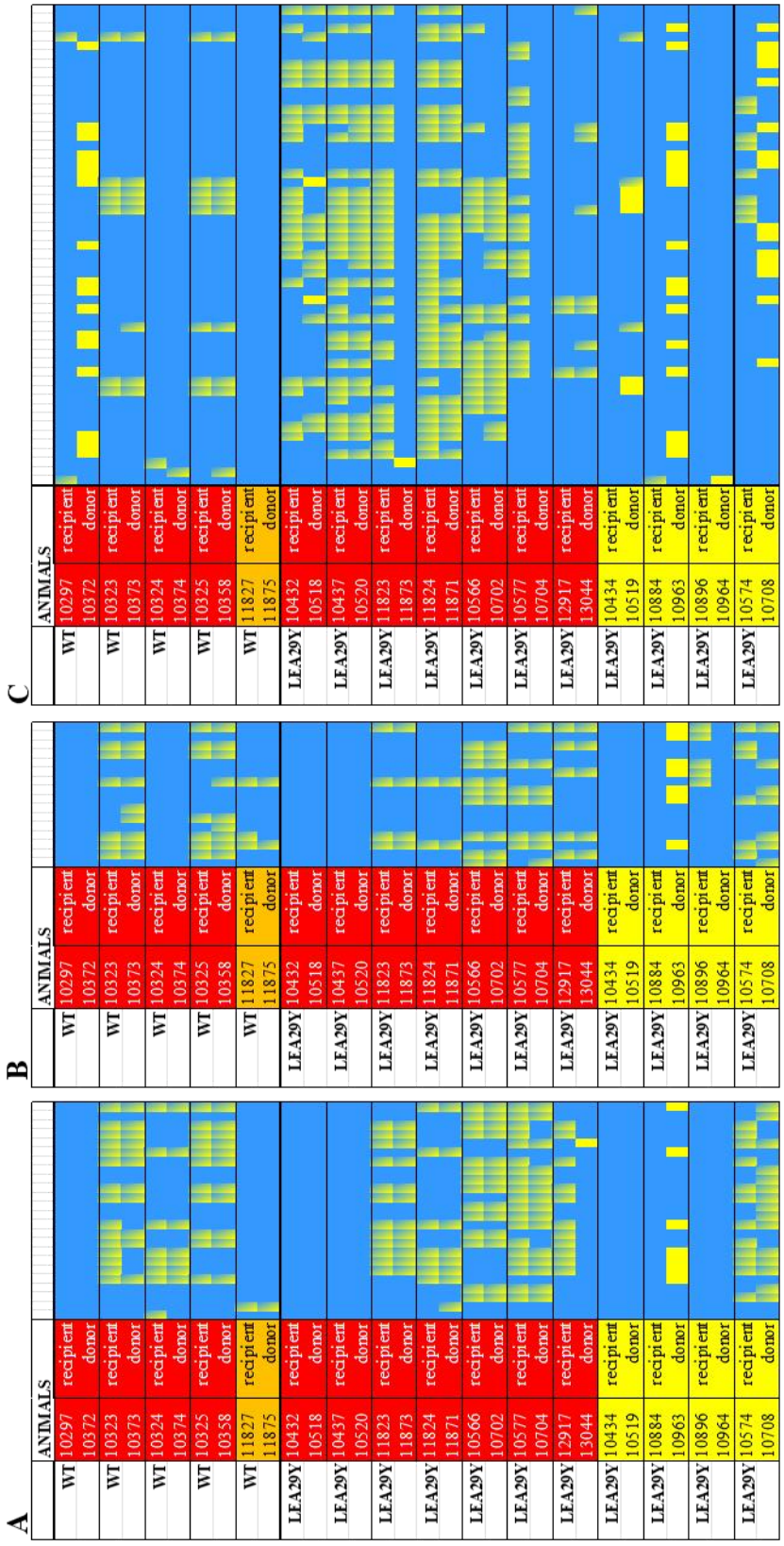

## 4.9. Variation of amino acids between donor-recipient pairs

The codons containing SNPs identified in exon 2 and 3 in SLA1 and SLA2, and exon 2 in SLA-DRB1, SLA-DQB, and SLA-DQA were individually translated into corresponding amino acids using IUPAC nomenclature for standardized amino acid annotation.

**Fig. 38: Illustration of variation of amino acids.** For all donor-recipient pairs, amino acids spanning exons 2 and 3 of the SLA1 (A) and SLA2 (B) genes at polymorphic positions are indicated in color codes. Dark green: any homozygous constellation in the recipient and an identical constellation in the donor. Light green: any non-matching constellation in donor in regard to the recipient, without any immunological impact on the recipient. Green/blue: any heterozygous constellation in the donor with immunological impact on the recipient. Blue: completely different constellation than the recipient with an immunological impact. The scoring of amino acid interaction is as per Tab. 40. The cumultative score of interaction due to amino acid mismatches is also displayed.

A

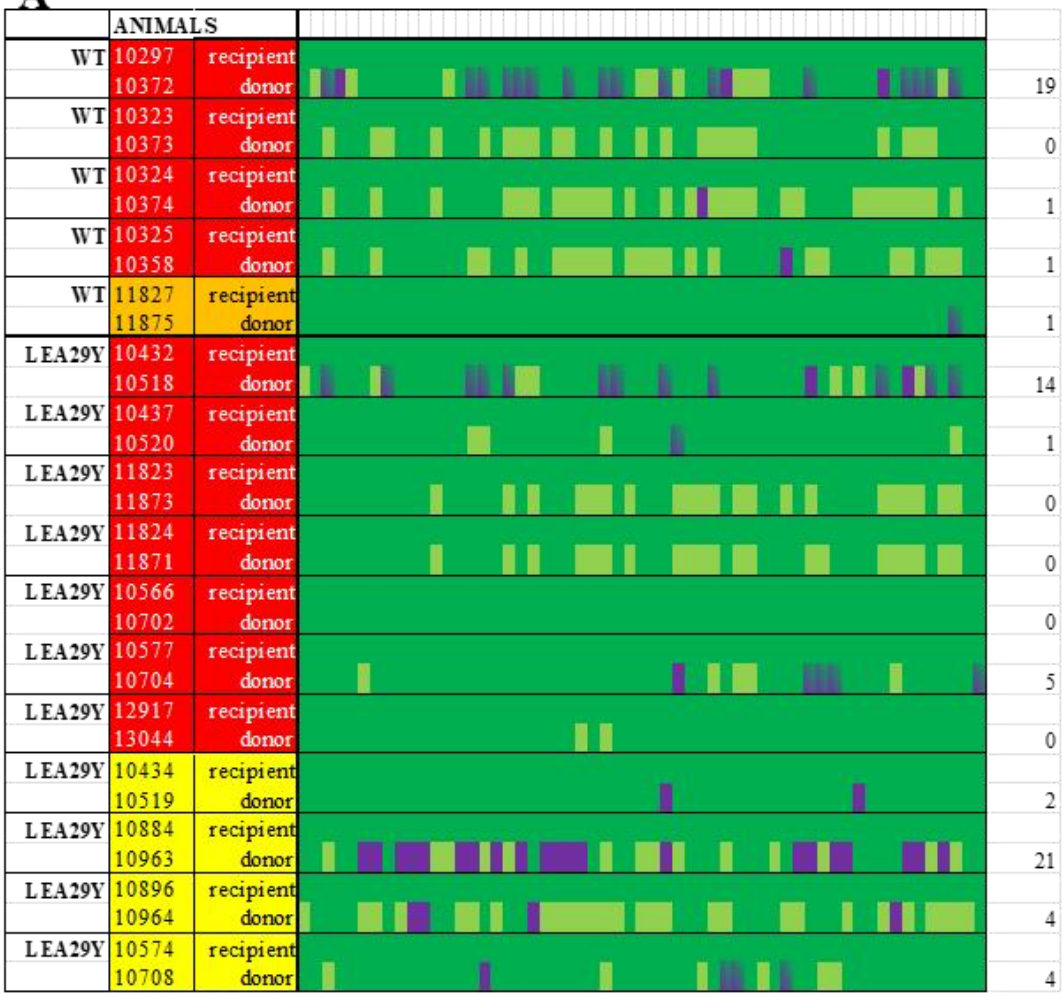

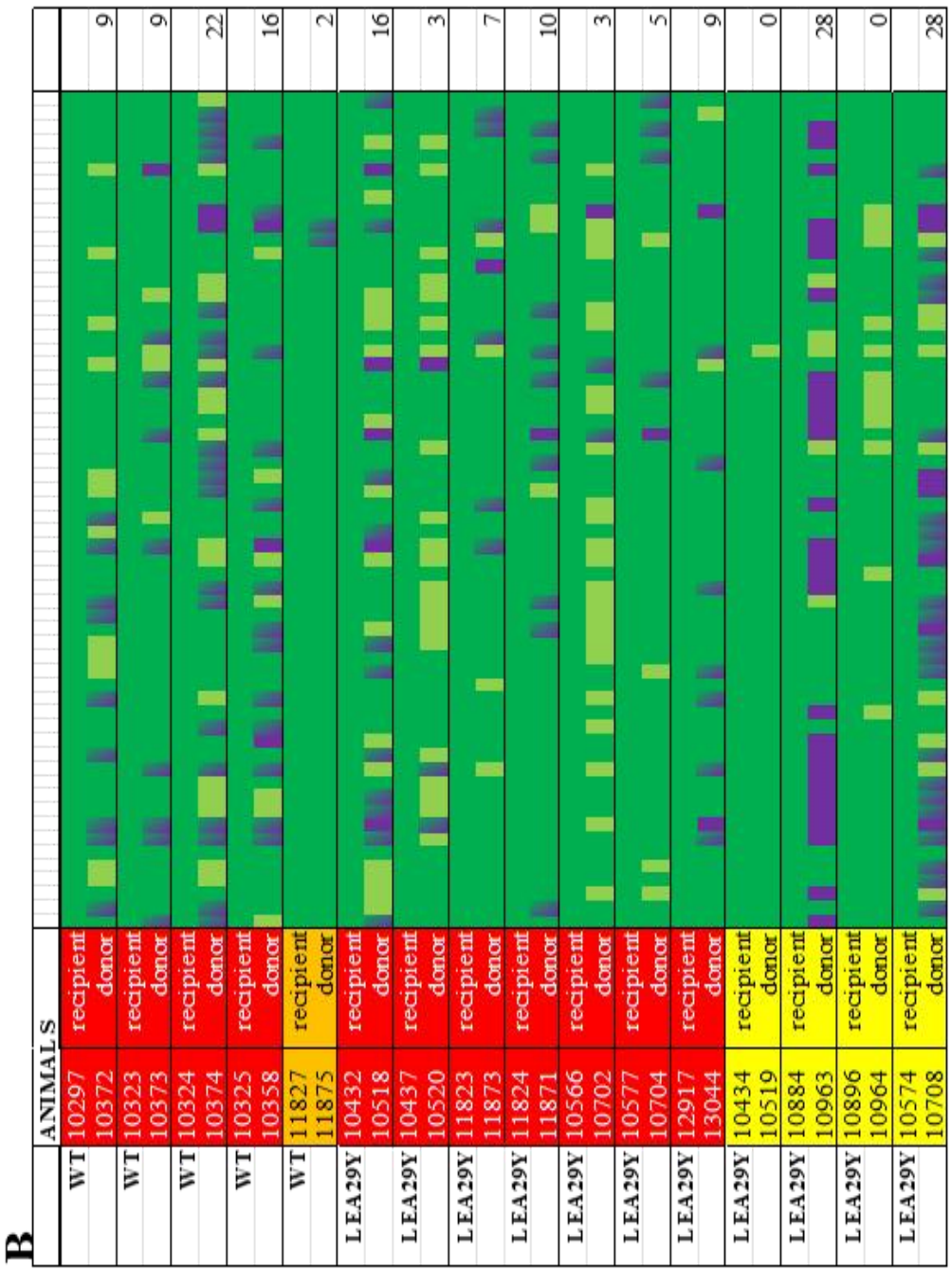
B
ANIMALS
WT 10297 recipient 9
10372 donor
WT 10323 recipient 9
10373 donor
WT 10324 recipient 22
10374 donor
WT 10325 recipient 16
10358 donor
WT 11827 recipient 2
11875 donor
LEA29Y 10432 recipient 16
10518 donor
LEA29Y 10437 recipient 3
10520 donor
LEA29Y 11823 recipient 7
11873 donor
LEA29Y 11824 recipient 10
11871 donor
LEA29Y 10566 recipient 3
10702 donor
LEA29Y 10577 recipient 5
10704 donor
LEA29Y 12917 recipient 9
13044 donor
LEA29Y 10434 recipient 0
10519 donor
LEA29Y 10884 recipient 28
10963 donor
LEA29Y 10896 recipient 0
10964 donor
LEA29Y 10574 recipient 28
10708 donor

**Fig. 39: Illustration of variation of amino acids.** For all donor-recipient pairs, amino acids spanning exons 2 in SLA-DQA (A), SLA-DQB1 (B), SLA-DRB1(C) genes translated from the amplicons. Color coding of amino acid constellations and donor-recipient pairs is as in Fig. 38.

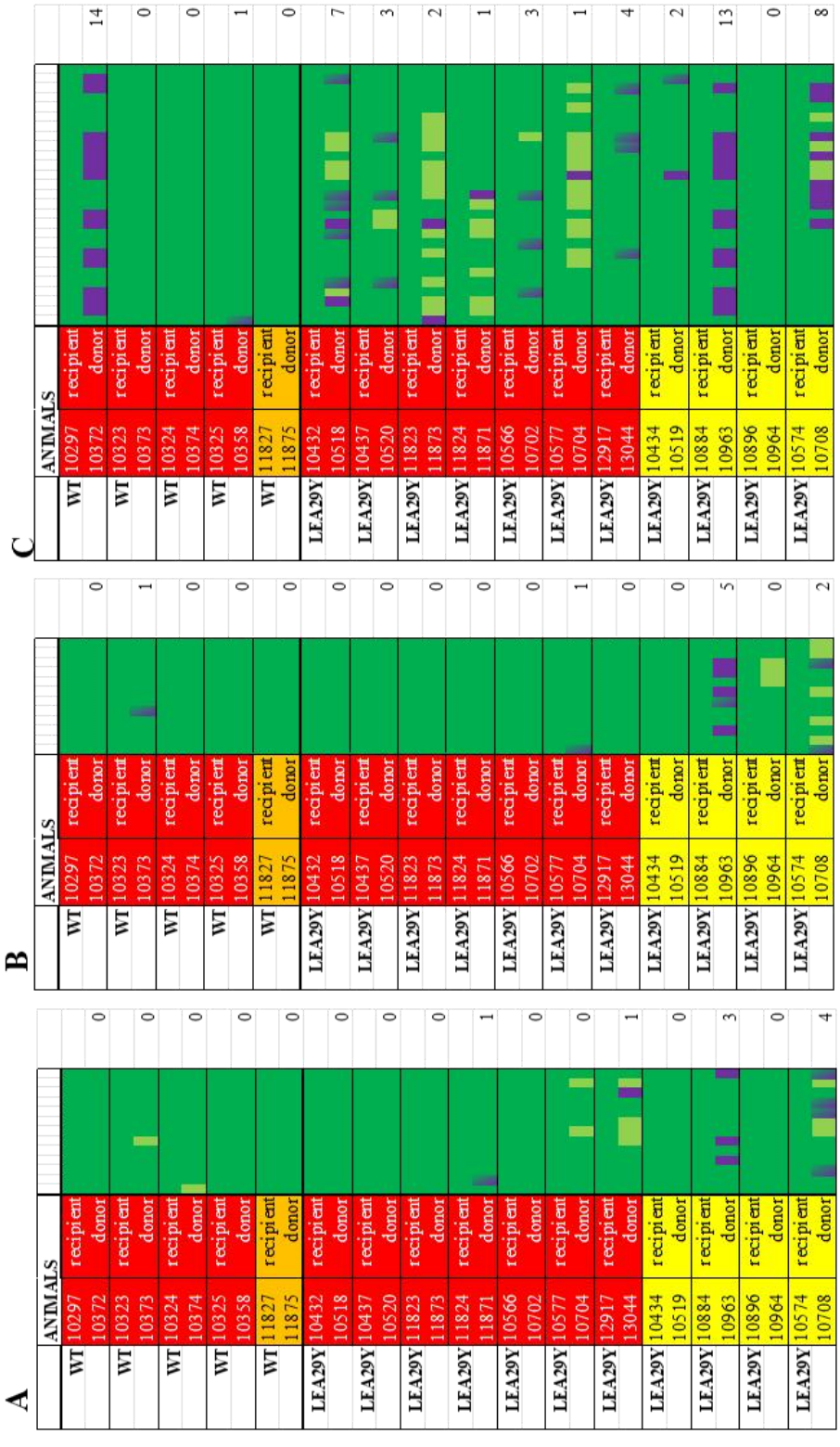

## 4.10. Demonstration of amino acid variation variation in HHTx with rejection grading of grafts

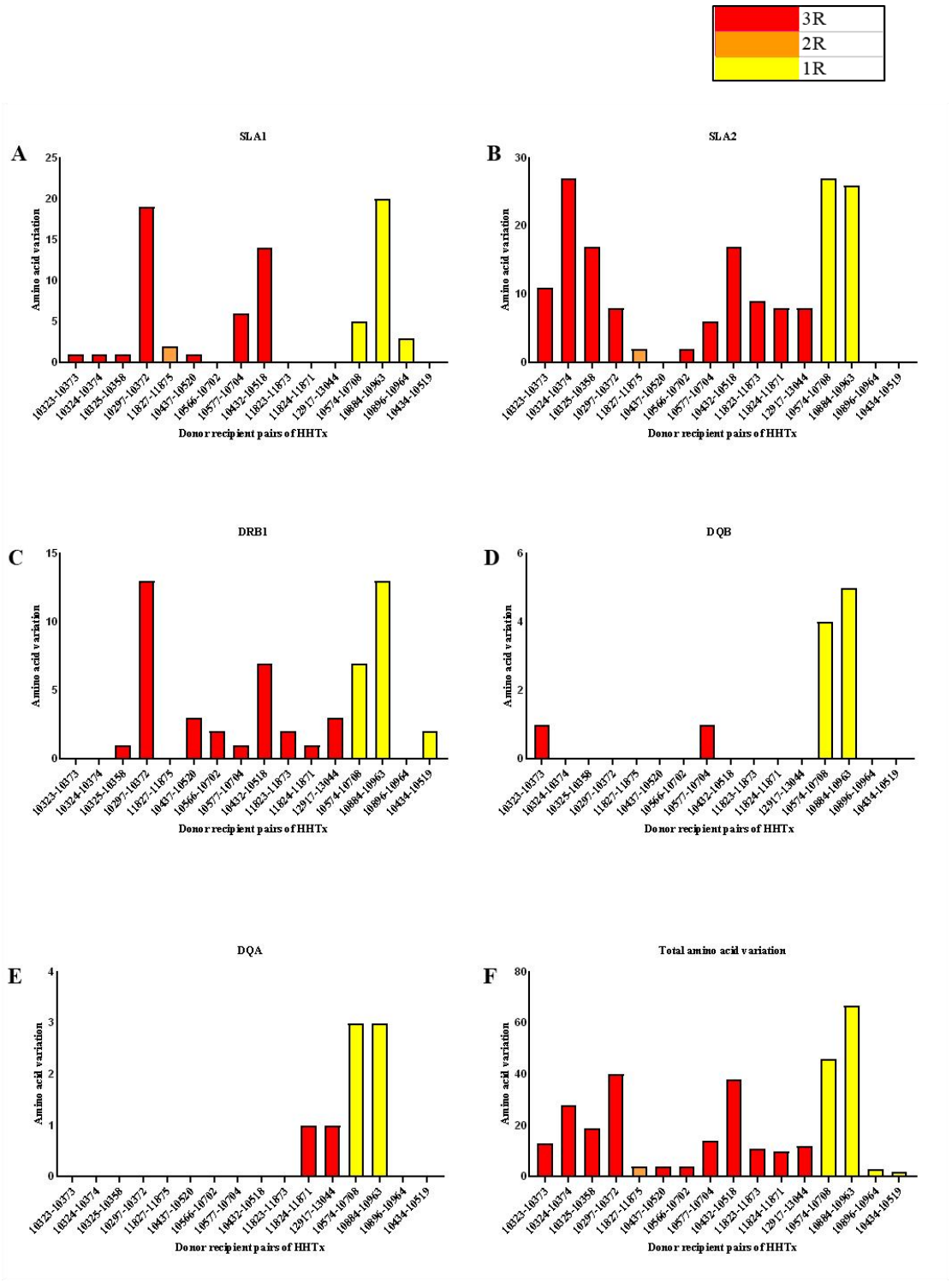


**Fig. 40: Illustration of amino acids variation between donor-recipient pairs in HHTx animals.** (A) Amino acids variation in SLA1. (B) Amino acids variation in SLA2. (C) Amino acids variation in SLA-DRB1. (D) Amino acids variation in SLA-DQB. (E) Amino acids variation in SLA-DQA. (F) Total amino acids variation among the donor-recipient pairs in HHTx.

The amino acid variability between the donor-recipient pairs of HHTx was represented along with the colour grade in regard to the grade of rejection of graft (Fig. 19). Quantitative anlysis revealed total amino acid variability scores of 2 in graft 10434, 3 in graft 10896 in surviving LEA grafts, being lowest among the HHTx transplants. Distinctly, graft 10884 exhibited amino acid variability score of 67, the highest recorded among HHTx transplants. We could not notice any pattern or correlation between rejection grade of the HHTx and amino acid variability thus implying no correlation with SLA mismatch in donor- recipient pair in HHTx.

# V. DISCUSSION

Cardiac transplantation is the end-stage treatment for patients with heart failure. After decades of successful clinical heart allotransplantation, recent years have also provided success in pig-to-human heart xenotransplantation. Graft tolerance by the recipient using as little systemic immunosuppression as possible is, however, still the ultimate goal of allo- as well as xenotransplantation that has not been accomplished yet to its full extent. This thesis offers the distinctive opportunity to use transgenic CAG-LEA29Y pigs to study the impact of local LEA29Y (belatacept) expression to alleviate T cell-mediated graft rejection, thereby providing a possible route for lowering the systemic immunosuppressive burden on the recipient in transplantation settings.

In this work, we performed heterotopic abdominal heart transplantation of either LEA29Y transgenic (HHTx) or wildtype (WT) pig hearts into a WT recipient pig to study clinical outcomes of transplantation, as well as histological and molecular markers of rejection and the role of SLA matching between the donor and the recipient. The goal was to assess the protective potential of LEA29Y expression from the donor graft by comprehensive means.

A retrospective study in heart-transplanted individuals, conducted from 2012 to 2021, revealed that histopathological detection of rejection in biopsies taken from patients generally aligns with clinical data on cellular and antibody-mediated rejections (McDonald et al., 2022). In our study, rejection grading for the cardiac grafts from HHTx was performed based on the guidelines by Stewart et al. (2005), also known as the International Society for Heart and Lung Transplantation (ISHLT) grading. This type of rejection grading is a qualitative rather than a quantitative method of judging graft rejection. As other studies, for example by Arabyarmohammadi et al. (2024) have found that clinical allograft injuries are often considerably different from histological findings in conventional qualitative rejection grading, we decided to follow a strategy of simple random sampling to examine the histology of graft rejection and combine this with an evaluation of cytokine and immune cell marker expression. Similar qualitative guidelines for cardiac grading of rejection were followed by Wu et al. (1994), where the cardiac grading of rejection was split into 3 groups as grade 0, grade 1, and grade 2-4, who additionally compared histopathological grading with the gene expression of

cytokines.

Following clinical assessment and histological rejection grading, our first point of evaluation was the examination of cytokine production from immune cells in the graft tissue. Cytokines evoke proliferation of T and B cells, trigger cytotoxic T cells and NK cells, escalate the expression of MHC and have a cytotoxic impact on the grafted allograft via recruitment of immune cells in the graft (Pirenne et al., 1994) and are thus an excellent parameter for determining rejection of the graft. Evaluation of cytokine production from immune cells can be estimated by different techniques, either with assaying mRNA through quantitative PCR or RNA sequencing. Alternatively, estimation of cytokine expression can be done on protein level by immunoassays like ELISA intracellular flow cytometry (Corris & Kirby, 2005) or immunohistochemistry. Coalescence of histological analysis with cytokine analysis can be a good approach to understand and explore the graft rejection in a transplantation setting

However, since the production of cytokines is fundamentally regulated transcriptionally, assessment of cytokines' and cell markers' mRNA expression using real-time quantitative PCR (RT-PCR) can be an alternative to measuring cytokine protein levels, as changes from mRNA expression occur before protein production (Amsen et al., 2009). This technique is helpful in measuring cytokines that are expressed in low quantities, to detect immune response cytokine feedback earlier, and to identify particular cell types producing cytokines. As qPCR is a comparatively cheap technique to run and can be adapted quickly to include a wide range of target genes that can be added to the examination panel when needed, it is at a distinct advantage over protein evaluation methods when a broad range of markers is to be examined. For these reasons, we chose this technique to evaluate graft rejection on a molecular level within the scope of this dissertation.

However, qPCR has some limitations. The starting materials for the qPCR assay must be of very high quality to ensure the accuracy in gene expression of the immune panel. Poor quality of RNA is problematic as this causes variations in efficiency during reverse transcription for cDNA synthesis and ultimately leads to inaccurate and false quantification for gene expression (Liss, 2002). Representation of expression by mRNA may not always be correlated with the actual protein expression (Smith & Osborn, 2009), as posttranscriptional processing of the mRNA may lead to differing outcomes on protein level. The

expression of RNA is also affected by the amount of live tissue in the explanted graft during the time of explantation. Necrosis of the cells disrupts the cell membrane, resulting in the expulsion of cell contents along with damage associated molecular patterns (DAMPs) (Li & Lan, 2023). Thus, the presence of large amounts of necrotic cells can influence mRNA representation (Ahn et al., 2018). In our HHTx experiments, animal 11823, which was terminated after 12 days with a 3 R grade of rejection in histological analysis, demonstrated lower levels of transcripts for most of the genes in the immune panel. The lower transcript levels despite clearly visible functional and histological rejection, may be attributable to the loss of viable, transcriptionally active cells within the necrotic regions of the analyzed samples of this graft.

On the broad spectrum, we did not observe any significant differences in the expression of the inflammatory genes between the WT-transplanted animals and LEA29Y-transplanted animals in HHTx but we see certain tendencies that point towards a protective effect of LEA29Y expression. IL-6, TNFA and IFNG have been reported as good predictors of LV function while studying cytokine profiles (Diakos et al., 2021). For example, IL-6 is seen as an early indicator of imflammatory responses that conveys the communication between the innate and the adaptive immune response (Jones, 2005). Even though not significant, expression of IL6 in the three surviving LEA29Y grafts in the LV region was lowest amongst all of the transplanted grafts in HHTx, indicating a diminished graft rejection response by the recipient.

Regarding TNFA expression, the surviving LEA29Y grafts in our study did not represent the ones with the least expression of TNFA observed among the whole cohort of transplanted hearts. TNFA is responsible for the production of intracellular adhesion molecule type 1 (ICAM-1), increasing the adherence of monocytes (Timoshanko et al., 2003), which transform to macrophages to, in turn, escalate TNFA production. Experimental primate models underwent significant, prolonged allograft preservation with systemically neutralizing TNFA (Li et al., 2019). According to Yang et al., utilization of macrophage function inhibitors and TNFA antagonists ceased the progression of any histological and clinical changes in chronic allograft nephropathy. In that sense, it is surprising that in our context, improved survival of the grafts did not correlate with reduced levels of TNFA, for which we do not have an explanation currently.

On the other hand, lowest expression of TGFB was demonstrated in the LV of the three surviving LEA29Y grafts in HHTx. TGFB is a primary cytokine responsible for fibrosis during chronic allograft rejection, resulting in delayed graft loss, for example post kidney transplantation (Campistol et al., 2001). The success or the failure of a graft is associated with TGFB, elevated TGFB levels in cardiac transplanted patients were reported to indicate graft dysfunction leading to a high risk of subsequent kidney failure due to the dysfunctional heart (Brunet, 2012; Mompart et al., 2021; van de Wetering et al., 2006). Thus, the fact that TGFB as well as IL6 levels in the non-rejected transgenic transplants were markedly lower than in rejected grafts points to a considerable protective effect of LEA29Y expression in our setting.

The region of RA of the surviving LEA29Y grafts in HHTx exhibited the lowest expression of IL1A, IL1B and IL18 amongst all of the transplanted grafts. Although the current literature does not have sufficient direct evidences that correlate the gene expressions of cytokines and cell markers specifically within right atrium with the survival outcomes of cardiac allografts, the pattern of expression of IL1A, IL1B and IL18 in surviving LEA29Y hearts is noteworthy.

Attempts to arrest T cell-mediated graft rejection by immune response modulation of CD45 have been performed by Ko et al. (2002). They demonstrated that the blockade of CD45 obstructs the proliferation and differentiation of T cells during allogenic stimulation (Ko et al., 2002). Our analysis did not display significant differences for the expression of CD45 between the transplanted LEA29Y grafts and transplanted WT grafts. Despite CD45 being a firmly established marker for graft rejection, as it is indicative of leucocyte infiltration, the surviving LEA29Y grafts from HHTx did not demonstrate the lowest degree of expression of CD45. Similarly, the surviving LEA29Y grafts did not demonstrate a consistent pattern of least expression of CD68. However, the future performance of a renal graft could be predicted with surveillance of the macrophage density, for which CD68 is a marker, during the earliest post transplantation phase(Bräsen et al., 2017). Significantly elevated CD68 numbers in the renal cortex were associated with histologically determined rejection at a later time point, thus demonstrating CD68 as a powerful predictor of prognosis for renal grafts during earliest phases after transplantation (Bräsen et al., 2017). In our context, this leads to the conclusion that, even though some LEA29Y grafts were still functional at the time point of

termination of the experiment, a longer follow-up may have resulted in chronic rejection nevertheless.

The study of the expression of cytokines and cell markers in our transplantations only gave a limited insight into the protective effect of the LEA29Y transgene, as results did not always reflect the mixed clinical outcome of graft survival. To assess a possible cause for this, retrospective Swine leukocyte antigen (SLA) profiling of the donor and recipient animals of the HHTx experiments was performed to determine the immunological compatibility between the graft donor and recipient.

UC Davis Health, Transplant Center states that the graft donors for liver, kidney and heart transplantations are evaluated by three tests, blood group, crossmatching and HLA testing, among which the first factor for the compatibility is determined by blood group match between the donor and the recipient. The rule for blood group match in organ transplantation is similar to the rule for transfusion of blood, thus setting blood group O as a universal donor and blood group AB as the universal recipient. Pre-transplantation HLA matching of donor and recipient is not routinely in application in cardiac transplantation because of time constraints between explantation and implantation (Holzhauser et al., 2020). However, retrospective studies show that HLA mismatch has consequences over the clinical outcomes of the transplantation. HLA typing, which was traditionally performed via serological testing, is now conducted with sequence-specific primer amplification and sequence-based typing (Jung, 2011), similar to what has been done on SLA within the scope of this thesis.

Holzhauser et al. (2020) performed an evaluation of HLA class I and HLA class II in clinically firm cardiac transplant recipients. In this retrospective study, a greater match in HLA was discovered in the donor-recipient pairs without donor-specific antigen (DSA) compared to the ones with DSA, suggesting the necessity to surveil HLA mismatch to improve clinical outcomes in cardiac transplants. However, in the same study, clinically stable cardiac transplants had no significant association observed between HLA matches and cellular rejection of the cardiac transplants in these patients. Firoz et al. (2024) reviewed the survival and chronic rejection consequences due to HLA mismatch at the loci level and total HLA groups in modern heart transplantation techniques. The study conducted in 33,060 adult heart transplanted patients from 2005-2021 revealed an

interesting association of increased incidences of acute organ rejection in the recipients with a higher mismatch of HLA. Mismatch in the HLA-DR in the heart transplanted patients from the same study had an upsurge in cardiac allograft vasculopathy. However, the incidence of mortality in the same group of heart transplanted patients did not demonstrate any association with mismatch of HLA among these patients. The HLA mismatch at any specific HLA loci level or the total cumulative HLA mismatch was taken into consideration while studying the mortality in these heart transplanted patients (Firoz et al., 2024).

Swine leukocyte antigen (SLA) is structurally equivalent to human leukocyte antigen (HLA). The findings from HLA were taken into consideration to dig deeper into the data set from SLA, as published data on SLA are still in the initial phases compared to HLA (Carnel et al., 2023). During the process of optimization of SLA-typing, Sørensen et al., designed universal primers for exons 2 and 3 of SLA class I genes. In order to obtain the accurate, clean and reliable sequencing data throughout the entire chromatogram, additional internal primers were developed to generate overlapping reads that span the complate target region. The PCR amplicons were sequenced with the universal primers as well as the inner primer to assemble the complete sequence of the target, i.e., exons 2 and 3 (Sørensen et al., 2017). We used a similar strategy to design primers to assemble the complete sequence of exons 2 and 3 in SLA class I. Inner reverse primers SLA1_2R and SLA1_2R were strategically located and designed for SLA1. Similarly, inner forward primer SLA2_fx1 and inner reverse primers SLA2_1R and SLA2_2R were also designed for SLA2. With this strategy, we were able to successfully assemble a complete sequence of exons 2 and 3 of SLA class I genes.

The lack of data and patterns of the impact of SLA variation between the donor-recipient pair for pig organ allotransplantation impelled us to compare the influence of SLA on organ rejection with the influence of HLA. An increasing number of HLA mismatches are linked to recurrent incidents of rejection (Zachary & Leffell, 2016). Each HLA mismatch increased the graft failure hazard by 13% (Williams et al., 2016). Each mismatch between the donor and the recipient HLA in pediatric kidney transplants increased the risk of allograft failure, and 6 mismatches increased the risk of rejection by 92% (Li et al., 2022). Comparing this knowledge from human allotransplantation with our Tx outcomes, we found that two surviving LEA29Y-WT transplanted hearts had a high ratio of SLA

match. Meanwhile, another surviving LEA29Y-WT transplanted heart, 10884, had a high SLA mismatch, also leading to higher amino acid mismatch between the donor-recipient combinations. So, in our case, there was no clear correlation between SLA mismatch between donor-recipient pairs and the clinical outcome of graft survival.

However, SLA class I (SLA1 and SLA2) and SLA class II (SLA-DRB1, SLA-DQA, SLA-DQB) interact with CD8+ T cells and CD4+ T cells, respectively, and contribute to graft rejection through distinct mechanisms. The relative impact of SLA class I and SLA class II on graft rejection differs in magnitude. Among SLA class I molecules, SLA2 exhibits higher expression than SLA1 (Hammer et al., 2020) . SLA class I molecules (SLA1 and SLA2) exhibit higher expression during the early post-transplantation phase, typically within the first six months, leading to allograft loss within this period (Lutz et al., 2013). In contrast, SLA class II expression occurs at a lower density and is primarily restricted to antigen-presenting cells (APCs). The impact of SLA class II on allograft rejection becomes more evident over an extended period, usually beyond six months. Therefore, assessing anti-SLA class I antibodies is crucial for predicting early graft loss within six months post-transplantation. Meanwhile, evaluating SLA class II compatibility becomes essential once a certain degree of clinical success has been achieved in transplantation (Lutz et al., 2013). In our study, the duration of transplantation experiments was relatively too short to study the impacts mediated by the SLA class II compatibility. Thus, the fact that variation in SLA class II between donors and recipients was very low, did likely not impact the outcome

In addition to SLA compatibility, assessing preformed antibodies and inflammation levels before transplantation is crucial for predicting post-transplant immune responses. Understanding the impact of pre-existing inflammation helps interpret cytokine expression following transplantation. In humans, donor-specific antibodies (DSA) increase the risk of acute rejection in kidney transplanted patients by 15% in non-sensitized patients and 46% in sensitized patients(Nin et al., 2018). For example, the presence of DSA in kidney transplant recipients raises the risk of allograft failure to 34%, compared to just 1% in patients without DSA (Wang et al., 2019).

A comprehensive evaluation of preformed antibodies and inflammatory markers

before transplantation can therefore improve graft survival and patient outcomes and may be a strategy for future transplantation experiments involving LEA29Y transgenic organs that may undergo a longer follow up to also monitor putative chronic rejection in these grafts. For the purpose of this thesis, preformed antibody levels and determination of pre Tx inflammation levels were not determined in donors and recipients. It may be valuable to assess these parameters retrospectively in the LEA29Y Tx settings to determine their influence on survival or failure of the grafts.

In conclusion, this thesis investigated the beneficial effects of local co-stimulation blockade by LEA29Y in a heterotopic abdominal heart transplantation model in pigs. To achieve this, pigs expressing LEA29Y were used as heart donors, and transplantation outcomes were compared to those with wild-type donor hearts. While transplantation outcomes varied and could not be attributed solely to LEA29Y expression, molecular analyses revealed a positive association of the surviving LEA29Y grafts and LEA29Y expression. However, no clear correlation was observed between SLA mismatch and graft survival in the HHTx transplant cohorts. The work in this thesis highlights the potential beneficial role of LEA29Y expression in improving graft survival under specific immunological conditions. This knowledge can be utilized as a foundation for further deciphering the benefits of local immunosupression with the long-term goal of easing the immunosuppressive burden on the recipient.

# VI. SUMMARY

**Impact of LEA29Y expression in porcine heterotopic abdominal heart transplantation model**

Cardiovascular disease (CVD) remains a major public health concern and one of the leading causes of death worldwide. Genetically modified pigs are increasingly used in preclinical research to overcome species-specific barriers and physiological incompatibilities in transplantation. Bähr et al. (2016) developed a genetically modified pig line, CAG-LEA29Y, which ubiquitously synthesizes biologically active LEA29Y (belatacept). Belatacept has a higher affinity for CD80/CD86 than CD28 on antigen-presenting cells (APCs), thereby blocking the co-stimulation pathway of T-cell activation and protecting transplanted organs from rejection. The CAG-LEA29Y pig is a promising model for studying graft protection mechanisms.

This study aimed to investigate the protective role of LEA29Y in an intra-abdominal heterotopic cardiac allotransplantation (HHTx) model. Transcript analysis of graft samples was performed to examine the cellular and molecular responses of the donor transgenic pig and the immune responses of the recipient. Understanding these responses is crucial for ensuring the long-term effectiveness of LEA29Y in regulating T-cell-mediated rejection. Real-time quantitative PCR (RT-PCR) was used to assess cytokine and cell marker mRNA expression, as mRNA changes precede protein production.

The surviving LEA transplants (10434, 10884, and 10886) exhibited lower expression levels of most cytokines and cell markers compared to both non-surviving LEA transplants and wild-type (WT) transplants. WT transplants and non-surviving LEA transplants showed severe rejection (grade 3R) with extensive myocyte damage and multifocal infiltrations, whereas surviving LEA transplants displayed only mild rejection (grade 1R) with interstitial and perivascular infiltration but no myocyte damage.

SLA mismatch was identified as a potential factor influencing the mixed outcomes of LEA29Y's protective effects on pig heart allografts. Single nucleotide polymorphisms (SNPs) were detected in exon 2 and exon 3 of SLA class I (SLA1, SLA2) and exon 2 of SLA class II (SLA-DRB1, SLA-DQA, SLA-

DQB). SLA mismatches were numerically graded based on donor-recipient amino acid interactions. However, gene expression of cytokines and cell markers, as well as rejection severity, did not strictly correlate with SLA mismatch scores.

To improve transplantation outcomes, it may be advisable to assess preformed antibodies and inflammation levels before transplantation. Evaluating pre-existing immune activation is crucial for understanding post-transplant cytokine responses. Flow cytometry crossmatching (FXCM) could be used to screen for alloantibody levels, helping to predict potential immune responses and improve graft survival.

# VII. ZUSAMMENFASSUNG

**Auswirkungen der LEA29Y-Expression im Modell der heterotopen abdominalen Herztransplantation bei Schweinen**

Herz-Kreislauf-Erkrankungen (CVD) bleiben ein bedeutendes Problem der öffentlichen Gesundheit und eine der weltweit führenden Todesursachen. Genetisch modifizierte Schweine werden zunehmend in der präklinischen Forschung eingesetzt, um artspezifische Barrieren und physiologische Inkompatibilitäten in der Transplantation zu überwinden. Bähr et al. (2016) entwickelten eine genetisch modifizierte Schweinelinie, CAG-LEA29Y, die das biologisch aktive LEA29Y (Belatacept) ubiquitär synthetisiert. Belatacept weist eine höhere Affinität zu CD80/CD86 als zu CD28 auf antigenpräsentierenden Zellen (APCs) auf und blockiert so den Co-Stimulationsweg der T-Zell-Aktivierung, wodurch transplantierte Organe vor Abstoßung geschützt werden. Das CAG-LEA29Y-Schwein ist ein vielversprechendes Modell zur Untersuchung von Mechanismen des Transplantatschutzes.

Ziel dieser Studie war es, die schützende Rolle von LEA29Y in einem intraabdominalen heterotopen kardialen Allotransplantationsmodell (HHTx) zu untersuchen. Eine Transkriptanalyse von Transplantatproben wurde durchgeführt, um die zellulären und molekularen Reaktionen des transgenen Spenderschweins sowie die Immunantworten des Empfängers zu analysieren. Das Verständnis dieser Reaktionen ist entscheidend für die langfristige Wirksamkeit von LEA29Y bei der Regulation der T-Zell-vermittelten Abstoßung. Die Echtzeit-quantitative PCR (RT-PCR) wurde eingesetzt, um die mRNA-Expression von Zytokinen und Zellmarkern zu bewerten, da mRNA-Veränderungen der Proteinproduktion vorausgehen.

Die überlebenden LEA-Transplantate (10434, 10884 und 10886) zeigten niedrigere Expressionsniveaus der meisten Zytokine und Zellmarker im Vergleich zu nicht überlebenden LEA-Transplantaten und Wildtyp- (WT) Transplantaten. WT-Transplantate und nicht überlebende LEA-Transplantate wiesen eine schwere Abstoßung (Grad 3R) mit ausgeprägten Myozytenschäden und multifokalen Infiltrationen auf, während überlebende LEA-Transplantate nur eine milde Abstoßung (Grad 1R) mit interstitieller und perivaskulärer Infiltration, aber ohne Myozytenschäden zeigten.

Ein SLA-Mismatch wurde als potenzieller Faktor für die unterschiedlichen Schutzwirkungen von LEA29Y auf Schweineherz-Allotransplantate identifiziert. Einzelnukleotid-Polymorphismen (SNPs) wurden in Exon 2 und Exon 3 der SLA-Klasse-I-Gene (SLA1, SLA2) sowie in Exon 2 der SLA-Klasse-II-Gene (SLA-DRB1, SLA-DQA, SLA-DQB) nachgewiesen. SLA-Mismatches wurden numerisch anhand der Aminosäureinteraktionen zwischen Spender und Empfänger bewertet. Allerdings korrelierten die Genexpression von Zytokinen und Zellmarkern sowie der Schweregrad der Abstoßung nicht strikt mit den SLA-Mismatch-Scores.

Um die Ergebnisse von Transplantationen zu verbessern, könnte es sinnvoll sein, vor der Transplantation vorgebildete Antikörper und Entzündungsniveaus zu untersuchen. Die Bewertung einer bereits bestehenden Immunaktivierung ist entscheidend für das Verständnis der posttransplantativen Zytokinreaktionen. Die Durchflusszytometrie-Kreuzprobe (FXCM) könnte zur Bestimmung der Alloantikörper-Spiegel verwendet werden, um potenzielle Immunreaktionen vorherzusagen und das Überleben des Transplantats zu verbessern.

# VIII. INDEX OF FIGURES

# IX. INDEX OF TABLES

# X. REFERENCES

Ahn, S.-H., Ahn, J.-H., Ryu, D.-R., Lee, J., Cho, M.-S., & Choi, Y.-H. (2018). Effect of necrosis on the miRNA-mRNA regulatory network in CRT-MG human astroglioma cells. *Cancer Research and Treatment: Official Journal of Korean Cancer Association*, *50*(2), 382-397.

Amsen, D., de Visser, K. E., & Town, T. (2009). Approaches to determine expression of inflammatory cytokines. *Methods Mol Biol*,

Arabyarmohammadi, S., Yuan, C., Viswanathan, V. S., Lal, P., Feldman, M. D., Fu, P., Margulies, K. B., Madabhushi, A., & Peyster, E. G. (2024). Failing to Make the Grade: Conventional Cardiac Allograft Rejection Grading Criteria Are Inadequate for Predicting Rejection Severity. *Circulation: Heart Failure*, *17*(2), e010950.

Bähr, A., Käser, T., Kemter, E., Gerner, W., Kurome, M., Baars, W., Herbach, N., Witter, K., Wünsch, A., Talker, S. C., Kessler, B., Nagashima, H., Saalmüller, A., Schwinzer, R., Wolf, E., & Klymiuk, N. (2016). Ubiquitous LEA29Y Expression Blocks T Cell Co-Stimulation but Permits Sexual Reproduction in Genetically Modified Pigs. *PLoS One*, *11*(5), e0155676.

Ballet, C., Renaudin, K., Degauque, N., Mai, H., Boeffard, F., Lair, D., Berthelot, L., Feng, C., Smit, H., & Usal, C. (2009). Indirect CD4+ TH1 response, antidonor antibodies and diffuse C4d graft deposits in long-term recipients conditioned by donor antigens priming. *American Journal of Transplantation*, *9*(4), 697-708.

Ballingall, K. T., Bontrop, R. E., Ellis, S. A., Grimholt, U., Hammond, J. A., Ho, C.-S., Kaufman, J., Kennedy, L. J., Maccari, G., & Miller, D. (2018). Comparative MHC nomenclature: report from the ISAG/IUIS-VIC committee 2018. *Immunogenetics*, *70*, 625-632.

Bassoy, E. Y., Walch, M., & Martinvalet, D. (2021). Reactive Oxygen Species: Do They Play a Role in Adaptive Immunity? *Front Immunol*, *12*, 755856.

Bentley, G., Higuchi, R., Hoglund, B., Goodridge, D., Sayer, D., Trachtenberg, E., & Erlich, H. (2009). High-resolution, high-throughput HLA genotyping by next-generation sequencing. *Tissue antigens*, *74*(5), 393-403.

Berger, M., Baliker, M., Van Gelder, T., Böhmig, G. A., Mannon, R. B., Kumar, D., Chadban, S., Nickerson, P., Lee, L. A., & Djamali, A. (2024). Chronic Active Antibody-mediated Rejection: Opportunity to Determine the Role of Interleukin-6 Blockade. *Transplantation*, *108*(5), 1109-1114.

Billingham, R. E. (1971). The passenger cell concept in transplantation immunology. *Cellular immunology*, *2*(1), 1-12.

Bode, J., Dutow, P., Sommer, K., Janik, K., Glage, S., Tümmler, B., Munder, A., Laudeley, R., Sachse, K. W., & Klos, A. (2012). A new role of the complement system: C3 provides protection in a mouse model of lung infection with intracellular Chlamydia psittaci. *PLoS One*, *7*(11), e50327.

Boneva, R. S., Folks, T. M., & Chapman, L. E. (2001). Infectious disease issues in xenotransplantation. *Clin Microbiol Rev*, *14*(1), 1-14.

Bräsen, J. H., Khalifa, A., Schmitz, J., Dai, W., Einecke, G., Schwarz, A., Hallensleben, M., Schmidt, B. M. W., Kreipe, H. H., Haller, H., & von Vietinghoff, S. (2017). Macrophage density in early surveillance biopsies predicts future renal transplant function. *Kidney international*, *92*(2), 479-489.

Braza, F., Brouard, S., Chadban, S., & Goldstein, D. R. (2016). Role of TLRs and DAMPs in allograft inflammation and transplant outcomes. *Nat Rev Nephrol*, *12*(5), 281-290.

Breart, B., Lemaître, F., Celli, S., & Bousso, P. (2008). Two-photon imaging of intratumoral CD8+ T cell cytotoxic activity during adoptive T cell therapy in mice. *The Journal of clinical investigation*, *118*(4), 1390-1397.

Bretscher, P. A. (1999). A two-step, two-signal model for the primary activation of precursor helper T cells. *Proceedings of the National Academy of Sciences*, *96*(1), 185-190.

Brunet, M. (2012). Cytokines as predictive biomarkers of alloreactivity. *Clinica chimica acta*, *413*(17-18), 1354-1358.

Bühler, L., Basker, M., Alwayn, I. P. J., Goepfert, C., Kitamura, H., Kawai, T., Gojo, S., Kozlowski, T., Ierino, F. L., Awwad, M., Sachs, D. H., Sackstein, R., Robson, S. C., & Cooper, D. K. C. (2000). COAGULATION AND THROMBOTIC DISORDERS ASSOCIATED WITH PIG ORGAN AND HEMATOPOIETIC CELL TRANSPLANTATION IN NONHUMAN PRIMATES. *Transplantation*, *70*(9), 1323-1331.

Byrne, G. W., Davies, W. R., Oi, K., Rao, V. P., Teotia, S. S., Ricci, D., Tazelaar, H. D., Walker, R. C., Logan, J. S., & McGregor, C. G. (2006). Increased immunosuppression, not anticoagulation, extends cardiac xenograft survival. *Transplantation*, *82*(12), 1787-1791.

Campistol, J. M., Iñigo, P., Larios, S., Bescos, M., & Oppenheimer, F. (2001). Role of transforming growth factor-beta1 in the progression of chronic allograft nephropathy. *Nephrol Dial Transplant*, *16 Suppl 1*, 114-116.

Carnel, N., Lancia, H. H., Guinier, C., & Benichou, G. (2023). Pathways of Antigen Recognition by T Cells in Allograft Rejection. *Transplantation*, *107*(4), 827-837.

Corris, P., & Kirby, J. (2005). A role for cytokine measurement in therapeutic monitoring of immunosuppressive drugs following lung transplantation. *Clinical & Experimental Immunology*, *139*(2), 176-178.

Costanzo-Nordin, M. (1992). Cardiac allograft vasculopathy: relationship with acute cellular rejection and histocompatibility. *The Journal of heart and lung transplantation: the official publication of the International Society for Heart Transplantation*, *11*(3 Pt 2), S90-103.

Courtney, A. H., Shvets, A. A., Lu, W., Griffante, G., Mollenauer, M., Horkova, V., Lo, W. L., Yu, S., Stepanek, O., Chakraborty, A. K., & Weiss, A. (2019). CD45 functions as a signaling gatekeeper in T cells. *Sci Signal*, *12*(604).

Cui, J., Qin, L., Zhang, J., Abrahimi, P., Li, H., Li, G., Tietjen, G. T., Tellides, G., Pober, J. S., & Mark Saltzman, W. (2017). Ex vivo pretreatment of human vessels with siRNA nanoparticles provides protein silencing in endothelial cells. *Nature Communications*, *8*(1), 191.

Cullen, P. P., Tsui, S. S., Caplice, N. M., & Hinchion, J. A. (2021). A state-of-the-art review of the current role of cardioprotective techniques in cardiac transplantation. *Interactive cardiovascular and thoracic surgery*, *32*(5), 683-694.

Diakos, N. A., Taleb, I., Kyriakopoulos, C. P., Shah, K. S., Javan, H., Richins, T. J., Yin, M. Y., Yen, C. G., Dranow, E., Bonios, M. J., Alharethi, R., Koliopoulou, A. G., Taleb, M., Fang, J. C., Selzman, C. H., Stellos, K., & Drakos, S. G. (2021). Circulating and Myocardial Cytokines Predict Cardiac Structural and Functional Improvement in Patients With Heart Failure Undergoing Mechanical Circulatory Support. *J Am Heart Assoc*, *10*(20), e020238.

Egen, J. G., Rothfuchs, A. G., Feng, C. G., Horwitz, M. A., Sher, A., & Germain, R. N. (2011). Intravital imaging reveals limited antigen presentation and T cell effector function in mycobacterial granulomas. *Immunity*, *34*(5), 807-819.

Esensten, J. H., Helou, Y. A., Chopra, G., Weiss, A., & Bluestone, J. A. (2016). CD28 Costimulation: From Mechanism to Therapy. *Immunity*, *44*(5), 973-988.

Ezzelarab, M. B., Ekser, B., Azimzadeh, A., Lin, C. C., Zhao, Y., Rodriguez, R., Echeverri, G. J., Iwase, H., Long, C., & Hara, H. (2015). Systemic inflammation in xenograft recipients precedes activation of coagulation. *Xenotransplantation*, *22*(1), 32-47.

Firoz, A., Geier, S., Yanagida, R. O. H., Hamad, E., Rakita, V. A. L., Zhao, H., Kashem, M., & Toyoda, Y. (2024). Heart Transplant Human Leukocyte Antigen Matching in the Modern Era. *Journal of Cardiac Failure*, *30*(2), 362-372.

Flécher, E., Fouquet, O., Ruggieri, V. G., Chabanne, C., Lelong, B., & Leguerrier, A. (2013). Heterotopic heart transplantation: where do we stand? *Eur J Cardiothorac Surg*, *44*(2), 201-206.

Fu, X., Segiser, A., Carrel, T. P., Tevaearai Stahel, H. T., & Most, H. (2016). Rat Heterotopic Heart Transplantation Model to Investigate Unloading-Induced Myocardial Remodeling. *Front Cardiovasc Med*, *3*, 34.

Gabriel, C., Fürst, D., Faé, I., Wenda, S., Zollikofer, C., Mytilineos, J., & Fischer, G. (2014). HLA typing by next-generation sequencing–getting closer to reality. *Tissue antigens*, *83*(2), 65-75.

Gao, C., He, X., Quan, J., Jiang, Q., Lin, H., Chen, H., & Qu, L. (2017). Specificity characterization of SLA class I molecules binding to swine-origin viral cytotoxic T lymphocyte epitope peptides in vitro. *Frontiers in Microbiology*, *8*, 2524.

Gottfried, E., Kunz-Schughart, L., Weber, A., Rehli, M., Peuker, A., Müller, A., Kastenberger, M., Brockhoff, G., Andreesen, R., & Kreutz, M. (2008). Expression of CD68 in non-myeloid cell types. *Scandinavian journal of immunology*, *67*(5), 453-463.

Gueler, F., Rong, S., Gwinner, W., Mengel, M., Bröcker, V., Schön, S., Greten, T. F., Hawlisch, H., Polakowski, T., & Schnatbaum, K. (2008). Complement 5a receptor inhibition improves renal allograft survival. *Journal of the American Society of Nephrology*, *19*(12), 2302-2312.

Hammer, S., Duckova, T., Groiss, S., Stadler, M., Jensen-Waern, M., Golde, W., Gimsa, U., & Saalmueller, A. (2021). Comparative analysis of swine leukocyte antigen gene diversity in European farmed pigs. *Animal Genetics*, *52*(4), 523-531.

Hammer, S. E., Ho, C.-S., Ando, A., Rogel-Gaillard, C., Charles, M., Tector, M., Tector, A. J., & Lunney, J. K. (2020). Importance of the major histocompatibility complex (swine leukocyte antigen) in swine health and biomedical research. *Annual review of animal biosciences*, *8*(1), 171-198.

Hara, H., Long, C., Lin, Y. J., Tai, H. C., Ezzelarab, M., Ayares, D., & Cooper, D. K. (2008). In vitro investigation of pig cells for resistance to human antibody-mediated rejection. *Transplant International*, *21*(12), 1163-1174.

Hoffmann, M. W., Wonigeit, K., Steinhoff, G., Herzbeck, H., Flad, H. D., & Pichlmayr, R. (1993). Production of cytokines (TNF-alpha, IL-1-beta) and endothelial cell activation in human liver allograft rejection. *Transplantation*, *55*(2), 329-335.

Holzhauser, L., Misra, M., Miller, T., Kalantari, S., Smith, B., Nguyen, A., Chung, B., Sarswat, N., Kim, G., Marino, S., & Grinstein, J. (2020). HLA Matching in Cardiac Transplantation - Impact on Cardiac Allograft Vasculopathy, Rejection and Donor Specific Antibodies. *Journal of Cardiac Failure*, *26*(10, Supplement), S157.

Hossen, M. M., Ma, Y., Yin, Z., Xia, Y., Du, J., Huang, J. Y., Huang, J. J., Zou, L., Ye, Z., & Huang, Z. (2023). Current understanding of CTLA-4: from mechanism to autoimmune diseases. *Frontiers in Immunology*, *14*, 1198365.

Houser, S. L., Kuwaki, K., Knosalla, C., Dor, F. J., Gollackner, B., Cheng, J., Shimizu, A., Schuurman, H. J., & Cooper, D. K. (2004). Thrombotic microangiopathy and graft arteriopathy in pig hearts following transplantation into baboons. *Xenotransplantation*, *11*(5), 416-425.

Hryhorowicz, M., Zeyland, J., Słomski, R., & Lipiński, D. (2017). Genetically modified pigs as organ donors for xenotransplantation. *Molecular Biotechnology*, *59*, 435-444.

Huse, M., Lillemeier, B. F., Kuhns, M. S., Chen, D. S., & Davis, M. M. (2006). T cells use two directionally distinct pathways for cytokine secretion. *Nature immunology*, *7*(3), 247-255.

Ingulli, E. (2010). Mechanism of cellular rejection in transplantation. *Pediatric nephrology*, *25*(1), 61-74.

Jackson, S. H., Devadas, S., Kwon, J., Pinto, L. A., & Williams, M. S. (2004). T cells express a phagocyte-type NADPH oxidase that is activated after T cell receptor stimulation. *Nature immunology*, *5*(8), 818-827.

Jones, S. A. (2005). Directing transition from innate to acquired immunity: defining a role for IL-6. *The Journal of Immunology*, *175*(6), 3463-3468.

Jordan, S. C., Choi, J., Kim, I., Wu, G., Toyoda, M., Shin, B., & Vo, A. (2017). Interleukin-6, A Cytokine Critical to Mediation of Inflammation, Autoimmunity and Allograft Rejection: Therapeutic Implications of IL-6 Receptor Blockade. *Transplantation*, *101*(1), 32-44.

Jung, H. L. (2011). Shedding a new light on the HLA matching. *The Korean Journal of Hematology*, *46*(1), 1-2.

Kadner, A., Chen, R. H., & Adams, D. H. (2000). Heterotopic heart transplantation: experimental development and clinical experience. *European journal of cardio-thoracic surgery*, *17*(4), 474-481.

Kenmochi, T., Mullen, Y., Miyamoto, M., & Stein, E. (1994). Swine as an allotransplantation model. *Veterinary Immunology and Immunopathology*, *43*(1-3), 177-183.

Khan, M. A., & Shamma, T. (2019). Complement factor and T-cell interactions during alloimmune inflammation in transplantation. *Journal of Leukocyte Biology*, *105*(4), 681-694.

Kirk, F. G. (2003). Where is the alloimmune response initiated? *American Journal of Transplantation*, *3*(3), 241-242.

Ko, S., Jaeger, M. D., Dahlke, M. H., Nakajima, Y., & Schlitt, H. J. (2002). Manipulation of CD45 antigen in transplantation tolerance. *Curr Mol Med*, *2*(3), 249-255.

Lalli, P. N., Strainic, M. G., Yang, M., Lin, F., Medof, M. E., & Heeger, P. S. (2008). Locally produced C5a binds to T cell–expressed C5aR to enhance effector T-cell expansion by limiting antigen-induced apoptosis. *Blood, The Journal of the American Society of Hematology*, *112*(5), 1759-1766.

Li, J., Li, C., Zhuang, Q., Peng, B., Zhu, Y., Ye, Q., & Ming, Y. (2019). The Evolving Roles of Macrophages in Organ Transplantation. *J Immunol Res*, *2019*, 5763430.

Li, K., Anderson, K. J., Peng, Q., Noble, A., Lu, B., Kelly, A. P., Wang, N., Sacks, S. H., & Zhou, W. (2008). Cyclic AMP plays a critical role in C3a-receptor–mediated regulation of dendritic cells in antigen uptake and T-cell stimulation. *Blood, The Journal of the American Society of Hematology*, *112*(13), 5084-5094.

Li, Q., & Lan, P. (2023). Activation of immune signals during organ transplantation. *Signal transduction and targeted therapy*, *8*(1), 110.

Li, W., Nava, R. G., Bribriesco, A. C., Zinselmeyer, B. H., Spahn, J. H., Gelman, A. E., Krupnick, A. S., Miller, M. J., & Kreisel, D. (2012). Intravital 2-photon imaging of leukocyte trafficking in beating heart. *The Journal of clinical investigation*, *122*(7), 2499-2508.

Li, Y., Nieuwenhuis, L. M., Keating, B. J., Festen, E. A. M., & de Meijer, V. E. (2022). The Impact of Donor and Recipient Genetic Variation on Outcomes After Solid Organ Transplantation: A Scoping Review and Future Perspectives. *Transplantation*, *106*(8), 1548-1557.

Liss, B. (2002). Improved quantitative real-time RT-PCR for expression profiling of individual cells. *Nucleic Acids Res*, *30*(17), e89.

Liu, J., Lin, F., Strainic, M. G., An, F., Miller, R. H., Altuntas, C. Z., Heeger, P. S., Tuohy, V. K., & Medof, M. E. (2008). IFN-γ and IL-17 production in experimental autoimmune encephalomyelitis depends on local APC–T cell complement production. *The Journal of Immunology*, *180*(9), 5882-5889.

Lunney, J. K., Ho, C.-S., Wysocki, M., & Smith, D. M. (2009). Molecular genetics of the swine major histocompatibility complex, the SLA complex. *Developmental & Comparative Immunology*, *33*(3), 362-374.

Lutz, A. J., Li, P., Estrada, J. L., Sidner, R. A., Chihara, R. K., Downey, S. M., Burlak, C., Wang, Z. Y., Reyes, L. M., & Ivary, B. (2013). Double knockout pigs deficient in N-glycolylneuraminic acid and G alactose α-1, 3-G alactose reduce the humoral barrier to xenotransplantation. *Xenotransplantation*, *20*(1), 27-35.

Ma, Q., Li, D., Nurieva, R., Patenia, R., Bassett, R., Cao, W., Alekseev, A. M., He, H., Molldrem, J. J., & Kroll, M. H. (2012). Reduced graft-versus-host disease in C3-deficient mice is associated with decreased donor Th1/Th17 differentiation. *Biology of Blood and Marrow Transplantation*, *18*(8), 1174-1181.

Maccari, G., Robinson, J., Ballingall, K., Guethlein, L. A., Grimholt, U., Kaufman, J., Ho, C.-S., De Groot, N. G., Flicek, P., & Bontrop, R. E. (2017). IPD-MHC 2.0: an improved inter-species database for the study of the major histocompatibility complex. *Nucleic acids research*, *45*(D1), D860-D864.

Magee, C. N., Boenisch, O., & Najafian, N. (2012). The role of costimulatory molecules in directing the functional differentiation of alloreactive T helper cells. *Am J Transplant*, *12*(10), 2588-2600.

Manikwar, P., Kiptoo, P., Badawi, A. H., Büyüktimkin, B., & Siahaan, T. J. (2012). Antigen-specific blocking of CD4-specific immunological synapse formation using BPI and current therapies for autoimmune diseases. *Med Res Rev*, *32*(4), 727-764.

Marchal, G., Dausset, J., & Colombani, J. (1962). Frequency of anti-platelet iso-antibodies in polytransfused patients. *Bibliotheca haematologica*, *13*, 319-323.

McDonald, M. M., Mihalj, M., Zhao, B., Nathan, S., Matejin, S., Ottaviani, G., Jezovnik, M. K., Radovancevic, R., Kar, B., Gregoric, I. D., & Buja, L. M. (2022). Clinicopathological correlations in heart transplantation recipients complicated by death or re-transplantation. *Front Cardiovasc Med*, *9*, 1014796.

Mehta, A. K., Gracias, D. T., & Croft, M. (2018). TNF activity and T cells. *Cytokine*, *101*, 14-18.

Meier-Kriesche, H. U., Schold, J. D., & Kaplan, B. (2004). Long-term renal allograft survival: have we made significant progress or is it time to rethink our analytic and therapeutic strategies? *American Journal of Transplantation*, *4*(8), 1289-1295.

Mendiola Pla, M., Evans, A., Lee, F. H., Chiang, Y., Bishawi, M., Vekstein, A., Kang, L., Zapata, D., Gross, R., Carnes, A., Gault, L. E., Balko, J. A., Bonadonna, D., Ho, S., Lezberg, P., Bryner, B. S., Schroder, J. N., Milano, C. A., & Bowles, D. E. (2022). A Porcine Heterotopic Heart Transplantation Protocol for Delivery of Therapeutics to a Cardiac Allograft. *J Vis Exp*(180).

Mohiuddin, M. M., Reichart, B., Byrne, G. W., & McGregor, C. G. A. (2015). Current status of pig heart xenotransplantation. *Int J Surg*, *23*(Pt B), 234-239.

Mompart, F., Kamgoué, A., Lahbib-Mansais, Y., Robelin, D., Bonnet, A., Rogel-Gaillard, C., Kocanova, S., & Yerle-Bouissou, M. (2021). The 3D nuclear conformation of the major histocompatibility complex changes upon cell activation both in porcine and human macrophages. *BMC Molecular and Cell Biology*, *22*(1), 45.

Mori, D. N., Kreisel, D., Fullerton, J. N., Gilroy, D. W., & Goldstein, D. R. (2014). Inflammatory triggers of acute rejection of organ allografts. *Immunological reviews*, *258*(1), 132-144.

Müller, A. J., Filipe-Santos, O., Eberl, G., Aebischer, T., Späth, G. F., & Bousso, P. (2012). CD4+ T cells rely on a cytokine gradient to control intracellular pathogens beyond sites of antigen presentation. *Immunity*, *37*(1), 147-157.

Nakamura, T., Shirouzu, T., Nakata, K., Yoshimura, N., & Ushigome, H. (2019). The Role of Major Histocompatibility Complex in Organ Transplantation- Donor Specific Anti-Major Histocompatibility Complex Antibodies Analysis Goes to the Next Stage. *Int J Mol Sci*, *20*(18).

Nakanishi, K. (2018). Unique Action of Interleukin-18 on T Cells and Other Immune Cells. *Front Immunol*, *9*, 763.

Nin, M., Tiscornia, A., Zulberti, C., Lorenzo, M., Curi, L., Orihuela, S., Carretto, E., Burgnstaller, E., Dibello, N., Gonzalez-Martinez, F., Noboa, O., & Bengochea, M. (2018). Presence of Pre-Existing HLA Antibodies in Renal Transplant Patients and its Impact During the First Year Post Transplant. *Transplantation*, *102*, S686.

Nozaki, T., Rosenblum, J. M., Ishii, D., Tanabe, K., & Fairchild, R. L. (2008). CD4 T Cell-Mediated Rejection of Cardiac Allografts in B Cell-Deficient Mice1. *The Journal of Immunology*, *181*(8), 5257-5263.

Peng, Q., Li, K., Wang, N., Li, Q., Asgari, E., Lu, B., Woodruff, T. M., Sacks, S. H., & Zhou, W. (2009). Dendritic cell function in allostimulation is modulated by C5aR signaling. *The Journal of Immunology*, *183*(10), 6058-6068.

Perona-Wright, G., Mohrs, K., & Mohrs, M. (2010). Sustained signaling by canonical helper T cell cytokines throughout the reactive lymph node. *Nature immunology*, *11*(6), 520-526.

Phelps, C. J., Koike, C., Vaught, T. D., Boone, J., Wells, K. D., Chen, S. H., Ball, S., Specht, S. M., Polejaeva, I. A., Monahan, J. A., Jobst, P. M., Sharma, S. B., Lamborn, A. E., Garst, A. S., Moore, M., Demetris, A. J., Rudert, W. A., Bottino, R., Bertera, S.,…Ayares, D. L. (2003). Production of alpha 1,3-galactosyltransferase-deficient pigs. *Science*, *299*(5605), 411-414.

Pietra, B. A., Wiseman, A., Bolwerk, A., Rizeq, M., & Gill, R. G. (2000). CD4 T cell-mediated cardiac allograft rejection requires donor but not host MHC class II. *J Clin Invest*, *106*(8), 1003-1010.

Pirenne, J., Pirenne-Noizat, F., de Groote, D., Vrindts, Y., Lopez, M., Gathy, R., Jacquet, N., Meurisse, M., Honore, P., & Franchimont, P. (1994). Cytokines and organ transplantation. A review. *Nuclear Medicine and Biology*, *21*(3), 545-555.

Pittman, K., & Kubes, P. (2013). Damage-associated molecular patterns control neutrophil recruitment. *Journal of innate immunity*, *5*(4), 315-323.

Rheinländer, A., Schraven, B., & Bommhardt, U. (2018). CD45 in human physiology and clinical medicine. *Immunology letters*, *196*, 22-32.

Riha, P., & Rudd, C. E. (2010). CD28 co-signaling in the adaptive immune response. *Self Nonself*, *1*(3), 231-240.

Saadi, S., Takahashi, T., Holzknecht, R. A., & Platt, J. L. (2004). Pathways to acute humoral rejection. *The American journal of pathology*, *164*(3), 1073-1080.

Santamore, W. P., & Dell'Italia, L. J. (1998). Ventricular interdependence: significant left ventricular contributions to right ventricular systolic function. *Prog Cardiovasc Dis*, *40*(4), 289-308.

Saunders, A., & Johnson, P. (2010). Modulation of immune cell signalling by the leukocyte common tyrosine phosphatase, CD45. *Cellular signalling*, *22*(3), 339-348.

Seto, T., Kamijo, S., Wada, Y., Yamaura, K., Takahashi, K., Komatsu, K., Otsu, Y., Terasaki, T., Fukui, D., & Amano, J. (2010). Upregulation of the apoptosis-related inflammasome in cardiac allograft rejection. *The Journal of Heart and Lung Transplantation*, *29*(3), 352-359.

Sharpe, A. H., & Freeman, G. J. (2002). The B7–CD28 superfamily. *Nature Reviews Immunology*, *2*(2), 116-126.

Siu, J. H. Y., Surendrakumar, V., Richards, J. A., & Pettigrew, G. J. (2018). T cell Allorecognition Pathways in Solid Organ Transplantation. *Front Immunol*, *9*, 2548.

Smith, C. J., & Osborn, A. M. (2009). Advantages and limitations of quantitative PCR (Q-PCR)-based approaches in microbial ecology. *FEMS Microbiol Ecol*, *67*(1), 6-20.

Snell, G. (1978). T cells, T cell recognition structures, and the major histocompatibility complex. *Immunological reviews*, *38*(1), 3-69.

Sommer, S. (2005). The importance of immune gene variability (MHC) in evolutionary ecology and conservation. *Frontiers in zoology*, *2*, 1-18.

Sørensen, M. R., Ilsøe, M., Strube, M. L., Bishop, R., Erbs, G., Hartmann, S. B., & Jungersen, G. (2017). Sequence-Based Genotyping of Expressed Swine Leukocyte Antigen Class I Alleles by Next-Generation Sequencing Reveal Novel Swine Leukocyte Antigen Class I Haplotypes and Alleles in Belgian, Danish, and Kenyan Fattening Pigs and Göttingen Minipigs. *Front Immunol*, *8*, 701.

Srivastava, S., & Ernst, J. D. (2013). Cutting Edge: Direct Recognition of Infected Cells by CD4 T Cells Is Required for Control of Intracellular Mycobacterium tuberculosis In Vivo. *The Journal of Immunology*, *191*(3), 1016-1020. https://doi.org/10.4049/jimmunol.1301236

Steinmuller, D. (1980). Passenger leukocytes and the immunogenicity of skin allografts. *Journal of Investigative Dermatology*, *75*(1), 107-115.

Stewart, S., Winters, G. L., Fishbein, M. C., Tazelaar, H. D., Kobashigawa, J., Abrams, J., Andersen, C. B., Angelini, A., Berry, G. J., Burke, M. M., Demetris, A. J., Hammond, E., Itescu, S., Marboe, C. C., McManus, B., Reed, E. F., Reinsmoen, N. L., Rodriguez, E. R., Rose, A. G.,…Billingham, M. E. (2005). Revision of the 1990 Working Formulation for the Standardization of Nomenclature in the Diagnosis of Heart Rejection. *The Journal of Heart and Lung Transplantation*, *24*(11), 1710-1720.

Strainic, M. G., Liu, J., Huang, D., An, F., Lalli, P. N., Muqim, N., Shapiro, V. S., Dubyak, G. R., Heeger, P. S., & Medof, M. E. (2008). Locally produced complement fragments C5a and C3a provide both costimulatory and survival signals to naive CD4+ T cells. *Immunity*, *28*(3), 425-435.

Stussi, G., West, L., Cooper, D. K., & Seebach, J. D. (2006). ABO-incompatible allotransplantation as a basis for clinical xenotransplantation. *Xenotransplantation*, *13*(5), 390-399.

Tchilian, E. Z., & Beverley, P. C. (2006). Altered CD45 expression and disease. *Trends in immunology*, *27*(3), 146-153.

Techakriengkrai, N., Nedumpun, T., Golde, W. T., & Suradhat, S. (2021). Diversity of the Swine Leukocyte Antigen Class I and II in Commercial Pig Populations. *Front Vet Sci*, *8*, 637682.

Timoshanko, J. R., Sedgwick, J. D., Holdsworth, S. R., & Tipping, P. G. (2003). Intrinsic renal cells are the major source of tumor necrosis factor contributing to renal injury in murine crescentic glomerulonephritis. *J Am Soc Nephrol*, *14*(7), 1785-1793.

Tseng, Y.-L., Kuwaki, K., Dor, F. J., Shimizu, A., Houser, S., Hisashi, Y., Yamada, K., Robson, S. C., Awwad, M., & Schuurman, H.-J. (2005). α1, 3-Galactosyltransferase gene-knockout pig heart transplantation in baboons with survival approaching 6 months. *Transplantation*, *80*(10), 1493-1500.

van de Wetering, J., Weimar, C. H., Balk, A. H., Roodnat, J. I., Holweg, C. T., Baan, C. C., van Domburg, R. T., & Weimar, W. (2006). The impact of transforming growth factor-β1 gene polymorphism on end-stage renal failure after heart transplantation. *Transplantation*, *82*(12), 1744-1748.

van der Zwan, M., Hesselink, D. A., van den Hoogen, M. W. F., & Baan, C. C. (2020). Costimulation Blockade in Kidney Transplant Recipients. *Drugs*, *80*(1), 33-46.

Ville, S., Poirier, N., Blancho, G., & Vanhove, B. (2015). Co-Stimulatory Blockade of the CD28/CD80-86/CTLA-4 Balance in Transplantation: Impact on Memory T Cells? *Front Immunol*, *6*, 411.

Werfel, T., Kirchhoff, K., Wittmann, M., Begemann, G., Kapp, A., Heidenreich, F., Gö tze, O., & Zwirner, J. r. (2000). Activated human T lymphocytes express a functional C3a receptor. *The Journal of Immunology*, *165*(11), 6599-6605.

Wieczorek, M., Abualrous, E. T., Sticht, J., Álvaro-Benito, M., Stolzenberg, S., Noé, F., & Freund, C. (2017). Major histocompatibility complex (MHC) class I and MHC class II proteins: conformational plasticity in antigen presentation. *Frontiers in Immunology*, *8*, 292.

Williams, R. C., Opelz, G., McGarvey, C. J., Weil, E. J., & Chakkera, H. A. (2016). The Risk of Transplant Failure With HLA Mismatch in First Adult Kidney Allografts From Deceased Donors. *Transplantation*, *100*(5), 1094-1102.

Wu, C. J., Kurbegov, D., Lattin, B., Burchard, E., Finkle, C., Valantine, H., Billingham, M. E., Starnes, V. A., & Clayberger, C. (1994). Cytokine gene expression in human cardiac allograft recipients. *Transplant Immunology*, *2*(3), 199-207.

Yamada, J., Hamuro, J., Terai, K., & Kinoshita, S. (2007). Major histocompatibility complex semi-matching improves murine corneal allograft survival under oxidative macrophage dominancy. *Transplantation*, *84*(7), 899-907.

Yang, L., Wu, H., Jin, X., Zheng, P., Hu, S., Xu, X., Yu, W., & Yan, J. (2020). Study of cardiovascular disease prediction model based on random forest in eastern China. *Scientific Reports*, *10*(1), 5245.

Ye, N., Cai, J., Dong, Y., Chen, H., Bo, Z., Zhao, X., Xia, M., & Han, M. (2022). A multi-omic approach reveals utility of CD45 expression in prognosis and novel target discovery. *Frontiers in Genetics*, *13*, 928328.

Zachary, A. A., & Leffell, M. S. (2016). HLA Mismatching Strategies for Solid Organ Transplantation - A Balancing Act. *Front Immunol*, *7*, 575.

Zeiser, R., Zambricki, E. A., Leveson-Gower, D., Kambham, N., Beilhack, A., & Negrin, R. S. (2007). Host-Derived Interleukin-18 Differentially Impacts Regulatory and Conventional T Cell Expansion During Acute Graft-Versus-Host Disease. *Biology of Blood and Marrow Transplantation*, *13*(12), 1427-1438.

Zhang, J., Li, S., Liu, F., & Yang, K. (2022). Role of CD68 in tumor immunity and prognosis prediction in pan-cancer. *Sci Rep*, *12*(1), 7844.

Zhuang, Q., & Lakkis, F. G. (2015). Dendritic cells and innate immunity in kidney transplantation. *Kidney international*, *87*(4), 712-718.

# XI. ACKNOWLEDGEMENT

First of all, I want to express my sincere gratitude to Prof. Dr. Eckhard Wolf for accepting my thesis and welcoming me as a guest scientist at the Chair for Molecular Animal Breeding and Biotechnology, LMU Munich.

I am very thankful to Prof. Dr. Christian Kuppatt for granting me the opportunity to pursue my doctoral thesis within his research group at the Department of Internal Medicine I, Klinikum rechts der Isar, TU Munich.

I am very grateful to Dr Josep Miquel Cambra for his valuable guidance, support, and encouragement throughout the research period of my thesis. This provided me with extremely useful insights to shape my research ideas.

I extend my appreciation to Prof. Dr. Nikolai Klymiuk for his contribution to development of this work.

Thank you to my mentor Dr. Andrea Bähr, for introducing me to preclinical research and guidance.

Thank you my colleague Heinke Heymer (Klinikum rechts der Isar, TU Munich) for preparing the histological staining.

Thank you, Carolina Cabrera, for helping with the animal breeding and management. Thank you to all the colleagues from Moorversuchsgut.

In the end, I owe all the motivation and love from my family: my mother, father, and brother. I am indebted to constant support from my husband Sagar and my sister Manila.